WOODS HOLE OCEANOGRAPHIC INSTITUTION
Woods Hole, Massachusetts

REFERENCE NO. 68-62

TURBULENCE AND TURBULENT FLUXES OVER THE INDIAN OCEAN

by

Andrew F. Bunker

September 1968

TECHNICAL REPORT

Submitted to the National Science Foundation under Grants G-22389 and GA-1490.

Approved for Distribution N.P. Fofonoff

N.P. Fofonoff, Chairman
Department of Physical Oceanography

Abstract

A C-54Q aircraft equipped with meteorological instruments was flown three times to India to participate in the International Indian Ocean Expedition. Flights were made out of Bombay, Gan, and Aden to observe winds, temperatures, humidities, clouds, radiation, carbon dioxide, tritium, turbulence, and turbulent fluxes of heat, water vapor, momentum and kinetic energy. The present paper reports the values of 405 measurements of the turbulence and turbulent fluxes and interprets them in terms of the monsoon circulation and the effect upon currents and temperatures of the Arabian Sea. Analyses of other data have been reported and interpreted elsewhere.

The aircraft turbulence measuring system used was developed earlier by Bunker (1955) (1960). It consisted of a vertical accelerometer, a strain-guage air-speed transducer, a vertical gyro, a platinum wire thermometer and a microwave refractometer for humidity measurements. The data was recorded on a nine-channel oscillograph. A digitizing reader was used to read and punch the data on cards. The turbulent quantities and fluxes were computed and tabulated by machine. The accuracy and limitations of the system are discussed. While much is left to be desired in terms of accuracies and spectral range, the results are meteorologically useful and comparison shows good agreement with other techniques.

Graphs are presented which show the vertical variation of the turbulence, fluctuations of temperature and humidity, sensible and latent heat fluxes and shearing stresses for both the northeast and southwest monsoons. The atmosphere of the southwest monsoon is more turbulent than the northeast monsoon air. Average root-mean-square vertical velocities generally range between 30 to 40 cm sec^{-1} in the northeast monsoon air and between 40 to 60 cm sec^{-1} in the southwest monsoon air. The turbulent velocities decrease with height to about 20 cm sec^{-1} at 2 to 4 km, except in cumulus clouds where one root-mean-square value of 174 cm sec^{-1} was encountered. The sensible heat flux is small and directed downward during both seasons at all heights except in the lowest 30 meters of the northeast monsoon air. The latent heat flux is directed upward in both seasons. It averages about 3.1 mcal cm^{-2} sec^{-1} in the lowest layers of the northeast monsoon and 1.6 mcal cm^{-2} sec^{-1} in the southwest monsoon. This is the equivalent of about 0.4 and 0.2 cm day^{-1} evaporation of water. Shearing stresses measured in the lowest layers during the northeast monsoon averaged less than 1 dyne cm^{-2}. The stress in the lowest layers during the southwest monsoon averaged about 3 dynes cm^{-2}.

Charts and tables are presented to show the regional variation of the turbulence and the fluxes. The air over the western part of the Arabian Sea during the southwest monsoon is more turbulent and shows greater variability than the eastern Arabian Sea. Frequent negative water vapor fluxes were observed west of 65 E. Dew-point temperature gradients observed from the R/V Atlantis II frequently changed from negative to positive in this region. The flux measurements in conjunction with the gradient observations are interpreted to mean that large scale intrusions of dry air displaced the moist surface air, thereby causing negative small-scale fluxes aloft, but increased evaporation from the sea surface. Regional variations are discussed in terms of wind strength, atmospheric stability, sea temperature, scale of motion and convergence patterns of the air.

It is demonstrated that the sensible heat flux has little or no effect upon the monsoon circulation of either season. The latent heat flux increases the strength of northeast monsoon circulation by furnishing energy to the equatorial convergence regions of the Indian Ocean. The evaporation of water from the Arabian Sea increases the rainfall over India and feeds energy into the southwest monsoon circulation. The stress of the wind off the Somalia coast causes upwelling of cold water which indirectly, through thermal winds, produces convergence and showers off the west coast of India.

I. Meteorological Background and Aircraft System of Turbulence Measurements

A. Meteorological Background

The International Indian Ocean Expedition was organized to study the oceanography and meteorology of the Indian Ocean. This ocean was selected for study because of the unique large-scale monsoons that occur during the summer and winter seasons and their interaction with the ocean currents and temperatures. During the summer season the winds blow strongly and steadily from the southwest into India and Asia, creating strong currents in the Arabian Sea and heavy rainfall over the land. In the winter the winds blow lightly out of Asia over the Indian Ocean and generally clear skies prevail. To study these phenomena and their interrelations, many research vessels, aircraft, land and island stations were utilized by many nations to obtain observations.

The Woods Hole Oceanographic Institution flew a C-54Q research aircraft, loaned by the U.S. Navy through the Office of Naval Research, to the Indian Ocean in 1963 and 1964. From this aircraft, observations were made of temperature and humidity, wind velocity, solar radiation and albedo, cloud types, heights and amounts, turbulence and turbulent fluxes of heat, water vapor and momentum. The flight paths flown during the 1964 trips are presented in Figure 1.

Most of the raw data has been reduced to meteorological parameters and distributed to investigators conducting studies on the monsoons. Several papers have been published using observations obtained from the aircraft. See, for example, Miller and Keshavamurthy (1967), Bunker and Chaffee (1968), Bunker (1967), Srivastava and Ronne (1966), Bunker (1965), and Ramage (1968).

This report presents 405 values of the turbulence and turbulent fluxes computed from the aircraft observations. The values are averaged both geographically and vertically and related to the observed gradients and winds. Comparisons of the fluxes have been made with the fluxes of the University of Washington group and the values found by the Internation Meteorological Centre from ship observations. Useable turbulence data was obtained only during the second and third flights of the C-54Q to the Indian Ocean. During the northeast monsoon, 172 one-minute series of turbulence observations were made. During the southwest monsoon, 233 series were made.

B. The Aircraft-acceleration Technique of Measuring Turbulent Vertical Velocities

The technique developed by Bunker (1955) (1960) to measure the vertical component of atmospheric turbulence and the turbulent fluxes of heat, water vapor and momentum was used during the IIOE flights of the C-54Q.

The instrumentation used was essentially as described in the two quoted papers. A Kearfott vertical gyro replaced the C-1 gyro used previously. A micro-wave refractometer was used to measure the rapid fluctuations of the water vapor content of the air.

The system allows the computation of the vertical velocity of the air from the following equation:

$$w_i' = a\Delta n/\rho V - b\Delta V/\rho V^2 - V\Delta\alpha_{att} + \sum_{0}^{t_i} \Delta n \Delta t \qquad (1)$$

Here Δn is the deviation of the measured vertical acceleration of the aircraft from a line of regression; ΔV is the deviation of the indicated air-speed from its line of regression; and $\Delta\alpha_{att}$ is the deviation of the measured attitude of the aircraft from its line of regression. All the lines of regression are least-squares fits to a straight line over the observing period. All runs were 1 minute long and measurements were made each fifth of a second. V is the true air-speed of the aircraft; ρ, the air density; Δt the measuring interval of 1/5 second. The constants a and b are values determined by the wing area, mass of the aircraft, the change in lift of the wings with angle of attack, and the gravitational acceleration.

The observations were recorded by a nine channel oscillograph on a 5 inch chart. The records were measured by a chart reader which digitized the readings and punched them on cards. The cards were fed into a computer which computed the lines of regression, determined the deviations from the lines of regression and solved the vertical velocity equations. Individual values of the vertical velocity were printed out and the root-mean-square value given. Records of the indicated air-speed, temperature of the air, and the refractometer output were treated similarly. The transport of heat, water vapor and momentum were computed from the following equations:

$$H = c_p \overline{\rho w' T'} \qquad (2)$$

$$E = L \overline{w' q'} \qquad (3)$$

$$\tau = -\overline{\rho w' u'} \qquad (4)$$

C. Limitations and Errors of the Measurement and Computational Systems

The turbulence measuring system has limitations and errors that should be understood before the results are interpreted. Ideally, the turbulence system should have had a high precision inertial navigation unit as its reference to give records of the exact attitude, speed and accelerations of the aircraft. Since one was not available for the IIOE, inexact instruments had to be used, and the effects of their shortcomings minimized by the method of reduction of the records. The two most serious faults of the system used are (1) inexact values of the attitude of the aircraft given by a vertical-seeking gyro and (2) the lack of a measure of the ground-speed of the aircraft. To minimize the errors arising from these deficiencies, only 1-minute units of 5-minute to 45-minute turbulence runs were reduced, deviations

from a line of regression obtained, and used in subsequent calculations. It was anticipated that a recording of the ground speed indicated by a Doppler radar set would give a valid series of ground-speeds. It was found, however, that the set was unstable and the output signal oscillated randomly while hunting for the true value. The assumption was made, therefore, that the ground-speed of the aircraft was either constant or varied linearly during the one-minute runs. The horizontal turbulent components of the wind were accordingly defined as the deviation from the line of regression of the indicated air-speed.

Other errors entering into the calculations are the usual ones of calibration errors of the sensors, instabilities of the bridge circuits, reading errors and other errors common to instrument systems. These errors combined are small (probably less than 5 percent) in comparison to the inaccuracies just described.

One result of using records with a length of 1 minute and deviations from a line of regression is to lose any information that might be contained in the records about the longer period fluctuations of the atmosphere. Thus, for an airplane flying 80 m per second, the length of run is 4800 m and the contributions to the fluctuations by wave-lengths greater than about 2400 m are lost. While flying at low levels in the boundary layer of the atmosphere most of the fluctuation energy is contained in wavelengths smaller than 2400 m and the statistics may be expected to represent approximately 80 percent of the fluctuations. As the aircraft altitude is increased, a smaller proportion of the energy is contained in wavelengths less than 2400 m and hence the turbulence values are less meaningful.

A comparison of the water vapor fluxes found by Fleagle, Badgley and Hsueh (1967) over the Arabian Sea with values found by the present technique verifies that the aircraft technique does not measure all of the flux. The flux of water vapor measured by the aircraft system averaged 60% of the flux measured by the integral method and 75% of the value found by the profile method. Previously (Bunker, 1960) it was shown that the aircraft technique gave values 25% smaller than the Jacobs (1942) bulk aero-dynamic formula.

The aircraft covariance system showed a much greater spread in the individual values than the other methods. This greater variation results from the small samples measured and large scale variations in the atmosphere. When the aircraft measurements are interpreted in conjunction with ship observations of the low-level water vapor gradients the processes operating in the atmosphere can be deduced. This point is discussed later with regard to the moisture fluxes west of 65 E during the southwest monsoon.

The errors of the system are difficult to estimate and have been the subject of much discussion in the past. Bunker (1955) estimated the σ_w errors involved with the system used in a PBY-6A aircraft and averaged over 30 seconds of flight to be $\pm$ 2 cm sec^{-1} exclusive of aircraft deformation, phugoid motion, and unsteady lift. An error of $\pm$ 5 percent is estimated if the phugoid motion is corrected for by subtracting 7-second averages from the individual values before computing the root-mean-square values. This correction, however, loses much of the low frequency energy of the atmosphere. Without the correction, the error may remain small or range up to 100%

if the aircraft has a strong phugoid motion. Telford and Warner (1962) have pointed out that this estimate may be unduly optimistic because the vertical-seeking gyro is influenced by horizontal accelerations of the aircraft. This point was discussed further by Bunker (1963) and Telford and Warner (1963). The magnitude of the error caused by horizontal accelerations cannot be estimated well because the Doppler radar did not give a useable record of the changes in the ground-speed of the aircraft.

The errors of the present system installed in the C-54Q aircraft, averaged over 1-minute units, are undoubtedly greater than the errors produced by the PBY-6A system averaged over half a minute.

While it is believed that the values of σ_w computed from the lines of regression and averaged over 60 seconds may be of the order of 10 percent accuracy, serious trouble arises in the computation of the shearing stress, $-\rho\overline{w'u'}$. It was found that the values of the stress did not change sign with the direction of the aircraft relative to the wind. That is, positive stresses were measured from the data obtained while the aircraft was flying upwind and downwind. The following averages were obtained during the third flight of the C-54Q aircraft to the Indian Ocean in 1964.

TABLE A

Averages of the Measured Stress

Relative Wind	Stress	
Head Wind	1.14	dynes cm^{-2}
Cross Wind	0.55	"
Tail Wind	0.38	"

In the frictional boundary layer an aircraft flying (a) upwind should record a positive value, (b) crosswind should record a zero value, and (c) downwind should record a negative stress. Hence, it is obvious that a hidden negative correlation is generated by the sensing or reduction system. The magnitude of this error in stress is about 0.7 dy cm^{-1}. With a $\sigma_w = \sigma_u = 50$ cm sec^{-1} a correlation coefficient of -0.3 is indicated, using the formula

$$\tau = -\rho r \sigma_w \sigma_u \qquad (5)$$

Such a correlation could arise from several sources and reflect the basic accuracy of the determinations of the individual values of w' and u'. One possibility of error arises from the second term $-b\Delta V/\rho V^2$, of equation (1) used for the computation of the vertical velocity values. If there were a positive 10 percent error in the calibration of the air-speed, then the stress for a headwind would be increased by + 27% and for a tail-wind it would be increased by + 6%. Checking the calibration does not reveal any such positive error.

Another possible source of error in the stress computation investigated was the effect of an undetected change in the ground speed of the aircraft. A sinusoidal variation with a period of 60 seconds and an amplitude of 1 m sec^{-1} was assumed. Considering only the effects of $u_{measured} = u' + \Delta GS$ where ΔGS is the ground speed changes and

$$w' = a\Delta n - bu_{measured}$$

it is seen that $\overline{w'w'_{error}} = -0.2\ \Delta \overline{GS^2}$

$$\tau_{error} = +.68 \text{ dynes cm}^{-2}$$

This error is exactly the amount found to be the error in the stress from comparing headwind stresses with tailwind stresses. However, a sinusoidal wave of ground speed with an amplitude of 100 cm sec^{-1} gives a root-mean-square horizontal velocity of 58 cm sec^{-1}. Since the average value of σ_u for the 203 measurements made in the boundary layer was 53 cm sec^{-1}, a ground-speed variation of such a large amplitude could not have occurred.

Approaching the problem empirically, it may be assumed that the difference between the $\overline{\sigma_w}$ and the $\overline{\sigma_u}$ represents the variation in u' caused by variations in the ground-speed of the aircraft. Since $\overline{\sigma_w} = 44$ cm sec^{-1} and $\overline{\sigma_u} = 53$ cm sec^{-1}, $\overline{\sigma_{GS}} = 9$ cm sec^{-1} the error in the stress determination is .02 dynes cm^{-2}; a negligible amount that does not explain the difficulty.

If one evaluates the effect of the ground-speed accelerations upon the gyro and hence upon the w' values, it is found that $\overline{\sigma_w}$ should be 39 cm sec^{-1} rather than 44 cm sec^{-1}. The $\overline{\sigma_{GS}}$ is the 14 cm sec^{-1} and the stress error $\pm$ .04 dy cm^{-2}. This is still a negligible error. If $\overline{\sigma_w} = \overline{\sigma_u} = 39$ cm sec^{-1} then the measured $\overline{\sigma_w}$ is 11% high and the $\overline{\sigma_u}$ is 26% high.

An attempt to resolve the problem of the hidden correlation between w' and u' was made by modifying the computational procedure and recomputing 19 runs. Twelve of the runs were tailwind runs with positive stresses. The other seven were headwind runs and crosswind runs. The computational procedure was changed by first subtracting only the mean value of the raw data from the individual values rather than finding deviations from a linear line of regression. The individual values of w_i, u_i, T_i, and q_i were then computed. Lastly, w', u', T', and q' were found as deviations from (a) a linear line of regression and (b) a quadratic line of regression. The following table shows how the computational changes modified the average stresses.

TABLE B

Average Stresses Grouped by Relative Winds

Computational System	Tailwind	Crosswind	Headwind
Standard	0.85	3.84	1.24
Linear Reg.	0.41	3.75	1.91
Quadratic Reg.	0.64	4.02	1.97

It is seen that the stresses for tailwinds decreased while the headwind stresses increased. Since the tailwind stresses decreased as was hoped, and the headwind stresses increased as is reasonable, but not anticipated, it is concluded that the newer computational systems eliminate small, random, uncorrelated variations of w' and u'. Thus the systems give slightly better results, but the major, hidden correlation remains.

It is possible that a correction system could be devised that would improve the results by correcting for changes in the attitude of the accelerometer, gyro variations with some assumed form of the ground-speed variations, flexing of the airframe, and other aerodynamic effects. Such an investigation would be costly and have a high probability of failure. Since work on the design of a new observing system utilizing a high-precision inertial navigation unit has been started, it seems unprofitable to spend more time on devising the corrections and recomputing the present data.

Based on the findings contained in Tables A and B, corrections could be made to the shearing stresses. First, the headwind stresses could be increased by 50% and the tailwind stresses decreased by 50% to account for the uncorrelated variations of w' and u'. Second, both the headwind and tailwind stresses could be decreased by 0.78 dynes cm^{-2} to account for the hidden correlation between w' and u'. This correction has not been applied to the stress data contained in the following tables. Correcting them would imply a higher degree of confidence in the corrections than is justified.

Since the headwind stresses would be changed only a small amount by applying the proposed corrections, it is recommended that they be accepted as measured. The crosswind and tailwind stresses are obviously wrong as measured, and should be discarded or corrected. If corrected, they should be interpreted and used with great care.

In summary, the root-mean-square vertical velocities are estimated to have a probable error of about $\pm$ 10 to 15 percent, exclusive of the energy lost by the limited frequency range of the system. The root-mean-horizontal velocities have a larger probable error, possibly $\pm$ 20 percent, caused by the inclusion of ground-speed variations in the average. The stress values measured while flying upwind are estimated to have an error of about $\pm$ 50 percent. The stresses measured downwind and crosswind have errors that exceed 100 percent. The root-mean-square temperature fluctuations are probably accurate to about 10 percent. The values of the specific humidity are not as accurate since the signal from the refractometer had to be corrected for the temperature and pressure fluctuations. The root-mean-square values of the specific humidity are estimated to have a probable error of about 20 percent. Judging by the comparison of moisture fluxes obtained by Fleagle, et. al., (1967) with the aircraft fluxes, the overall accuracy seems to be in the 20 to 25 percent range except for that part of the flux lost by the limited spectral range of the aircraft method. The flux of sensible heat is assumed to be of the same order of accuracy and subject to the same limitations.

II Tabulation of Fluctuation and Flux Data

Values of the fluctuations and fluxes are presented in the following tables with supplementary information and identification. The data has been grouped by days. The first column gives an identifying number corresponding to the run number photographed on the oscillograph trace. The letters indicate different one-minute sections of the run that have been measured. The

TABLE C: Turbulence and Flux Data Over the Indian Ocean

RUN	GMT hr min	LAT N	LONG E	HEIGHT meters	σ_w cm sec^{-1}	σ_u cm sec^{-1}	σ_T ^oC	σ_q $gm\ m^{-3}$	$c_p\overline{\rho w'T'}$ mcal cm^{-2} sec^{-1}	$L\overline{w'q'}$ mcal cm^{-2} sec^{-1}	$-\overline{\rho w'u'}$ dynes cm^{-2}	WIND ^oT m sec^{-1}	$(-\overline{\rho w'u'})(\cos\phi)^{-1}$ dynes cm^{-2}	KE FLUX ergs cm^{-2} sec^{-1}
8 February 1964														
4414A	1226	23.8N	59.7E	4430	27	62	.39	.32	-.1	1.0	-.2	270/2.6	0.3	
4414B	1227	23.8N	59.7E	4430	16	27	.11	.09	-.1	-.3	-.0	270/2.6	0.0	
12 February 1964														
4417A	0545	18.8N	71.5E	460	16	28	.28	.15	-.1	.1	.2	110/9.4	-0.2	8
4417B	0546	18.8N	71.5E	460	14	17	.18	.19	-.0	.2	.0	110/9.4	0.0	
4418	0600	19.0N	70.5E	305	18	17	.10	.20	.2	-.2	-.0	94/12.3	0.0	2
4419A	0624	19.3N	69.2E	140	24	21	.06	.59	-.1	3.5	.3	82/4.1	-0.3	11
4419B	0625	19.3N	69.2E	140	33	23	.04	.54	.1	7.4	.1	82/4.1	-0.1	
4420A	0635	19.5N	68.7E	20	24	35	.05	.45	.1	3.6	.2	82/5.1	-0.2	2
4420B	0636	19.5N	68.7E	20	27	35	.04	.45	.1	3.4	.2	82/5.1	-0.2	
15 February 1964														
4421	0548	18.1N	73.0E	2730	58	58	.16	.26	.2	-1.5	-.0H	180/3.5	0.0	
4425A	0715	18.7N	71.4E	4420	24	20	.05	.08	.1	.2	.1	19/6.4	-0.2	
4425B	0716	18.7N	71.4E	4420	13	13	.11	.12	.1	.0	.0	19/6.4	.0	
4426A	0815	18.3N	72.9E	4420	25	10	.07	.08	-.2	.5	-.0	108/5.2	ind.	
4426B	0816	18.3N	72.9E	4420	11	12	.05	.20	-.0	.5	.0	108/5.2	ind.	
4427A*	0918	18.9N	74.0E	4420	31	19	.13	.12	.2	-.2	.1	55/7.7	-.2	
4427B*	0919	18.9N	74.0E	4420	45	91	.16	.13	-.4	-.4	2.9	55/7.7	-3.5	
4428A	0946	18.9N	72.5E	4420	8	6	.04	.11	-.0	.0	.0	50/7.3	.0	
4428B	0947	18.9N	72.5E	4420	18	18	.05	.16	-.0	-.3	.1	50/7.3	-.1	
4429A	1030	18.8N	71.5E	2570	20	30	.02	.30	.0	.1	.1	315/4.3	-.2	
4429B	1031	18.8N	71.5E	2570	17	18	.02	.29	.0	.4	.0	315/4.3	.0	
4430A#	1056	18.9N	72.9E	2580	26	32	.13	.25	.0	-.2	.0H	68/5.8	.0	
4430B#	1057	18.9N	72.9E	2580	33	42	.09	.27	-.1	.5	.3H	68/5.8	.4	
4431A*	1149	18.9N	73.4E	1325	29	38	.05	.30	.0	.7	.2	63/6.9	-.2	
4431B*	1150	18.9N	73.4E	1325	14	28	.06	.30	.1	.2	-.2	63/6.9	-.2	

* Over the mountains east of Bombay
\# Over shoreline at Bombay

RUN	GMT hr min	LAT N	LONG E	HEIGHT meters	σ_w cm sec^{-1}	σ_u cm sec^{-1}	σ_T ^oC	σ_q gm m^{-3}	$c_p\overline{\rho w'T'}$ mcal cm^{-2} sec^{-1}	$L\overline{w'q'}$ mcal cm^{-2} sec^{-1}	$-\overline{\rho w'u'}$ dynes cm^{-2}	WIND ^oT m sec^{-1}	$(-\overline{\rho w'u'})(\cos\phi)^{-1}$ dynes cm^{-2}	KE FLUX ergs cm^{-2} sec^{-1}
15 February 1964 (cont.)														
4432A	1208	18.9N	17.0E	1325	14	14	.04	.55	.0	.4	.1	90/7.2	-.1	
4432B	1209	18.9N	17.0E	1325	15	23	.07	.95	.1	-2.3	.0	90/7.2	.0	
4432C	1210	18.9N	17.0E	1325	22	27	.07	.46	-.1	1.4	.3	90/7.2	-.3	
4432D	1211	18.9N	17.0E	1325	17	31	.08	.42	.0	1.1	.2	90/7.2	-.2	
17 February 1964														
4433A	0615	18.8N	71.2E	940	36	19	.09	.10	.2	-.2	-.2	80/3.0	ind.	
4433B	0616	18.8N	71.2E	940	13	12	.05	.16	-.0	-.1	.1	80/3.0	ind.	-2
4434A	0626	18.7N	71.2E	1905	13	16	.04	.07	-.0	.1	.0	155/5.8	0.0	0
4434B	0627	18.7N	71.2E	1905	15	27	.04	.06	-.0	.0	.2	155/5.8	-0.2	-1
4435A	0632	19.1N	71.1E	2375	11	23	.04	.06	.0	-.1	-.1	178/7.0	0.1	1
4435B	0633	19.1N	71.1E	2375	12	24	.07	.04	-.1	.0	.2	178/7.0	-0.2	1
4436A	0732	19.7N	71.5E	460	59	49	.16	.21	.3	.8	.8		ind.	
4436B	0733	19.7N	71.5E	460	22	30	.11	.18	-.3	.9	.4		ind.	
4437A	0814	19.2N	72.8E	460	16	26	.04	.49	-.1	.6	.1	310/4.6	-0.2	
4437B	0815	19.2N	72.8E	460	12	19	.05	.43	-.0	.5	.1	310/4.6	-0.1	
4438A	0840	18.6N	71.8E	490	10	11	.08	.35	.1	.1	.0	85/3.1	0.0	
4438B	0841	18.6N	71.8E	490	14	20	.11	.46	.2	.3	.2	85/3.1	-0.2	
4439A	0916	19.5N	70.9E	480	17	21	.06	.24	-.0	-.3	.1 H	5/5.3	0.1	
4439B	0917	19.5N	70.9E	480	23	19	.06	.27	.0	-1.2	.1 H	5/5.3	0.1	
4440A	0935	19.9N	71.5E	490	14	16	.05	.18	.0	.3	.1	16/7.9	ind.	0
4440B	0936	19.9N	71.5E	490	17	19	.07	.16	.1	-.2	.1	16/7.9	ind.	1
4441A	1008	19.4N	72.6E	470	27	36	.07	.16	.1	.3	.7	1/5.9	-0.8	
4441B	1009	19.4N	72.6E	470	30	42	.07	.18	-.1	.5	.3	1/5.9	-0.3	
4442A	1036	19.2N	71.5E	480	18	17	.05	.18	.0	.2	.1	15/8.1	ind.	1
4442B	1037	19.2N	71.5E	480	12	17	.05	.17	-.0	.1	.1	15/8.1	ind.	
4443A	1057	19.1N	70.5E	310	21	30	.53	.09	.1	-.1	.2	360/8.8	ind.	1
4443B	1058	19.1N	70.5E	310	31	27	.43	.08	.2	.2	.3	360/8.8	ind.	5
4446A	1109	19.1N	69.9E	140	35	37	.05	.19	.1	.4	.3	360/7.4	ind.	1
4446B	1110	19.1N	69.9E	140	46	39	.07	.14	.1	-.8	.2	360/7.4	ind.	

RUN	GMT hr min	LAT N	LONG E	HEIGHT meters	σ_w cm sec^{-1}	σ_u cm sec^{-1}	σ_T ^oC	σ_q $gm\ m^{-3}$	$c_p\rho\overline{w'T'}$ mcal cm^{-2} sec^{-1}	$L\overline{w'q'}$ mcal cm^{-2} sec^{-1}	$\overline{\rho w'u'}$ dynes cm^{-2}	WIND ^oT m sec^{-1}	$(\overline{\rho w'u'})(\cos\phi)^{-1}$ dynes cm^{-2}	KE FLUX ergs cm^{-2} sec^{-1}
17 February 1964 (cont.)														
4447A	1117	19.0N	69.6E	45	27	52	.08	.09	-.1	.0	.6	360/7.7	ind.	6
4447B	1118	19.0N	69.6E	45	30	55	.08	.08	-.1	.2	.5	360/7.7	ind.	28
4448A	1158	19.0N	71.0E	140	50	49	.15	.16	-.4	-1.1	.5	340/7.4	ind.	65
4448B	1159	19.0N	71.0E	140	28	44	.21	.21	-.7	-.4	.6	340/7.4	ind.	5
19 February 1964														
4450A	0623	14.0N	74.2E	455	19	17	.15	.18	-.0	-.1	.2	315/2.9	-.2	2
4450B	0624	14.0N	74.2E	455	22	13	.23	.39	-.5	1.3	.1 H	100/3.2	+.1	
4450C	0625	13.9N	74.2E	455	15	16	.43	1.54	-1.0	7.9	-.1 H	100/3.2	-.1	
4450D	0626	13.9N	74.3E	455	26	20	.35	1.24	-.1	-.9	.1 H	100/3.2	+.1	
4451A	0725	11.4N	75.4E	445	23	29	.17	1.08	-.1	1.0	.3	288/5.0	-.4	
4451B	0726	11.4N	75.4E	445	24	28	.22	.79	.1	-.3	.0	288/5.0	.0	
4451C	0727	11.3N	75.4E	445	26	32	.16	.92	-.1	1.9	.3	288/5.0	-.4	
4451D	0728	11.3N	75.4E	445	29	37	.16	.93	-.4	6.8	.5	288/5.0	-.8	
4452A	0818	9.3N	76.4E	440	19	24	.06	.16	-.0	.1	.0	310/3.0	.0	-4
4452B	0819	9.3N	76.4E	440	17	31	.21	.24	-.3	.4	.3	310/3.0	-.4	
4452C	0820	9.2N	76.4E	440	81	136	.35	.26	-3.0	-5.2	6.4	90/3.1	ind.	
4452D	0821	9.2N	76.4E	440	116	149	.40	.31	-5.4	-8.6	13.5	90/3.1	ind.	1545
4452E	0822	9.1N	76.4E	440	103	111	.17	.43	-.6	11.0	6.4	90/3.1	ind.	
4453A	0916	6.6N	76.1E	435	38	35	.12	.66	.1	.7	-.2	70/12.2	+.3	
4453B	0917	6.6N	76.0E	435	51	38	.12	.71	-.7	10.9	.7	70/12.2	-1.0	
4454	1010	4.2N	75.1E	435	22	30	.10	.64	-.2	1.0	.3	100/9.1	ind.	
4455A	1014	4.0N	75.1E	435	39	38	.11	.49	-.2	4.3	.6	65/8.4	-.7	
4455B	1015	3.9N	75.1E	435	29	37	.10	.52	-.0	-.4	.7	65/8.4	-.9	
4456A	1115	1.3N	74.0E	430	21	20	.11	.65	-.1	1.9	.2	112/5.9	ind.	
4456B	1116	1.3N	73.9E	430	27	21	.20	1.36	-.8	12.5	.0	112/5.9	ind.	
20 February 1964														
4458A	0636	0.0N	70.3E	450	19	17	.11	.50	.1	-.9	.2 H	227/3.0	0.2	-26
4458B	0637	0.0N	70.3E	450	26	13	.17	.88	.3	-5.5	-.0 H	227/3.0	0.0	

RUN	GMT hr min	LAT N	LONG E	HEIGHT meters	σ_w cm sec^{-1}	σ_u cm sec^{-1}	σ_T ^oC	σ_q $gm\ m^{-3}$	$c_p\rho\overline{w'T'}$ mcal cm^{-2} sec^{-1}	$L\overline{w'q'}$ mcal cm^{-2} sec^{-1}	$\rho\overline{w'u'}$ dynes cm^{-2}	WIND ^oT m sec^{-1}	$(\rho\overline{w'u'})(\cos\phi)^{-1}$ dynes cm^{-2}	KE FLUX ergs cm^{-2} sec^{-1}
20 February (cont.)														
4458C	0638	0.0N	70.2E	450	14	12	.10	.63	-.1	2.7	.0H	227/3.0	0.1	
4458D	0639	0.0N	70.2E	450	26	15	.12	.71	-.2	3.3	.2H	227/3.0	0.2	
4458E	0640	0.0N	70.1E	450	13	19	.14	.85	.1	.3	.0H	227/3.0	0.0	
4458F	0641	0.0N	70.1E	450	27	34	.14	.80	-.0	-1.3	.2H	227/3.0	0.3	
4458G	0642	0.0N	70.0E	450	38	28	.12	.84	-.3	7.2	.5H	227/3.0	0.6	
4459A	0715	0.0N	68.7E	305	35	26	.12	.86	-.2	4.7	.4	35/5.2	-0.6	19
4459B	0716	0.0N	68.7E	305	24	29	.06	.42	-.1	.5	.4	35/5.2	-0.6	
4460A	0729	0.0N	68.1E	140	41	34	.05	.36	-.2	3.1	.8H	238/2.1	0.9	28
4460B	0730	0.0N	68.1E	140	36	32	.08	.40	-.0	1.8	.6H	238/2.1	0.7	
4461A	0745	0.0N	67.4E	10	25	37	.07	.53	.1	2.0	.5H	275/1.5	0.5	16
4461B	0746	0.0N	67.4E	10	29	46	.07	.62	.0	3.2	.7H	275/1.5	0.7	
4463	0856	0.0N	64.4E	450	27	37	.15	.87	-.3	5.4	.4	31/7.0	-0.8	15
4466A	1104	0.0N	63.9E	4375	15	14	.04	.04	-.0	0.0	.1H	109/4.6	0.1	-1
4466B	1105	0.0N	63.9E	4375	21	14	.04	.04	-.0	.1	.1H	109/4.6	0.1	
4467A	1219	0.1S	67.4E	4375	41	30	.20	.20	-.3	.3	.3	360/3.0	ind.	
4467B	1220	0.1S	67.5E	4375	53	34	.16	.23	-.2	.4	.2	360/3.0	ind.	
4468	1233	0.2S	68.1E	4375	114	84	.32	.18	-.4	2.7	.6	200/5.6	ind.	
22 February 1964														
4470A	0520	1.7N	74.1E	4145	29	20	.08	.14	-.1	-.1	.1H	38/9.9	0.1	
4470B	0521	1.7N	74.1E	4145	29	23	.13	.11	.2	.4	.0H	38/9.9	0.0	
4471A	0805	9.5N	76.1E	2220	57	33	.14	.14	-1.0	1.4	-.4	94/9.8	ind.	
4471B	0806	9.6N	76.1E	2220	35	21	.11	.08	-.3	.2	.1	94/9.8	ind.	
4472A	0820	10.2N	76.0E	1240	28	30	.13	.44	.1	-1.3	.2H	35/5.5	0.4	-2
4472B	0821	10.3N	75.9E	1240	28	29	.24	.82	-.3	5.5	-.1H	35/5.5	-0.1	
4473	0834	10.8N	75.7E	430	35	32	.12	.19	-.1	-2.5	.9H	293/2.1	+1.5	-7
4474A	0844	11.2N	75.5E	115	43	46	.13	.43	-.0	3.4	.4	264/3.3	ind.	6
4474B	0845	11.2N	75.5E	115	41	38	.06	.49	.1	2.5	.0	264/3.3	ind.	
4475A	0849	11.4N	75.4E	60	36	51	.07	.53	.1	3.5	.9H	330/0.5	0.9	1
4475B	0850	11.5N	75.4E	60	59	47	.07	.51	.5	6.0	.7H	330/0.5	0.7	
4477A	0930	13.0N	74.7E	275	41	38	.07	.60	-.1	4.7	.9	280/4.3	ind.	

RUN	GMT hr min	LAT N	LONG E	HEIGHT meters	σ_w cm sec^{-1}	σ_u cm sec^{-1}	σ_T ^oC	σ_q gm m^{-3}	$c_p\rho\overline{w'T'}$ mcal cm^{-2} sec^{-1}	$L\overline{w'q'}$ mcal cm^{-2} sec^{-1}	$-\rho\overline{w'u'}$ dynes cm^{-2}	WIND ^oT m sec^{-1}	$(-\rho\overline{w'u'})(\cos\phi)^{-1}$ dynes cm^{-2}	KE FLUX ergs cm^{-2} sec^{-1}
22 February 1964 (cont.)														
4477B	0931	13.1N	74.7E	275	51	39	.07	.70	-.2	3.4	1.1	280/4.3	ind.	
4478	1022	15.2N	73.7E	275	47	38	.11	.82	-.8	8.2	1.1	2/5.5	1.2	
26 February 1964														
4481A	0450	18.5N	71.4E	430	26	41	.09	.42	-.0	..6	.4	171/4.5	ind.	
4481B	0451	18.5N	71.3E	430	31	40	.09	.46	-.1	3.0	.2	171/4.5	ind.	
4482A	0635	17.8N	72.6E	415	31	21	.08	.09	.2	-.3	-.0	90/4.5	0.0	
4482B	0636	17.8N	72.6E	415	28	23	.11	.06	.3	.1	-.1	90/4.5	0.1	
4486A	0757	16.0N	69.9E	425	34	40	.16	1.39	-.4	4.5	.7	33/7.4	-0.9	
4486B	0758	16.0N	69.9E	425	39	47	.19	1.42	-.4	4.2	1.0	33/7.4	-1.2	
4487	0832	14.3N	69.9E	120	46	40	.05	.36	.2	7.6	.5	112/2.8	ind.	
28 February 1964														
4490A	0444	19.0N	72.3E	430	8	18	.03	.05	.0	.1	.1 H	275/3.5	0.1	
4490B	0445	19.0N	72.2E	430	9	17	.06	.04	-.1	.0	.0 H	275/3.5	0.0	
4491A	0535	19.2N	69.9E	305	26	40	.16	1.30	-.6	8.7	.7 H	284/2.7	1.3	
4491B	0536	19.3N	69.9E	305	27	42	.20	1.54	-.4	7.1	.6 H	284/2.7	1.1	
4492A	0544	19.6N	69.8E	150	32	47	.09	.53	-.1	2.7	.7 H	282/4.6	1.3	
4492B	0545	19.7N	69.7E	150	32	32	.06	.58	-.1	2.2	.3 H	282/4.6	0.6	
4493A	0600	19.9N	69.2E	25	37	40	.07	.69	.1	5.5	.5	351/5.2	-0.6	
4493B	0601	19.9N	69.1E	25	33	45	.05	.55	.0	5.0	.6	351/5/2	-0.8	
4495A	0646	20.0N	68.6E	300	20	38	.12	.83	.1	-1.0	.1 H	313/3.3	0.2	
4495B	0647	20.0N	68.6E	300	28	46	.17	.90	-.3	4.9	.7 H	313/3.3	1.0	
4495C	0648	20.1N	68.6E	300	25	32	.09	.57	-.2	1.4	.3 H	313/3.3	0.4	
4495D	0649	20.1N	68.6E	300	26	33	.11	.81	-.2	2.5	.5 H	313/3.3	0.8	
4497	0807	20.0N	70.0E	300	24	33	.16	.70	-.2	1.5	.5	18/4.4	-0.6	
4498	0847	19.0N	69.6E	1250	15	13	.05	.70	.0	.1	.1 H	228/6.5	0.1	
4499	0925	19.8N	68.6E	1280	34	18	.05	.06	.0	.4	.3	130/6.1	-0.5	
4500	0958	20.6N	69.3E	1280	9	13	.04	.06	-.0	.0	.0	130/6.1	ind.	

RUN	GMT hr min	LAT N	LONG E	HEIGHT meters	σ_w cm sec^{-1}	σ_u cm sec^{-1}	σ_T ^oC	σ_q gm m^{-3}	$c_p\rho\overline{w'T'}$ mcal cm^{-2} sec^{-1}	$L\overline{w'q'}$ mcal cm^{-2} sec^{-1}	$\rho\overline{w'u'}$ dynes cm^{-2}	WIND ^oT m sec^{-1}	$(\rho\overline{w'u'})(\cos\phi)^{-1}$ dynes cm^{-2}	KE FLUX ergs cm^{-2} sec^{-1}
28 February 1964 (cont.)														
4501A	1015	20.8N	70.1E	1280	38	56	.05	.05	-.0	-.1	.7	265/3.2	-1.0	
4501B	1016	20.8N	70.2E	1280	40	51	.07	.06	-.0	.1	.5	265/3.2	-0.8	
4502	1039	20.3N	70.0E	1280	21	20	.05	.09	.0	.2	.1	289/4.0	ind.	
4505	1123	19.0N	70.9E	1280	15	15	.05	.06	.0	.1	.1	244/11.8	-0.1	
2-3 March 1964														
4509	2146	18.9N	68.9E	470	11	13	.05	.07	-.0	.2	.1	009/2.9	ind.	
4510A	2222	20.3N	68.8E	470	18	15	.07	.09	-.0	-.1	.1	272/6.4	ind.	
4510B	2223	20.3N	68.8E	470	13	26	.13	.34	.0	.1	.3	272/6.4	ind.	
4511	0022	18.8N	68.9E	970	25	22	.04	.05	-.0	-.0	.0H	299/5.7	0.0	
4513	0329	20.1N	70.0E	4425	18	25	.05	.04	-.0	.0	.2	277/4.2	ind.	
4514A	0409	19.0N	69.8E	415	40	41	.16	1.32	-.7	8.1	.7	354/3.0	ind.	
4514B	0410	19.0N	69.8E	415	35	37	.18	1.42	-1.0	16.1	.8	354/3.0	ind.	
4515A	0434	19.0N	70.4E	1280	10	16	.08	.15	.0	.2	.1H	63/9.3	0.1	
4515B	0435	19.0N	70.4E	1280	17	16	.09	.13	.2	.5	.2H	63/9.3	0.2	
4-5 March 1964														
4517	2044	19.0N	71.8E	460	37	47	.26	1.18	-1.0	2.2	1.2	32/3.0	-1.8	
4518A	2111	18.8N	71.3E	1280	43	37	.07	.15	-.2	-.2	.7	295/3.7	-1.0	
4518B	2112	18.9N	71.3E	1280	34	34	.06	.19	-.1	-.9	.4	295/3.7	-0.6	
4519	2200	19.1N	72.4E	2575	14	15	.05	.12	.0	.1	.1H	213/6.1	+0.1	
4520	2248	18.8N	71.3E	3810	12	12	.04	.11	-.0	.2	.0	299/8.3	-0.1	
4521	2326	19.2N	73.4E	3810	15	14	.07	.06	-.0	-.2	.1	272/9.5	-0.1	
4522	0015	19.1N	72.5E	1250	36	39	.06	.32	.0	-.5	.1	25/3.4	-0.2	
4523A	0056	18.9N	71.6E	480	27	61	.15	.20	-.3	-.3	.9	9/6.5	ind.	
4523B	0057	18.9N	71.6E	480	24	33	.27	.92	-.0	1.3	.1	9/6.5	ind.	
4524	0125	19.2N	72.6E	330	23	42	.53	.82	-.1	2.0	.5	29/8.5	ind.	
4525A	0130	19.2N	72.3E	150	22	45	.18	1.32	-.3	5.6	.7H	330/4.3	+1.0	
4525B	0131	19.2N	72.3E	150	24	41	.14	.96	-.1	1.9	.2H	330/4.3	+0.2	

RUN	GMT hr min	LAT N	LONG E	HEIGHT meters	σ_w cm sec^{-1}	σ_u cm sec^{-1}	σ_T ^oC	σ_q gm m^{-3}	$c_p\overline{\rho w'T'}$ mcal cm^{-2} sec^{-1}	$L\overline{w'q'}$ mcal cm^{-2} sec^{-1}	$-\overline{\rho w'u'}$ dynes cm^{-2}	WIND ^oT m sec^{-1}	$(-\overline{\rho w'u'})(\cos\phi)^{-1}$ dynes cm^{-2}	KE FLUX ergs cm^{-2} sec^{-1}
4-5 March 1964 (cont.)														
4526A	0144	19.3N	72.1E	35	23	48	.08	.61	-.0	2.4	.4	346/9.7	ind.	
4526B	0145	19.3N	72.1E	35	27	41	.08	.61	-.1	4.1	.5	346/9.7	ind.	
7 March 1964														
4528	0345	19.7N	72.4E	300	18	23	.16	.36	-.1	0.2	.1	54/5.8	ind.	
4529	0410	20.5N	71.6E	300	52	66	.92	.53	1.4	0.6	1.6	119/4.1	- 1.8	
4530A	0500	20.0N	69.8E	240	26	27	.78	-.49	-.5	5.2	.4	27/4.0	-0.5	
4530B	0501	20.0N	69.8E	240	28	29	.55	-.22	-.2	3.4	.3	27/4.0	-0.3	
4531A	0617	18.5N	68.0E	120	52	51	.23	.14	.2	1.4	1.4	10/6.3	-1.4	
4531B	0618	18.4N	68.0E	120	42	46	.27	-.01	-.0	3.9	.6	10/6.3	-0.6	
4532A	0621	18.3N	68.0E	20	45	55	.32	.30	.3	1.4	1.1	18/2.5	-1.1	
4532B	0622	18.3N	68.0E	20	40	49	.31	.39	.4	3.1	.4	18/2.5	-0.4	
4533A	0719	15.4N	68.0E	300	45	37	.60	-.14	-.1	1.6	.3	6/9.3	-0.3	
4533B	0720	15.4N	68.0E	300	42	48	.15	-.03	-.0	1.2	.9	6/9.3	-0.9	
4534	0735	14.4N	68.0E	110	58	52	.29	-.15	-.2	-1.0	1.5	7/5.0	-1.5	
4535	0743	13.9N	68.0E	20	32	49	.34	.09	.1	2.6	.5	360/5.1	-0.5	
4536	1009	12.8N	69.6E	4410	10	17	.18	.01	.0	0.1	.1	139/4.8	ind.	
9 August 1964														
4571	0950	24.4N	58.0E	2967	28	15	.03	.26	.1	-2.1	.2 H	58/9.6	0.2	
4572	1055	23.3N	61.3E	3101	14	17	.04	.38	-.0	.7	.1	247/12.1	-0.1	
4574	1206	22.2N	64.8E	2992	38	15	.08	.17	.2	-1.0	.2	225/4.0	ind.	
4576	1313	20.9N	68.0E	3004	38	27	.05	.17	-.0	.0	.1 H	69/8.8	0.1	
4577A	1338	20.4N	69.2E	2992	80	33	.13	.19	-.4	.8	.1	342/5.8	-0.1	
4577B	1339	20.4N	69.3E	2992	81	28	.09	.22	.0	.2	.8	342/5.8	-0.1	
14 August 1964														
4578	0441	18.2N	71.8E	536	27	32	.12	.36	.3	-2.8	.1	252/9.8	ind.	

RUN	GMT hr min	LAT N	LONG E	HEIGHT meters	σ_w cm sec^{-1}	σ_u cm sec^{-1}	σ_T ^oC	σ_q gm m^{-3}	$c_p\overline{\rho w'T'}$ mcal cm^{-2} sec^{-1}	$L\overline{w'q'}$ mcal cm^{-2} sec^{-1}	$\overline{\rho w'u'}$ dynes cm^{-2}	WIND ^oT m sec^{-1}	$(\overline{\rho w'u'})(\cos\phi)^{-1}$ dynes cm^{-2}	KE FLUX ergs cm^{-2} sec^{-1}
14 August 1964														
4579	0455	17.7N	72.0E	372	52	38	.06	.33	-.2	3.7	.4	290/9.3	-0.6	51
4580	0503	17.4N	72.1E	220	53	33	.05	.20	-.0	1.0	-.1	267/6.2	ind.	36
4582	0508	17.2N	72.2E	105	44	55	.05	.32	.0	2.7	.0	255/6.2	ind.	14
16 August 1964														
4586A	0425	18.3N	71.4E	455	36	40	.09	.28	-.1	1.8	.3 H	258/6.4	0.3	
4586B	0426	18.2N	71.4E	455	41	39	.09	.28	-.1	2.2	.1 H	258/6.4	0.1	
4588A	0459	17.6N	70.2E	304	36	41	.09	.29	-.3	1.6	.8 H	218/4.9	0.8	35
4588B	0500	17.5N	70.2E	304	33	37	.07	.21	-.1	1.5	.2 H	218/4.9	0.2	
4589A	0506	17.5N	70.0E	146	54	64	.07	.24	-.1	2.0	1.1 H	235/5.1	1.1	
4589B	0507	17.5N	69.9E	146	50	57	.05	.21	-.1	3.0	1.5 H	235/5.1	1.5	
4590A	0513	17.3N	69.7E	26	46	69	.26	.50	-1.4	7.4	2.1 H	210/8.8	2.5	
4590B	0514	17.3N	69.7E	26	40	59	.07	.25	-.2	1.0	1.2 H	210/8.8	1.4	
4591A	0553	16.6N	68.4E	464	55	55	.12	.32	-.3	.6	1.1 H	230/10.8	1.1	
4591B	0554	16.6N	68.3E	464	51	25	.13	.38	-.2	.7	.5 H	230/10.8	0.5	
4591C	0555	16.5N	68.3E	464	32	51	.14	.45	-.1	2.7	.5 H	230/10.8	0.5	
4591D	0556	16.5N	68.2E	464	36	46	.10	.30	-.3	2.3	.7 H	230/10.8	0.7	
4593	0852	12.9N	68.5E	4679	46	14	.05	.04	.1	-.2	.1	310/6.0	ind.	-29
18 August 1964														
4596	0350	18.4N	71.6E	520	67	62	.16	.40	-.2	2.9	1.0 H	283/9.9	1.3	
4597	0437	17.3N	69.7E	502	36	23	.06	.44	.0	.3	-.1	267/11.9	-0.1	
4599	0452	17.0N	69.2E	363	37	49	.07	.31	-.1	-1.5	.6 H	231/9.4	0.6	
4600	0458	16.3N	69.0E	194	51	59	.07	.18	-.0	.9	1.4 H	251/7.3	1.4	
4601	0505	16.8N	68.7E	70	57	91	.08	.23	-.3	2.1	3.1 H	228/10.9	3.1	
4602	0740	17.4N	70.0E	4834	20	24	.04	.19	.0	.3	.1 H	002/5.7	0.2	26
20 August 1964														
4603	0349	20.0N	71.4E	467	62	63	.11	.25	-.8	2.2	2.3 H	239/9.8	3.6	

RUN	GMT hr min	LAT N	LONG E	HEIGHT meters	σ_w cm sec^{-1}	σ_u cm sec^{-1}	σ_T ^{o}C	σ_q gm m^{-3}	$c_p\rho\overline{w'T'}$ mcal cm^{-2} sec^{-1}	$L\overline{w'q'}$ mcal cm^{-2} sec^{-1}	$-\rho\overline{w'u'}$ dynes cm^{-2}	WIND ^{o}T m sec^{-1}	$(-\rho\overline{w'u'})(\cos\phi)^{-1}$ dynes cm^{-2}	KE FLUX ergs cm^{-2} sec^{-1}
20 August 1964 (cont.)														
4604	0407	20.4N	70.6E	275	32	32	.16	.29	-.4	.9	.3	212/10.1	ind.	
4605A	0418	20.6N	70.2E	160	55	60	.05	.25	.2	2.0	1.7	222/11.5	ind.	
4605B	0419	20.6N	70.2E	160	42	44	.05	.35	-.1	3.1	.6	222/11.5	ind.	
4606A	0434	20.9N	69.5E	26	54	79	.06	.40	-.1	5.8	2.3	220/10.0	ind.	
4606B	0435	20.9N	69.6E	26	49	69	.07	.32	.1	2.5	1.7	220/10.0	ind.	
4608	0539	22.3N	67.0E	476	27	37	.23	.87	.3	-4.0	.2	221/6.7	ind.	
4609	0811	20.1N	70,1E	4973	25	15	.04	.37	.0	-2.1	.1	342/10.8	-0.1	
22 August 1964														
4611A	0358	17.7N	72.2E	503	14	30	.06	.11	.0	.0	.1	267/12.1	ind.	
5611B	0400	17.6N	72.2E	503	28	25	.04	.10	-.0	.1	.2	267/12.1	ind.	
4611C	0403	17.5N	72.3E	503	31	53	.08	.16	-.0	-.1	.6	267/11.8	ind.	
4611D	0406	17.3N	72.3E	503	53	47	.10	.17	.2	1.2	1.1	267/11.2	ind.	
4611E	0409	17.2N	72.4E	503	41	70	.15	.30	-.3	1.3	1.0	267/11.2	ind.	
4611F	0412	17.1N	72.4E	503	52	60	.14	.22	-.4	.1	1.8	268/9.7	ind.	
4611G	0415	16.9N	72.5E	503	46	47	.11	.23	-.2	1.3	1.4	268/9.7	ind.	
4611H	0418	16.8N	72.5E	503	37	37	.15	.38	.2	-.1	.1	271/8.8	ind.	
4611I	0421	16.7N	72.6E	503	39	40	.11	.31	.2	-.6	.6	271/8.8	ind.	
4611J	0424	16.5N	72.6E	503	31	39	.08	.30	.0	-.6	.1	271/9.4	ind.	
4611K	0427	16.4N	72.7E	503	38	34	.14	.48	.1	-2.1	.9	271/9.4	ind.	
4611L	0430	16.3N	72.7E	503	38	50	.14	.48	.5	-3.4	.5	277/9.8	ind.	
4611M	0432	16.3N	72.7E	503	35	54	.19	.62	.4	.5	-.1	277/9.8	ind.	
4611N	0434	16.1N	72.8E	503	32	58	.12	.33	.2	1.3	-.3	282/9.0	ind.	
4611O	0436	16.0N	72.8E	503	38	39	.12	.36	.2	-.3	.2	282/9.0	ind.	
4611P	0438	15.9N	72.9E	503	46	44	.09	.26	-.1	-.1	.6	291/8.0	-0.1	
4611Q	0440	15.9N	72.9E	503	35	53	.11	.31	+.1	1.7	.2	291/8.0	-0.4	
4611R	0442	15.8N	72.9E	503	34	28	.15	.49	.3	-1.2	.3	289/8.4	-0.6	
4611S	0444	15.7N	73.0E	503	35	53	.12	.24	-.1	.7	.1	289/8.4	-0.2	
4613A	0607	12.1N	74.3E	338	32	43	.05	.15	.1	1.0	.2	302/6.2	-0.2	
4613B	0609	12.0N	74.3E	338	32	43	.08	.20	.1	1.6	.3	302/6.2	-0.4	

RUN	GMT hr min	LAT N	LONG E	HEIGHT meters	σ_w cm sec^{-1}	σ_u cm sec^{-1}	σ_T ^oC	σ_q gm m^{-3}	$c_p\rho\overline{w'T'}$ mcal cm^{-2} sec^{-1}	$L\overline{w'q'}$ mcal cm^{-2} sec^{-1}	$-\overline{\rho w'u'}$ dynes cm^{-2}	WIND ^oT m sec^{-1}	$(-\overline{\rho w'u'})(\cos\phi)^{-1}$ dynes cm^{-2}	KE FLUX ergs cm^{-2} sec^{-1}
22 August 1964 (cont.)														
4615A	0619	11.6N	74.5E	176	44	37	.05	.22	-.1	1.5	.5	288/4.2	ind.	
4615B	0621	11.5N	74.5E	176	44	35	.06	.15	.1	1.4	.4	288/4.2	ind.	
4616A	0631	11.2N	74.7E	44	42	36	.05	.20	.2	2.4	.3	317/4.1	-0.4	
4616B	0633	10.9N	74.7E	44	34	50	.05	.29	.0	2.3	.2	317/4.1	-0.3	
4618A	0756	7.2N	75.8E	503	42	28	.07	.13	.0	.8	.3	273/4.6	ind.	
4618B	0758	7.1N	75.8E	503	39	30	.10	.46	.0	- .3	.1	273/4.6	ind.	
4619A	0803	6.9N	75.9E	329	40	60	.10	.25	-.0	.3	.7	320/6.2	-0.8	456
4619B	0805	6.8N	75.9E	329	33	33	.05	.23	-.0	-.1	.3	320/6.2	-0.3	24
4620A	0814	6.4N	76.1E	167	49	32	.04	.16	.0	1.0	-.1	325/3.5	0.0	
4620B	0816	6.3N	76.1E	167	50	34	.05	.31	.2	.5	-.1	325/3.5	+0.1	
4621A	0826	5.8N	76.2E	44	45	53	.06	.38	.1	4.3	.3	303/3.2	-0.5	
4621B	0828	5.8N	76.3E	44	42	44	.05	.38	.2	2.9	.4	303/3.2	-0.5	
4625	0914	5.8N	76.3E	2063	32	38	.05	.17	-.1	.1	.7	264/7.8	ind.	48
4626A	0940	6.9N	75.9E	2063	18	25	.20	.59	-.2	.6	.2	254/7.5	ind.	
4626B	0942	7.0N	75.9E	2063	13	17	.20	.50	-.1	.8	-.1	254/7.5	ind.	
4629A	1139	11.9N	74.2E	2085	174	127	.28	.45	-.4	3.6	1.6	238/11.4	ind.	1026
4629B	1141	12.2N	74.1E	2085	61	36	.20	.68	.1	2.7	.5	238/11.4	ind.	210
4630A	1154	12.6N	73.9E	2074	27	20	.03	.12	-.1	-1.0	.4	223/6.6	-0.7	-6
4630B	1156	12.7N	73.9E	2074	61	40	.22	.56	.7	-6.2	1.2	223/6.6	-2.3	
4630C	1158	12.7N	73.9E	2074	40	19	.08	.19	-.0	-.3	.0	223/6.6	-0.1	
4631	1320	16.4N	72.7E	2074	52	35	.06	.14	.3	1.3	.5	198/5.4	-0.7	26
4633A	1345	17.6N	72.4E	2074	35	35	.09	.27	.1	1.3	.1	195/7.7	-0.2	
4633B	1347	17.7N	72.4E	2074	39	36	.08	.41	.3	-2.9	.1	195/7.7	-0.1	-44
25 August 1964														
4635	0348	18.2N	71.4E	185	42	55	.07	.16	-.3	.2	1.6 H	296/7.1	+3.0	
4636	0353	18.1N	71.2E	44	38	54	.06	.18	-.0	.2	.6	307/4.6	ind.	
4638A	0440	17.1N	69.4E	995	25	53	.06	.80	-.0	.6	-.1	307/7.9	ind.	20
4638B	0442	17.1N	69.3E	995	32	24	.04	.13	-.0	-.2	.0	307/7.9	ind.	11
4639A	0547	15.7N	67.0E	484	37	49	.22	.38	-.3	.7	.1 H	247/9.1	+0.1	
4639B	0549	15.6N	66.9E	484	40	35	.07	.32	-.3	2.5	.7 H	247/9.1	+0.7	

RUN	GMT hr min	LAT N	LONG E	HEIGHT meters	σ_w cm sec^{-1}	σ_u cm sec^{-1}	σ_T ^oC	σ_q gm m^{-3}	$c_p\overline{\rho w'T'}$ mcal cm^{-2} sec^{-1}	$L\overline{w'q'}$ mcal cm^{-2} sec^{-1}	$\overline{\rho w'u'}$ dynes cm^{-2}	WIND ^oT m sec^{-1}	$(-\overline{\rho w'u'})(\cos\phi)^{-1}$ dynes cm^{-2}	KE FLUX ergs cm^{-2} sec^{-1}
25 August 1964 (cont.)														
4641A	0619	15.0N	65.9E	484	28	39	.13	.37	.0	-.5	.3 H	240/8.4	0.3	
4641B	0621	15.0N	65.8E	484	33	41	.10	.26	-.4	-1.2	.4 H	240/8.4	0.4	
4642	0641	14.6N	65.2E	365	44	54	.07	.18	-.1	.5	1.2 H	211/4.4	+1.4	109
4643A	0651	14.5N	64.8E	185	64	66	.07	.43	-.2	1.4	1.5 H	221/4.9	1.5	35
4643B	0653	14.3N	64.8E	185	44	68	.07	.20	-.2	.9	1.2 H	221/4.9	1.2	38
4644	0658	14.2N	64.6E	53	60	104	.07	.86	-.5	-3.3	3.6 H	245/7.7	3.9	93
4645A	0840	12.2N	61.7E	347	53	43	.09	.16	.1	.3	.6 H	197/4.6	0.7	-381
4645B	0845	12.2N	61.6E	170	40	51	.07	.14	-.1	-.6	1.1 H	220/9.0	+1.2	14
4646A	0856	11.9N	61.2E	44	67	118	.10	.19	-.7	-.6	4.8 H	210/4.5	5.3	-330
4646B	0858	11.9N	61.1E	44	47	73	.07	.29	-.2	-1.6	1.5 H	210/4.5	1.7	38
4647	1009	11.1N	60.2E	4136	18	16	.05	.08	-.0	-.2	.1	151/4.2	ind.	2
4648	1257	15.2N	67.4E	4150	17	20	.04	.19	.0	-.0	.1	345/4.1	ind.	-2
28 August 1964														
4650	0446	18.8N	72.1E	281	46	46	.07	.57	-.2	8.3	1.2 H	220/3.5	1.3	38
4651	0455	18.7N	71.8E	115	45	60	.08	.35	-.1	1.2	1.4 H	200/5.5	2.1	-48
4652	0500	18.7N	71.6E	10	46	55	.05	.28	-.2	1.3	1.5 H	220/6.0	1.7	15
4654A	0533	18.3N	70.3E	431	49	49	.10	.38	-.2	-2.4	.7 H	226/7.2	0.7	-21
4654B	0535	18.2N	70.2E	431	35	52	.14	.25	-.2	.5	.6 H	226/7.2	0.6	8
4654C	0537	18.2N	70.1E	431	43	59	.16	.23	-.7	-.7	1.4 H	226/7.2	1.5	-45
4654D	0539	18.2N	70.0E	431	31	50	.08	.50	-.0	1.2	.6 H	226/7.2	0.7	11
4654E	0541	18.2N	69.9E	431	40	61	.09	.31	-.0	-.3	1.3 H	226/7.2	1.4	59
4654F	0543	18.1N	69.8E	431	50	60	.13	.36	-.3	-3.2	.4 H	226/7.2	0.5	-359
4655A	0733	16.8N	65.6E	431	37	27	.09	.34	-.1	-.3	.3 H	220/8.0	0.4	-29
4655B	0735	16.7N	65.5E	431	33	42	.10	.37	-.3	.6	.8 H	220/8.0	0.9	-35
4656A	0747	16.6N	65.0E	281	37	50	.08	.43	-.1	1.0	.6 H	230/4.0	0.6	8
4656B	0749	16.6N	65.0E	281	46	39	.07	.28	-.1	+.0	.8 H	230/4.0	0.8	36
4657A	0755	16.5N	64.8E	115	48	55	.07	.30	-.1	.1	1.3 H	230/4.4	1.4	-1
4657B	0757	16.4N	64.7E	115	37	40	.06	.25	-.0	.1	.4 H	230/4.4	0.5	-9
4658A	0805	16.4N	64.4E	10	46	73	.06	.63	-.0	.3	1.7 H	230/4.9	1.8	41
4658B	0807	16.3N	64.3E	10	64	88	.08	.16	-.0	-1.9	2.2 H	230/4.9	2.8	1082

RUN	GMT hr min	LAT N	LONG E	HEIGHT meters	σ_w cm sec^{-1}	σ_u cm sec^{-1}	σ_T ^oC	σ_q $gm\ m^{-3}$	$c_p\overline{\rho w'T'}$ mcal cm^{-2} sec^{-1}	$L\overline{w'q'}$ mcal cm^{-2} sec^{-1}	$-\overline{\rho w'u'}$ dynes cm^{-2}	WIND ^oT m sec^{-1}	$(-\overline{\rho w'u'})$ $(\cos\phi)^{-1}$ dynes cm^{-2}	KE FLUX ergs cm^{-2} sec^{-1}
28 August 1964 (cont.)														
4659A	0858	15.7N	62.4E	459	84	129	.14	.21	-.2	-.9	5.3 H	220/14.0	5.7	-1818
4659B	0900	15.6N	62.3E	459	99	100	.11	.31	-.7	-1.1	5.5 H	220/14.0	5.9	-332
4660	1015	14.4N	59.0E	4455	31	17	.04	.13	.1	.6	.1	320/9.0	ind.	9
30 August 1964														
4662	0316	12.7N	46.1E	402	39	47	.07	.19	-.0	-1.2	.6	240/25.0	-0.7	-29
4663	0322	12.7N	46.4E	217	50	82	.11	.19	-.1	.2	1.9	240/22.5	-2.3	129
4664	0330	12.6N	46.9E	99	73	130	.10	.39	-.7	-.1	1.7	250/18.0	-1.9	-105
4667	0604	10.0N	53.4E	556	21	20	.09	.09	-.0	-.1	.2	236/19.5	ind.	2
4668A	0703	7.9N	54.6E	391	50	43	.08	.17	-.3	.8	.7	261/14.0	ind.	-47
4668B	0705	7.8N	54.6E	391	54	66	.07	.22	.1	.2	.9	261/14.0	ind.	-50
4669A	0713	7.6N	54.7E	229	57	50	.06	.15	.2	1.3	-.4	245/11.6	ind.	-128
4669B	0715	7.5N	54.8E	229	46	59	.06	.17	-.1	.3	1.1	245/11.6	ind.	-2
4669C	0717	7.4N	54.8E	229	54	77	.05	.17	.0	-.6	1.0	245/11.6	ind.	-66
4670A	0723	7.2N	54.9E	96	62	81	.08	.14	-.1	-.9	1.7	256/10.8	ind.	-168
4670B	0725	7.1N	54.9E	96	67	69	.08	.20	-.2	.4	.8	256/10.8	ind.	-89
4671A	0811	5.4N	55.8E	575	46	51	.11	.20	-.0	1.1	.5	272/9.5	ind.	-18
4671B	0813	5.3N	55.7E	575	43	63	.18	.24	.3	-.5	.6	272/9.5	ind.	-33
4672	0930	6.0N	54.8E	4628	29	27	.07	.09	.0	.2	.3 H	344/5.8	-0.3	-3
4673	1245	12.2N	51.8E	4600	27	30	.06	.10	.0	-.1	.2 H	19/6.2	+0.3	-1
1 September 1964														
4676A	0344	12.7N	46.5E	380	60	111	.21	.45	.1	.4	.3	260/16.3	-0.3	179
4676B	0345	12.7N	46.6E	380	48	66	.19	1.07	-.5	1.2	1.1	260/16.3	-1.2	-12
4677	0353	12.6N	47.0E	235	42	50	.05	.18	-.0	-.4	.3	250/15.0	-0.3	-74
4678	0359	12.6N	47.2E	95	24	34	.05	.15	-.0	-.1	.2	247/13.3	-0.2	-5
4680	0503	12.0N	50.3E	550	26	32	.15	.40	.6	-3.7	.2	257/6.5	-0.2	6
4681	0558	12.1N	53.0E	550	36	47	.33	.15	-.5	-.2	.4	230/21.0	ind.	-6

RUN	GMT Hr min	LAT N	LONG E	HEIGHT meters	σ_w cm sec^{-1}	σ_u cm sec^{-1}	σ_T ^oC	σ_q gm m^{-3}	$c_p\overline{\rho w'T'}$ mcal cm^{-2} sec^{-1}	$L\overline{w'q'}$ mcal cm^{-2} sec^{-1}	$\overline{\rho w'u'}$ dynes cm^{-2}	WIND ^oT m sec^{-1}	$(\overline{\rho w'u'})(\cos\phi)^{-1}$ dynes cm^{-2}	KE FLUX ergs cm^{-2} sec^{-1}
1 September 1964 (cont.)														
4682A	0618	11.9N	53.9E	560	115	105	.29	.42	-.5	-2.2	.2	236/22.3	ind.	-482
4682B	0620	11.9N	53.0E	560	80	94	.17	.32	-.8	1.2	-.2	236/22.3	ind.	191
4682C	0622	11.9N	54.1E	560	78	111	.14	.29	-.3	-0.0	1.6	236/22.3	ind.	212
4682D	0624	11.9N	54.2E	560	88	115	.12	.32	-.5	-.2	2.3	236/22.3	ind.	-255
4683A	0645	11.6N	55.2E	560	71	86	.14	.21	-.1	1.5	.1	254/16.1	-0.1	-158
4683B	0646	11.6N	55.3E	560	71	90	.13	.27	-.3	-.2	.9	254/16.1	-1.4	137
4683C	0648	11.6N	55.4E	560	61	69	.12	.24	-.0	-.8	1.0	254/16.1	-1.5	-36
4683D	0650	11.5N	55.4E	560	63	70	.12	.24	.1	1.7	.9	254/16.1	-1.4	2
4683E	0652	11.5N	55.5E	560	65	66	.12	.20	.4	1.6	.1	254/16.1	-0.1	75
4683F	0654	11.5N	55.6E	560	55	63	.11	.24	.2	1.5	.4	254/16.1	-0.6	-35
4684A	0705	11.3N	56.1E	395	59	76	.09	.21	.3	.9	-.6	256/16.5	+0.8	38
4684B	0706	11.3N	56.2E	395	64	74	.09	.19	.1	-1.4	1.8	256/16.5	-2.5	-93
4684C	0708	11.3N	56.3E	395	67	104	.11	.23	.0	.1	.5	256/16.5	-0.7	234
4684D	0710	11.3N	56.4E	395	62	85	.09	.21	-.1	1.2	-.4	256/16.5	+0.6	63
4685A	0714	11.2N	56.6E	235	54	81	.07	.18	.0	.1	.1	258/15.0	-0.2	61
4685B	0715	11.2N	56.6E	235	61	75	.06	.14	-.1	-.1	.4	258/15.0	-0.6	-99
4685C	0717	11.2N	56.7E	235	47	83	.06	.18	.0	.2	-.2	258/15.0	+0.3	150
4685D	0719	11.1N	56.8E	235	38	69	.06	.13	-.0	.3	.5	258/15.0	-0.7	-44
4686A	0724	11.1N	57.0E	100	41	58	.04	.14	-.1	-.7	.3	264/13.8	-0.3	-21
4686B	0725	11.0N	57.1E	100	38	60	.04	.17	-.0	-.3	.1	264/13.8	-0.2	-2
4686C	0727	11.0N	57.2E	100	36	66	.07	.21	-.1	-.4	1.1	264/13.8	-1.3	53
4686D	0729	11.0N	57.3E	100	29	43	.05	.13	-.0	.1	.6	264/13.8	-0.7	-8
4687A	0743	10.8N	58.0E	560	46	68	.12	.22	.1	.4	.1	265/18.0	-0.1	12
4687B	0745	10.8N	58.1E	560	50	72	.08	.18	.0	.4	1.2	265/18.0	-1.4	-12
4687C	0747	10.8N	58.2E	560	43	45	.08	.15	.0	-.1	.5	265/18.0	-0.6	-20
4687D	0749	10.7N	58.3E	560	35	49	.07	.19	.0	.9	.2	265/18.0	-0.2	11
4687E	0751	10.7N	58.4E	560	43	51	.08	.17	.1	-.6	.3	265/18.0	-0.4	-89
4687F	0753	10.7N	58.5E	560	63	78	.11	.16	.1	.2	.9	265/18.0	-0.1	-11
4687G	0755	10.7N	58.6E	560	46	76	.11	.20	-.0	.7	1.4	265/18.0	-1.6	-75
4687H	0757	10.6N	58.7E	560	45	62	.13	.19	.3	.9	.3	265/18.0	-0.4	29
4687I	0759	10.6N	58.8E	560	43	59	.12	.21	-.2	1.5	.1	265/18.0	-0.1	0
4688	0942	12.3N	63.4E	4140	18	22	.03	.07	.0	.1	.1	212/7.0	-0.1	0
4689	1226	17.6N	69.1E	4140	18	26	.08	.18	-.1	.1	.1	212/7.0	-0.1	-2

RUN	GMT hr min	LAT N	LONG E	HEIGHT meters	σ_w cm sec^{-1}	σ_u cm sec^{-1}	σ_T ^oC	σ_q gm m^{-3}	$c_p\overline{\rho w'T'}$ mcal cm^{-2} sec^{-1}	$L\overline{w'q'}$ mcal cm^{-2} sec^{-1}	$\overline{\rho w'u'}$ dynes cm^{-2}	WIND ^oT m sec^{-1}	$(\overline{\rho w'u'})(\cos\phi)^{-1}$ dynes cm^{-2}	KE FLUX ergs cm^{-2} sec^{-1}
3 September 1964														
4690A	0339	17.9N	72.3E	509	43	56	.06	.18	-.1	-.3	.4	325/5.0	ind.	-24
4690B	0341	17.8N	72.2E	509	39	42	.06	.17	.0	1.0	.7	325/5.0	ind.	-9
4690C	0343	17.8N	72.2E	509	28	32	.08	.19	-.0	.1	.3	325/5.0	ind.	-2
4690D	0345	17.7N	72.2E	500	28	44	.09	.14	-.0	.6	.8	325/5.0	ind.	14
4690E	0347	17.6N	72.2E	500	29	44	.07	.21	-.1	-.0	.6	325/5.0	ind.	-23
4690F	0349	17.5N	72.3E	490	26	47	.13	.17	-.2	.0	.4	325/5.0	ind.	-3
4691A	0420	16.2N	72.9E	354	41	36	.07	.14	-.1	1.0	-.2	330/4.5	+0.2	15
4691B	0422	16.1N	72.9E	354	49	41	.08	.22	.2	.9	.4	330/4.5	-0.4	-15
4692A	0427	15.8N	73.0E	175	36	45	.06	.18	.1	.6	.4	335/4.5	-0.4	11
4692B	0429	15.8N	73.0E	175	43	43	.07	.17	.0	1.6	.6	335/4.5	-0.6	42
4693A	0435	15.5N	73.1E	55	35	43	.07	.15	.2	1.0	-.1	335/4.5	+0.1	36
4693B	0437	15.4N	73.2E	55	39	41	.08	.17	.3	.8	.1	335/4.5	-0.1	42
4693C	0439	15.3N	73.2E	55	32	53	.09	.16	.0	.6	.3	335/4.5	-0.3	8
4694A	0514	13.7N	73.7E	509	81	85	.11	.21	-.9	2.5	.1	325/5.0	-0.1	-59
4694B	0516	13.6N	73.7E	509	55	67	.14	.20	.5	1.1	.6	325/5.0	-0.6	-161
4694C	0518	13.5N	73.8E	509	24	47	.10	.16	.1	1.2	-.1	325/5.0	+0.1	-6
4694D	0519	13.4N	73.8E	509	52	62	.13	.17	-.3	-1.0	.4	325/5.0	-0.4	-30
4694E	0520	13.3N	73.8E	509	37	43	.17	.23	.1	-.2	.7	325/5.0	-0.7	26
4694F	0522	13.2N	73.8E	509	35	71	.14	.20	-.3	2.0	.8	325/5.0	-0.8	-20
4695A	0548	12.1N	74.3E	515	26	48	.12	.15	.2	-.2	.5	325/5.0	-0.5	23
4695B	0550	12.0N	74.3E	515	22	26	.12	.16	.1	-.3	.2	325/5.0	-0.2	3
4696A	0557	11.7N	74.4E	372	31	44	.18	.17	.7	.2	.3	340/11.0	-0.3	-20
4696B	0559	11.6N	74.4E	372	42	43	.11	.15	-.2	-.4	-.0	340/11.0	0.0	48
4696C	0601	11.5N	74.4E	372	29	40	.12	.13	.4	-.3	.1	340/11.0	-0.1	12
4697A	0605	11.4N	74.5E	193	61	66	.12	.17	.4	-.2	.8	340/9.5	-0.8	48
4697B	0607	11.3N	74.5E	193	42	52	.11	.14	.1	.5	.2	340/9.5	-0.2	12
4698A	0613	11.0N	74.6E	56	51	65	.07	.19	.2	.2	.6	335/6.7	-0.6	48
4698B	0615	10.9N	74.7E	56	54	65	.09	.22	.3	-.4	.3	335/6.7	-0.3	51
4699	0725	9.6N	74.8E	4665	50	58	.08	.14	-.1	-.0	-.1H	006/8.2	-0.1	39

RUN	GMT hr min	LAT N	LONG E	HEIGHT meters	σ_w cm sec^{-1}	σ_u cm sec^{-1}	σ_T ^oC	σ_q gm m^{-3}	$c_p\rho\overline{w'T'}$ mcal cm^{-2} sec^{-1}	$L\overline{w'q'}$ mcal cm^{-2} sec^{-1}	$\rho\overline{w'u'}$ dynes cm^{-2}	WIND ^oT m sec^{-1}	$(\rho\overline{w'u'})$ $(\cos\phi)^{-1}$ dynes cm^{-2}	KE FLUX ergs cm^{-2} sec^{-1}
5 September 1964														
4700A	0414	16.5N	72.6E	304	25	36	.05	.20	-.0	-.1	.1	015/5.5	-0.1	24
4700B	0416	16.5N	72.6E	304	31	39	.08	.23	-.0	1.0	.0	015/5.5	0.0	17
4700C	0418	16.4N	72.6E	304	48	31	.09	.26	.1	.5	.1	015/5.5	-0.2	62
4701A	0423	16.1N	72.7E	145	33	40	.06	.22	.0	.8	.1	025/4.5	-0.2	15
4701B	0425	16.1N	72.7E	145	42	36	.07	.16	-.1	1.8	.4	025/4.5	-0.6	35
4702A	0430	15.8N	72.8E	22	36	31	.06	.15	.2	.7	-.0	040/3.5	+0.1	-12
4702B	0432	15.7N	72.8E	22	33	45	.07	.19	.2	.4	.2	040/3.5	-0.4	3
4703A	0443	15.2N	73.1E	470	36	37	.14	.45	.3	1.3	.3	010/5.8	-0.4	11
4703B	0445	15.2N	73.1E	470	51	34	.16	.37	.9	1.7	.1	010/5.8	-0.1	30
4704A	0513	13.9N	73.5E	470	28	34	.08	.21	-.1	1.1	.3	340/5.2	-0.3	-3
4704B	0515	13.8N	73.5E	470	48	43	.17	.25	.6	.3	-.0	340/5.2	0.0	3
4704C	0517	13.7N	73.5E	470	29	32	.09	.15	-.2	.7	.3	340/5.2	-0.3	-2
4704D	0519	13.7N	73.5E	470	31	24	.07	.16	.0	.0	.1	340/5.2	-0.1	-11
4704E	0521	13.6N	73.5E	470	18	21	.08	.14	.1	.3	.0	340/5.2	0.0	-3
4704F	0523	13.5N	73.5E	470	33	26	.09	.19	.3	-.0	.3	340/5.2	-0.3	-30
4704G	0525	13.5N	73.5E	470	25	27	.08	.17	.0	.2	.2	340/5.2	-0.2	-2
4704H	0527	13.4N	73.6E	470	23	22	.10	.24	.3	-.8	.2	340/5.2	-0.2	-6
4705	0611	11.2N	74.5E	313	28	44	.04	.02	.0	-.0	.8	355/5.5	-0.8	72
4706	0616	11.0N	74.5E	160	44	45	.07	.04	.3	.2	.7	010/4.2	-0.7	6
4707A	0621	10.8N	74.5E	15	31	27	.06	.16	.1	.7	.0	040/1.5	0.0	-9
4707B	0623	10.7N	74.5E	15	29	35	.06	.20	.0	.7	-.0	040/1.5	+0.1	8
4708	0707	10.2N	74.6E	3950	19	35	.04	.23	-.0	-.1	.3	072/7.2	ind.	-107
4709	0852	15.0N	74.6E	3950	26	19	.07	.07	-.2	.2	-.0	105/5.2	ind.	-3
9 September 1965														
4710A	0347	19.5N	71.7E	475	32	35	.06	.28	-.1	.5	.6	160/3.2	-0.9	18
4710B	0349	19.5N	71.7E	475	38	29	.10	.38	-.0	1.5	.2	160/3.2	-0.3	18
4711A	0355	19.6N	71.3E	300	40	33	.05	.30	.0	1.5	.2	140/8.5	-0.2	24
4711B	0357	19.7N	71.3E	300	45	38	.06	.27	.0	-.0	.4	140/8.5	-0.5	30
4712A	0406	19.8N	70.9E	162	47	39	.04	.27	.1	-.4	.9	145/6.5	-1.1	26
4712B	0408	19.9N	70.9E	162	63	39	.07	.20	.1	.0	.9	145/6.5	-1.0	-33
4713A	0413	20.0N	70.6E	26	64	42	.16	.43	-.0	3.4	.6	170/3.4	-1.1	-237
4713B	0415	20.0N	70.5E	26	30	34	.07	.24	-.0	.2	.3	170/3.4	-0.6	-9

next three columns give the Greenwich time in hours and minutes, the latitude and longitude in degrees and tenths of degrees. The height of the run in meters is given in the fifth column. The next four columns give the root-mean-square values of the vertical velocity, σ_w the horizontal velocity, σ_u the temperature, σ_T and the specific humidity σ_q. These values are computed from the deviations from linear lines of regression as described in the previous section. The column headed $C_p \rho \overline{w'T'}$ gives the flux of sensible heat in millicalories per square centimeter per second. The next column gives the flux of the latent heat of condensation of water vapor. The column is headed $L \overline{w'q'}$ and the units are the same as for the sensible heat flux. The column headed $-\rho \overline{w'u'}$ gives the shearing stress in dynes per square centimeter. The letter H following a stress value indicates that the aircraft was flying within 60° of the upward direction. Any value not followed by an H should be accepted with the reservations described in the preceding section. The wind direction and speed are given in the next column. The wind direction is given to the nearest degree and the speed to the nearest tenth of a meter per second. These values are either averages of several observations at the same level, or averages found graphically from values at the level and at several nearby levels. The column headed $(-\rho \overline{w'u'})(\cos\phi)$ is the stress corrected for the angle between the aircraft heading and the wind direction. A value labelled, ind., indicates an indefinite value because the aircraft was flying within 30° of the crosswind direction. The last column gives the flux of the turbulent kinetic energy in ergs per square centimeter per second. Not all of the rows contain this value since this quantity was an after-thought, and added to the computer program after many of the runs were processed. The flux of energy was computed by forming the average of $\frac{1}{2}\rho' w' (\frac{3}{2})(u'^2 + w^3)$ Here it is assumed that $v'^2 \approx u'^2$ and w'^2 .

III Vertical and Regional Variation of the Turbulence Parameters

The values of the fluctuation and turbulence values presented in the preceding section are now grouped seasonally, vertically, and regionally and discussed in relation to the gradients and the air flow patterns. The two seasonal divisions are (1) the northeast monsoon season and (2) the southwest monsoon season.

A. Northeast Monsoon Turbulence Characteristics

1. Meteorological Background

During the winter months an intense high pressure cell is formed over northern Asia by the cold air produced by radiational cooling. The air flows southwards over India and the Arabian Sea under the influence of the pressure gradient. Figure 2 shows the surface and 700 mb streamline charts for a typical day during the northeast monsoon. The air mass is warmed and dried by its passage over the northern mountains and its descent into the plains of India. As the surface air starts its southwestward passage over the Arabian Sea it is only slightly cooler in the lowest few meters than the water. A strong subsidence inversion usually occurs in the lowest

100 to 500 meters above the surface. The air is dry with only a trace of cirrus clouds present. As the air moves over the water, water vapor is accumulated by the air and cumulus clouds are formed after a passage of several hundred kilometers. Eventually, the air reaches the equatorial convergence zone, is lifted, and its water vapor precipitated. The subsequent graphs and tables show the changes in the fluctuations of temperature, water vapor, turbulence, and fluxes as the air mass moves from the west coast of India to the equatorial zone.

The vertical distribution of mixing ratio, potential temperature, and wind speed is given in Figure 3. The ordinate is given in percentages of the height of the base of the subsidence inversion. This ordinate was chosen since the height of the inversion varies greatly from day to day. If height was used as the ordinate, the characteristics of the boundary layer and the inversion would be smoothed out and only a simple decrease in mixing ratio and increase in potential temperature would appear on the plot. Data for the graph were taken in the region from 100 to 200 km from the northwest coast of India. This selection excluded soundings confused by the strong sea breeze off the Indian Coast, and soundings that were essentially land-formed radiational inversions. The graph thus gives the condition of the air mass, well away from land disturbances, as it starts its southward passage over the Arabian Sea. It is seen that the potential temperature increases by about 2C in a few meters at the top of the boundary layer. The mixing ratio drops rapidly through the inversion to a minimum at the 150% level. The wind shows the usual increase in speed with height to the top of the boundary layer. Above the layer, it varies in a different pattern according to the changed pressure gradient.

2. Fluctuation Statistics

Averages of the root-mean-square values of the vertical and horizontal components of the turbulent wind, of the specific humidity and the temperature fluctuation, and the fluxes of sensible and latent heat and momentum have been formed for the various levels of the atmosphere and presented in Table D. These are presented graphically in Figures 4 and 6. Here again the ordinate used is the percentage of the height of the base of the subsidence inversion. These averages are based on all the measurements made and hence include values made close to the coastline and in the equatorial region. The r-m-s values of the vertical velocity show only a small decrease with height through the boundary layer and in the air above the inversion. The averages are rather small and similar in magnitude to those measured previously (Bunker, 1955) in the northeast trade winds of the North Atlantic Ocean. To show this comparison Figure 5 is presented. Here, values of the r-m-s vertical velocity, $\sqrt{w}$, from several oceanic regions of the world are plotted. The values observed in the Somali jet region will be discussed later. The curve plotted from the North Atlantic westerlies region represents an extreme of high winds and intense heating of the air by a warmer sea surface. In the present case of the northeast monsoon, the heating from below is small and limited to the lowest 30 meters. At best, the surface air has a potential temperature that is only a fraction of a degree warmer than the air at 50 meters. This small temperature difference is insufficient to set up any organized convection currents buy may augment the turbulence generated mechanically.

The height variation of the vertical velocities observed over

TABLE D

Turbulence, Fluctuation, and Flux Averages During the Northeast Monsoon

Height % of Inv. Ht.	No.	σ_w cm sec^{-1}	σ_u cm sec^{-1}	σ_T ^oC	σ_q gm m^{-3}	$c_p\overline{\rho w'T'}$ mcal cm^{-2} sec^{-1}	$L\overline{w'q'}$ mcal cm^{-2} sec^{-1}	$-\overline{\rho w'u'}(\cos\phi)^{-1}$ dynes cm^{-2}	No.
13	16	37	45	.08	.46	.10	3.13	0.7	4
38	17	36	42	.15	.50	-.03	2.53	0.8	6
63	7	36	30	.08	.65	-.21	4.66	1.2	1
88	21	28	32	.15	.69	-.16	1.61	0.6	14
125	31	32	38	.17	.62	-.52	2.38	0.4	5
175	6	32	35	.12	.64	-.05	1.99	-	0
250	11	25	38	.20	.28	-.02	.54	0.1	3
350	22	22	25	.06	.17	.02	-.05	0.1	5

different regions of the Indian Ocean are presented in Figure 6. The series designated with a dash-dot-line was measured within 100 kilometers of the west coast of India. It shows an irregular increase with height to 300 meters and then a decrease. Much of the irregularity arises from the varying distances from the shoreline at which the observations were made. The values drawn with a dotted line were made 100 km to 200 km from shore. The magnitude of the turbulence is much less in this region. The full line indicates the data observed over the Arabian Sea at distances greater than 200 km. The magnitude of the vertical velocity rises to 50 cm sec^{-1} at the 100 m level and then decreases slowly to 35 cm sec^{-1} above 400 m. It is believed that the excess of turbulence in this region in comparison to other regions is caused by the action of cumulus clouds whose bases are quite low. The dashed line denotes observations made in the equatorial region. Here the turbulence is moderate and closely resembles the turbulence observed in the Atlantic trade wind region.

The horizontal turbulent component of the air is also moderate but slightly greater than the vertical component. Near the surface of the water, the vertical velocities are suppressed and much of the turbulent energy presumably is contained in the horizontal component. Near and above the inversion the stability of the air again suppresses the vertical component and the horizontal component is greater.

Figure 7 presents the vertical variation of the root-mean-square values of the temperature and the specific humidity. The values of the temperature fluctuations are moderate at all levels. The specific humidity values show the greatest fluctuations in the region of the inversion where the gradients are largest.

3. Turbulent Transport of Heat, Water Vapor and Momentum

Averages of the sensible heat flux, $c_p\overline{\rho w'T'}$ are presented in Figure 8. In the lowest 25% of the boundary layer sensible heat is transported upwards. Above this level the heat is transported downwards. This distribution is typical of subsiding air masses moving southward over warmer surfaces. It was observed by Bunker (1960) in regions off the east coast of North America. The magnitude of the flux and height at which the heat flux reverses depends upon the decrease in potential temperature in the lowest layer and the height at which the potential temperature reaches a minimum. Here the minimum potential temperature is only a fraction of a degree below the average in the layer and occurs close to the water surface. Above the minimum, which is barely recognizable in Figure 3 because of its small magnitude, the flow of heat is downward. Thus, the lower air is being heated both by the waters of the Arabian Sea and by transport from the warm subsiding air aloft.

The flux of the latent heat of condensation of water vapor shown in Figure 8 is upward at all levels except the highest level where a small negative value is indicated. The magnitude of the flux is great and indicates an amount of water vapor flux that is significant in terms of supplying the general circulation of the atmosphere with energy. The role of this energy supply will be discussed later. Locally, this transport is important in that it rapidly fills the air below the inversion with water vapor. When the air near the inversion base is saturated, cumulus clouds are formed and the process of the breakdown of the inversion begins. Bunker and Chaffee (1968)

present charts showing the formation of cumulus clouds in the region around 12 N. Once the inversion is broken down, the cumulus carry the water vapor to greater heights and eventually a thick layer of moist air is formed.

The preceding figures were drawn from averages over all regions of the Arabian Sea and the equatorial region of the Indian Ocean. Averages are formed and presented in Table E for four distinctive regions of the Indian Ocean. The averages are also grouped by two height ranges, 0 to 50m and 50m to 100m.

In the case of the sensible heat flux for the 0 to 50m height range, it is seen that all heat fluxes are directed upwards. There are minor variations between the groups. The flux is greatest near the west coast of India and least in the equatorial region. Other differences are small and probably represent sampling variations. In the 50m to 500m layer, the fluxes are all downward and show the same small regional and sampling variations.

The averages of the latent heat fluxes are all positive with regional and height range variations in magnitude. Near the western coast of India the fluxes are greatest in the lower level with a large drop at the higher level reflecting the suppression of transport by the temperature inversion. Over other regions of the Arabian Sea and along the equator the fluxes are less. They are maintained throughout a greater height range since the inversion is weaker or broken in these regions. The maintainance of high flux rates along the air trajectory is very significant in that it ensures that large amounts of water vapor are fed into the equatorial convergence zone.

The five turbulence records made at 4375m on 20 February 1964 describe the conditions near and in an active equatorial convergence zone. The first two runs were made west of the area where the cumulus activity was greatest. Only small cumulus and a few octas of cirrus were present. The records show that the air was smooth, the variations of temperature and humidity were small, and the fluxes of sensible and latent heat were all less than 0.06 mcal $cm^{-2}sec^{-1}$. The next two runs were made within a stratus cloud probably formed by the spreading out of cumulus towers. Here, the turbulence, the temperature and humidity variations, and the fluxes were all greatly increased. The fifth run was made through an active cumulonimbus tower. In the tower the σ_w exceeded 100 cm sec^{-1}, the temperature and humidity fluctuations were large, and the sensible and latent heat fluxes were -.42 and 2.70 mcal cm^{-2} sec^{-1} respectively.

The values of shearing stress, $-\overline{\rho w' u'}(\cos\phi)^{-1}$ are presented in Figure 9. These values must be interpreted with caution as described in Section I. Averages were formed from only those measurements made while the aircraft was flying upwind. The average stress in the air under the inversion is seen to be about 0.7 dynes cm^{-2}. This value is higher than would be computed using the equation:

$$\tau = C_D \rho u^2 \qquad (6)$$

Using a drag coefficient, C_D, of 0.001 and a mean speed in the layer of 5m sec^{-1}, τ=0.4 dynes cm^{-1}. Thus, the stresses determined by the covariance method appear to be too high by a factor of nearly 2.

B. Southwest Monsoon Season

1. Meteorological Background

The most pronounced and important feature of Indian weather is the south-

TABLE E

Averages of Sensible and Latent Heat Fluxes during the Northeast Monsoon

Area	Sensible Heat Flux		Latent Heat Flux	
	0 to 50m	50m to 500 m	0 to 50m	50m to 500m
	mcal cm^{-2} sec^{-1}			
All regions	+.10	-.21	3.08	2.01
0-100 km offshore	+.14	-.27	4.02	1.07
100-200 km offshore	+.08	-.15	4.39	1.80
Arabian Sea	+.11	-.23	1.45	5.03
Equatorial Region	+.04	-.14	2.64	2.39

west monsoon that blows continuously from June through September despositing large amounts of rain upon the land. Typical surface and 700 millibar streamline charts are presented in Figure 10. The surface chart shows the broad flow of air northward across the equator and northeastward across the Arabian Sea onto the Indian peninsula. The strength of the winds is indicated by isovels (dashed lines) for each 10 knots. The 700 mb chart shows the same general flow pattern. Above about 500 mbs, depending on the geographical position, the wind reverses and blows from the east.

The air-sea interactions are different over the eastern and western parts of the Arabian Sea. Off the coast of Somalia the stress of the wind transports the surface water to the east and cold water rises from below to replace the warm surface water. The body of cold water in the west cools the lower levels of the atmosphere. As the air leaves the region of cold water, it receives heat from the warmer water to the east. Thus the western region is characterized by strong localized cooling and heating while the eastern region is more homogeneous. The two sections are analysed separately with the 65 E meridian used as the separation line.

2. Average Meteorological Conditions Over the Eastern Arabian Sea

Averages of the potential temperature, mixing ratio, and wind speed have been found for many height ranges and presented in Figure 11. In the lowest 150 meters the air averages out to be exactly neutrally stable. The individual aircraft soundings show several very slight positive and negative vertical gradients of the potential temperature. These gradients are so small that they are within the error range of the dynamic temperature corrections, and it cannot be stated definitely that they are real. The air is slightly stable from 150m to the 500m level and more stable above 500m. The mixing ratio has a negative gradient at all levels. The average wind speed increases with height to the 1100 meter level and then varies irregularly. The wind profiles shown in Figure 18 should be studied to see the large variations of the wind speed with height and geographical location. In view of these large variations, the average wind speed curve is seen to have limited usefulness.

The cloud cover increases from west to east over the Arabian Sea. At 60 E there is an average of 3 octas of cumulus clouds with an average height of 1600 m. Near the coast of India, there are 4 octas of cumulus and cumulus congestus with a height of 2400 meters. Cumulonimbus clouds near the coast of India reach an average height of 8200 meters. Only a few isolated showers were observed near 60 E while near India frequent heavy showers were encountered.

3. Fluctuation Statistics Over the Eastern Arabian Sea

The turbulence statistics obtained over the eastern Arabian Sea between 9 August and 9 September 1964 are presented in Table F. During this month of observing, the monsoon was slowly diminishing in strength and the breaks in the shower activity became more frequent and of longer duration. The "retreat" of the monsoon began during the last week of September.

TABLE F

Turbulence, Fluctuation, and Flux Statistics Over the Arabian Sea East of 65° E

Height m	No.	σ_w cm sec^{-1}	σ_u cm sec^{-1}	σ_T °C	σ_q 2gm m^{-3}	$c_p\rho\overline{w'T'}$ mcal cm^{-2} sec^{-1}	L $\overline{w'q'}$ mcal cm^{-2} sec^{-1}	$-\rho\overline{w'u'}(\cos)^{-1}$ dy cm^{-2}	No.
25	16	41	49	.08	.28	-.06	2.26	1.9	3
75	6	45	60	.08	.19	+.12	+.70	3.1	1
150	21	45	47	.06	.19	.04	1.16	1.5	4
250	4	42	40	.09	.37	-.17	2.77	1.1	2
400	53	37	41	.10	.28	-.04	.48	0.3	23
625	37	38	47	.11	.27	.00	.18	0.6	2
875	2	29	39	.05	.47	-.03	.20	-	0
2500	15	58	35	.12	.33	.02	-.14	0.2	1
3750	9	29	26	.05	.18	-.03	-.20	0.1	3

The respective columns give the height, number of observations, averages of the vertical and horizontal root-mean-square turbulent velocities, the temperature and specific humidity fluctuations, the sensible and latent heat transports and the shearing stress. The last column gives the number of observations used in obtaining the averages of the shearing stress. Only stresses obtained while the aircraft was flying upwind were used for the averages.

The height variation of the root-mean-square values of the vertical and horizontal turbulent velocities, the temperature fluctuations, and the specific humidity fluctuations are presented in Figures 12 and 13. The vertical velocities, σ_w have values in the 40's in the lowest layers where the air is neutrally stable and the turbulence is generated solely by the mechanics of the flow of air over the water surface. Higher in the atmosphere the air is stable and the turbulence is damped. A high value of 58 cm sec^{-1} was observed in the 2000 to 3000 meter layer. Here many observations were made penetrating cumulus clouds. A maximum σ_w of 174 cm sec^{-1} was observed on one run through cumulus clouds. If penetrative runs and non-penetrative runs are grouped separately and averaged, it is found that 85 cm sec^{-1} is the average for cloud runs and 30 cm sec^{-1} is the average for runs outside of cumulus clouds.

The root-mean-square values of the horizontal turbulance, σ_u, are greater than the values of σ_w at the lower levels of the atmosphere and less than σ_w at the higher levels. In the case of the traverses through the cumulus clouds, the average σ_u is only 33 cm sec^{-1}. The large excess of vertical turbulence over horizontal turbulence undoubtedly occurs since the buoyancy of the clouds is the generating force of the turbulence and the vertical wind shear is not very great.

Figure 13 presents the fluctuation values of temperature and mixing ratio. None of the values are very high as might be expected from the small gradients. The σ_q's observed in the cloud traverses are surprisingly low. No study of this question has been made but it is supposed that the values result from rather thorough mixing of environmental air entrained into the clouds.

4. Turbulent Transports Over the Eastern Arabian Sea

The average values of the sensible and latent heat fluxes for several height ranges are presented in Figure 14. The sensible heat fluxes are all rather small with a zero average in the lowest 300m, and a -0.01 mcal cm^{-2} sec^{-1} average for the entire layer to 4500m. Thus, the exchange of sensible heat between the ocean and the atmosphere over the eastern Arabian Sea has little, if any, effect upon the monsoon circulation.

The occurrence of positive sensible heat fluxes between 50 and 200 meters can be traced to observations made south of about 15 N. In this region, the westerly wind frequently has a component from the north. When this occurs, the air moves toward water that is a few tenths of a degree warmer. See Miller and Jefferies (1967). This slight difference in temperature may be sufficient to cause an upward flow of sensible heat in the lowest layers. Twenty-four runs were made in this region with northwest winds. The average upward flux of these runs was 0.13 mcal cm^{-2} sec^{-1}. The average sensible heat flux averaged over the eastern Arabian Sea between 0 and 200 meters, exclusive of these 24 runs, was -0.13 mcal cm^{-2} sec^{-1}.

In the cloud layer, the sensible heat flux is positive with average of 0.02 mcal cm^{-2} sec^{-1}. This average does not arise from a consistent upward flux of heat by the clouds and a downward transport of heat by the environmental air. Rather, both the clouds and the environmental air show large individual positive and negative fluxes. In the clouds, the fluxes range from +0.69 to -0.44 mcal cm^{-2} sec^{-1}. One should not attempt to interpret these data without considering the spectral limitations of the measuring system. It was pointed out earlier that only one minute runs were reduced, and contributions by gusts greater than about 2.4 km are lost. Thus, a significant amount of heat and water vapor may be transported in the cloud layer by larger scales of motion.

The latent heat fluxes are much larger at all levels than the sensible heat fluxes, and have a significant influence on the monsoon circulation and weather which will be discussed later. The fluxes are high at the lowest level, averaging 1.6 mcal cm^{-2} sec^{-1} below 300 m, decrease rapidly above the 300m level, and become negative above 2000m. One characteristic of the latent heat flux determination is the wide range of the individual values. In the lowest 300 meters of air over the eastern Arabian Sea, the 47 individual measurements range between +8.3 and -0.41 mcal cm^{-2} sec^{-1}. The question arises as to whether this variation is an intrinsic characteristic of water vapor flux through the atmosphere or merely the result of an unstable, noisy measuring system. It was pointed out earlier that the mean of the measured fluxes were 20 to 25% smaller than the mean measured by other groups using different techniques. Such agreement is consistent with the restricted spectral range that the system can measure and the probable error, $\pm$ 0.18 mcal cm^{-2} sec^{-1}, of the mean $L\overline{w'q'}$ for the 47 observations in the lowest 300 meters.

The individual 1/5 second values of the vertical velocity and the specific humidity, which are printed out by the computer, have been scanned carefully for clues to the source of the variation. Runs with extreme values of $L\overline{w'q'}$ were inspected for reading or instrumental errors. Only a few minor errors were detected and corrected. After correction and recomputation, it was found that the values of $L\overline{w'q'}$ were changed by only a small percentage of the original values, and the large deviations remained. Suspiciously large deviations of the specific humidity were checked against the aircraft psychrograph record. In cases where the deviations lasted for more than a few seconds, the slower recording psychrograph confirmed the existence and magnitude of the deviations.

If the specific humidity variations are correct, and if there is any error, then it must lie in the vertical velocity amplitudes or correlation with the humidity fluctuations. A check of the records shows that the values of σ_w are only slightly greater than normal in the cases of runs with extremes of $L\overline{w'q'}$. Therefore, if an error is present, it must be associated with the phasing of the vertical velocities with the humidity variations. The nature of this phasing error would be such as to sometimes greatly increase the correlation coefficient between w' and q', and at other times make it go negative. If the vertical velocities were erroneously phased in some manner, then it would be expected that the sensible heat

fluxes would be similarly modified. A plot of all the values of $L\overline{w'q'}$ versus $c_p\rho\overline{w'T'}$ over the entire Arabian Sea for the 0 to 300 m height range shows that the downward flux of sensible heat is greater for the extremes of $L\overline{w'q'}$ regardless of whether the $L\overline{w'q'}$ values are positive or negative. Thus, an erroneous phasing is ruled out as a source of the variation. Further, inspection of the print-outs of the fluctuation data shows that most of the latent heat flux is transported by gusts of several seconds duration. Phasing errors would be smaller for these large gusts than for the smaller gusts of a few tenths of a second duration. Therefore, it is concluded that no erroneous phasing occurred and that the observed extremes are true variations of the flux through the atmosphere within the spectral range of the system.

The individual fluctuations of w' and q' for Run 4650, the run with the greatest flux, were inspected for a clue to the manner in which the large variations are produced. It was found that most of the water vapor was transported by three clear-cut upward gusts with high humidity and one downward gust of dry air. These four gusts totaled 27% of the time but accounted for 92% of the water vapor flux. Other runs with large fluxes have a few strong gusts that carry most of the heat and water vapor. Thus, the variation appears to be a sampling problem related to the size, number, and strength of the gusts.

Another factor that should not be overlooked is the local and short period variations of the humidity and temperature vertical gradients. In a turbulent atmosphere, the instantaneous gradient is rarely the same as the mean gradient, and may have the opposite sense for short periods of time. This was demonstrated by the three-aircraft traverses through the trade winds east of the Bahama Islands (Bunker, 1962). These flights also showed that an excess of water vapor frequently occurred at the top of the friction layer. All of these factors would contribute to large variations of fluxes measured over short periods of time or distance.

The latent heat fluxes in the 2 to 3 kilometer height range, where several cumulus clouds were penetrated, have an average of -0.14 mcal cm^{-2} sec^{-1}. When the runs are separated into runs that penetrated cumulus clouds, and those that did not, and averaged, it is found that the average of the penetrative runs is +0.40 mcal cm^{-2} sec^{-1}, while the non-penetrative runs averaged -0.50. The individual fluxes for the penetrative group ranged from -6.2 to +3.6 mcal $cm^{-2}sec^{-1}$. The non-penetrative group had values ranging from -2.9 to +1.3 mcal cm^{-2} sec^{-1}.

The spectral limitations of the system are particularly obvious in the cloud layer since a considerable portion of the vertical transport of heat, water vapor and momentum quite obviously is carried by long-period convective motions. Thus, there must be a large component of flux that the system fails to record.

On 22 August, 1964 when the majority of the cloud runs were made, one engine of the aircraft developed magneto trouble. As a result, it was decided to go around one particularly large, active cumulus cloud that lay on the straight-line course of the aircraft. Omission of this cloud biases the statistics of the clouds discussed in the next section. For what little it is worth, the author estimated that the $\overline{\tau w}$ in the cloud might have been

250 $\pm$ 50 cm sec^{-1}. The latent heat flux must have been very large, since it appeared to be a young, growing cloud.

The shearing stresses measured while the aircraft was flying upwind averaged 1.9 dynes cm^{-2} in the lowest 200 meters of the atmosphere. This average is based on only 8 measurements. By comparison, the stress computed from a drag coefficient of 0.0015 and the square of the average wind speed is 0.9 dynes cm^{-2}. Above the 300 meter level, the value of the stress decreases rapidly to a few tenths of a dyne cm^{-2}.

5. Meteorological Conditions Over the Western Arabian Sea

The western Arabian Sea is a region of strong contrasts, and great air-sea interaction which has profound effects upon both the atmosphere and the sea. The most outstanding interaction sequence in the area is (a) the build-up of an atmospheric shearing stress on the water as the southwest monsoon develops, (b) the offshore movement of the surface water under the influence of the stress, (c) the replacement of the surface water by cold upwelling water, (d) the cooling of the air by the cold water, (e) the development of a strong thermal wind jet as a result of the cooling of the air, and (f) low level convergence of the air in the eastern Arabian Sea as the thermal wind jet breaks down. The different aspects of these processes have been the subject of many recent papers. See Bunker (1965), Warren, et. al. (1966), Swallow and Bruce (1966), and Colón (1964).

Instead of presenting averages of temperature and humidity in this heterogeneous region, a potential temperature cross-section, two dropsonde records and several wind profiles are presented to demonstrate the meteorological conditions. Figure 16 is the cross-section constructed from 5 dropsonde records and the aircraft ascent and descent. The cross-section is roughly perpendicular to the wind. See Figures 1 and 10. The aircraft track did not pass over the coldest portion of the upwelling water which is closer to the Somali coast. The effect of the cold water upon the air temperature is very apparent. Figure 17 shows the temperature and mixing ratio distributions in the region of the coolest air measured and in the region about 250 kilometers to the southeast. In addition to the intense cooling of the air, it should be noted from the record of the 1030 GMT dropsonde that the air had lost considerable water vapor. It is presumed that the water vapor condensed directly on the surface of the cold water which had a temperature of only 14C nearer the shore.

To show the winds which vary greatly in speed with height and location over the Arabian Sea, 8 profiles are presented in Figure 18. The strong jet off the Coast of Somalia and its slow dissolution to the east is clearly shown. South and north of the main jet region, the profiles show irregular height variations and moderate speeds.

6. Fluctuation Statistics Over the Western Arabian Sea

The averages of the fluctuation and flux values over the western Arabian Sea have been collected in Table G. The parameters and their arrangement are the same as for Table F. Figure 19 presents a plot against height of the of the values $\overline{\sigma w}$ and $\overline{\sigma u}$. The values of $\overline{\sigma u}$ are generally in the 50's and reach an average of 62 cm sec^{-1} in the 300 to 500 meter height range. These values are greater than those observed over the eastern Arabian Sea and

TABLE G

Turbulence, Fluctuation, and Flux Statistics Over the Arabian Sea West of 65 E

Height m	No.	σ_w cm sec^{-1}	σ_u cm sec^{-1}	σ_T °C	σ_q gm m^{-3}	$c_p\rho\overline{w'T'}$ mcal cm^{-2} sec^{-1}	$L\overline{w'q'}$ mcal cm^{-2} sec^{-1}	$-\rho\overline{w'u'}(\cos\phi)^{-1}$ dynes cm^{-2}	No.
25	4	56	88	.08	.31	-.22	-.97	2.9	4
75	5	57	84	.08	.35	-.32	-.80	3.9	1
150	9	42	56	.06	.22	-.08	.68	1.2	5
250	10	50	67	.07	.18	-.01	.20	1.4	1
400	12	62	79	.11	.30	-.06	.03	4.3	3
625	24	56	68	.13	.23	-.04	.22	-	-
3750	6	23	22	.05	.14	.00	.20	0.3	2

show a different variation with height. The higher values in the 300 to 750m height range is attributed to the existence of large wind shears associated with the high velocity jet at 1 kilometer. The difference in variation of the turbulence with height between this case and other cases representing different turbulent processes is shown in Figure 5. On this diagram, the variation between individual runs at a given height within the Somalia Jet, is indicated by a bar. The steady increase in turbulence to the 545 meter level is seen to be quite different from the other observed cases. The observations of 14 January 1955 were made under conditions of great instability in the lower layers and strong winds. The trade wind averages are characteristic of weaker winds, and nearly neutral stability.

The values of $\overline{\sigma u}$ are 38% greater than the average of $\overline{\sigma w}$. This excess is believed to be associated with the high wind velocities and wind shears. During the northeast monsoon and over the eastern Arabian Sea during the southwest monsoon, the wind speeds and shears are more moderate and the excess of $\overline{\sigma u}$ over $\overline{\sigma w}$ amounts to about 16%.

Figure 20 presents the plot of $\overline{\sigma T}$ and $\overline{\sigma q}$ versus the height. These curves show rather small random variations with height. The magnitudes are nearly the same as those observed over the eastern section of the Arabian Sea.

Both the sensible and latent heat fluxes are directed downward below the 100 meter level as shown by the tabulated values and Figure 21. Above the 100 meter level, the latent heat fluxes become positive while the sensible heat flux remains downward. The downward flow of sensible heat is the direct result of warm subsiding air flowing over the cold upwelling water off Somalia. The pair of dropsonde records presented in Figure 17 shows the large amount of heat that has been exchanged between the air and the sea water. A rough calculation of heat transfer from the lowest 400 meters of the atmosphere to the ocean shows that about 50 calories are lost in about 2×10^4 seconds. Hence the sensible heat flux is about 2.5 mcal cm^{-2} sec^{-1}. This value is about ten times as high as the value observed by the aircraft covarience method. The difference is not too surprising, since the aircraft values were not measured over the coldest water which is found close to the shoreline.

The downward flux of water vapor in the lowest layers is an indication that the cold upwelling water acts as a sink rather than a source of water vapor. As the air leaves the coast of Somalia, it has a dewpoint of about 20C, although the relative humidity is fairly low. When this air encounters the 12C upwelling water, the water vapor condenses on the water surface. A positive gradient of mixing ratio is quickly established and a negative flux of water vapor results. At higher levels, the atmosphere apparently is not influenced by the cold water, and the mixing ratio gradient remains negative. The depletion of water vapor from the atmosphere is shown in Figure 17 by the mixing ratio curve of the 1130 GMT dropsonde at 11 N, 52.3 E.

The shearing stresses in the region off Somalia are of the greatest meteorological interest. It is regretted deeply that more confidence cannot be placed in the measured values, and that the many crosswind and tailwind values cannot be used. The fourteen values measured while flying upwind show that much higher values of the stress occur in this region of the Arabian Sea than in other regions. The average for the 0 to 500 m layer is 2.6 dynes cm^{-2}. None of these runs were made in the level where the winds were strongest. The height variation of the stress, Figure 22, shows that the

stress continues to increase up to the 500 m level. This increase is in contrast to the curve for the eastern Arabian Sea, Figure 15, which decreases to 0.3 dynes cm^{-2} in the 300 to 500 m layer. The high value in this layer over the western part is believed to be associated with the high velocity jet and the strong velocity gradients.

7. Regional Variations of the Turbulence and Fluxes over the Arabian Sea During the Southwest Monsoon

Averages have been formed and plotted by 5 degree squares of the values observed in the lowest 475 meters of the atmosphere during the southwest monsoon. In the case of two squares, the 50-55 E, 10-20 N square and the 55-60 E, 5 N-10 N square, no observations were made below 475 meters, so averages of values in the 500 to 600 meter range were included on the charts.

The first set of averages, presented in Figure 23, gives the distribution of the vertical component of the turbulent velocity. A region of maximum turbulence extends northeast across the Arabian Sea from the coast of Somalia to the coast of Northwest India. This band of turbulent air coincides roughly with the axis of the velocity maximum of the monsoon winds. Presumably, the excess turbulence is associated with the higher wind speeds, since the stability of the air is slightly greater within this band.

The second chart, Figure 24, shows the distribution of the sensible heat flux over the Arabian Sea. In the west over the cold upwelling water, the heat fluxes are directed downward as might be predicted. Between 55 and 60 E the heat flux is directed upward. This upward flow of heat must be associated with the readjustment of the cooled air to the warmer water of the Arabian Sea. The aircraft psychrograph records showed that the air was still stable in this region above 100m, but an unstable lapse rate may have existed below 100 meters, the lowest level to which the aircraft descended.

East of 60 E, the heat fluxes are directed downward again. Exceptions to this generalization are the regions south of 15 N along the coast of India. These positive fluxes have been noted earlier, and related to the flow of air from the northwest to areas where the water was a few tenths of a degree warmer.

The distribution of the latent heat flux over the Arabian Sea is presented in Figure 25. Over the western part of the sea, the latent heat flux is small or negative, while east of 65 E, all of the averages are positive. The negative values near the coast of Somalia are consistent with the decrease in mixing ratio observed by the dropsonde and the aircraft psychrograph. Between 60 and 65 E, negative values were also observed. These values are inconsistent with the mixing ratio gradients observed by the aircraft, and the latent heat fluxes computed by Suryanarayana and Sikka (1965) of the International Meteorological Centre at Bombay from ship reports. Since 14 runs were made in this area, it is hard to explain the negative values as sampling error. Of the 14 runs, 7 yielded small positive values, while the other 7 gave larger negative values. The records have been searched for errors, but the few that were found did not change the results significantly. The microwave refractometer used to measure the humidity variations showed high frequency variations of

large magnitude on the two days that the aircraft was observing in the 60 to 65 region. Several records were reread after drawing a smooth line through the high frequency variations. Computation using these smoothed values gave negative fluxes, with essentially the same magnitude. Thus it is concluded that the negative fluxes are real.

If one accepts the negative fluxes as real, then the question arises as to why the moisture flux was downward in this region on these two days. The streamline charts indicate a normal southwest flow of air with no unusual features. Similarly the aircraft psychrograph shows a normal horizontal and vertical distribution of the humidity and temperature. Inspection of the computer print-outs of the individual fluctuations shows how the negative fluxes were produced. In all of the runs with negative fluxes, several sustained updrafts of dry air and sustained downdrafts of moist air were observed. Such a distribution of vertical velocity and moisture could come about by a local, temporary layering of moist air above drier air.

Vertical gradients of dewpoint temperatures were measured hourly by R. Stanley from the R/V Atlantis II in August and September 1963, using a dewpoint hygrometer. It was found that in the region between 15 and 20 N and 55 and 65 E, positive gradients of dewpoint temperatures were observed 25% of the time. The average dewpoint temperature difference between 5m above the sea to 23m was -0.4C for the 60 to 65 E region, and -0.7C between 55 and 60 E. The average of the positive gradients between 60 and 65 E was +0.4C per 18m. The greatest positive gradient observed was +1.6C per 18m. The hourly observations preceding and following this large positive gradient were both negative gradients.

Most of the positive gradients were observed as single occurrences, but one case of 4 consecutive positive gradients and 2 cases of 3 consecutive positive gradients were observed. Thus it is seen that reversals of the normal water vapor gradient occur in the lowest 23 meters above the sea in this area.

The water temperature in the area varied from 27C near 65 E to 25C near 60 E. The dewpoint temperatures at the 5 meter level averaged about 24C. Therefore, there must have been a negative water vapor gradient in the lowest 5 meters. This layer of negative gradient is overlain by a layer which normally has a negative gradient but which frequently has its gradient reversed by invasions of drier air. These intrusions of drier air must be moistened rapidly until the normal gradient is restored. At some later time the moist air is displaced by another intrusion of dry air. This sequence of intrusion, moistening, and displacement is the equivalent of a large-scale upward transport process of water vapor. It appears, then, that the aircraft flux system is measuring the small-scale moistening of the dry air intrusions by the moist air aloft. Most of the moistening of the dry air is probably accomplished by the small-scale turbulent transport operating in the lowest 5 meters. The major upward transport above the 5 meter level is achieved by large-scale, intermittent processes. When this is realized, it is seen that no discrepancies exist between the aircraft measurements, the fluxes computed from the ship reports, and the Atlantis II gradients.

It is clear from this discussion that the aircraft system cannot yield reliable values of the evaporation from the sea surface under conditions where

large-scale reversals of the water vapor gradient occur at low levels. The aircraft system in conjunction with gradient measurements from ships does help to give a more complete picture of the processes operating in these unusual areas.

The shearing stresses observed while the aircraft was flying upwind are presented in Figure 26. Unfortunately, no values were recorded west of 60 E where the Somali jet occurs. Between 60 and 65 E where the jet is still strong the stress averages 2.5 dynes cm^{-2}. East of 65 E, the stress decreases to a little over 1 dyne cm^{-2}. This decrease is consistent with the decrease in the wind speed near the Indian coast.

IV Significance of Turbulent Fluxes in Relation to the Monsoon Circulations and Weather

One of the aims of the International Indian Ocean Expedition was to observe the interactions between the ocean and the atmosphere and to evaluate the degree to which one medium influences the circulation of the other. The oceanographers have made extensive measurements of the currents and the physical and chemical properties of the Indian Ocean which show the influence of the atmosphere upon the ocean. The present body of heat, water vapor and momentum fluxes are now examined to determine the influence of the ocean upon the two monsoon circulations and weather.

1. Relation Between the Northeast Monsoon and the Turbulent Fluxes

The winds of the northwest monsoon are moderate in strength and exert a shearing stress of less than 1 dyne cm^{-2} on the waters of the Arabian Sea. This stress, in combination with thermo-haline forces, causes a weak, irregular flow of surface water to the south and west. See Wooster, Schaefer, and Robinson (1967). In the northern Arabian Sea, the currents are weakest and most irregular with many northwest currents observed. No regions of upwelling are indicated by the temperature charts, but surface nutrient charts suggest weak upwelling along the east and north shores of the Arabian Sea.

The turbulent flux measurements show that in the lowest 50 meters of the atmosphere, sensible heat is being transported from the sea to the air at a rate of 0.1 mcal cm^{-2} sec^{-1}. Above the 50 meter level, heat is transported downward from the warm subsiding air aloft at a nearly equal rate. During the air's trajectory from 20 N to the equator, the air accumulates about 30 calories. If this heat is distributed throughout the lower equatorial air to the 300 mb level, the air temperature would be increased by only about 0.1 C. Since it is primarily the temperature gradient between the equator and the subarctic regions that drives the monsoon circulation, it is seen that the flux of sensible heat contributes a negligible amount of energy to the monsoon circulation. The small amount of heat added to the lower layer may have a slight effect by maintaining the turbulence at a greater level and thus increasing the flux of water vapor.

The latent heat flux was seen to average about 3 mcal cm^{-2} sec^{-1} over the Arabian Sea. This latent heat is accumulated in the atmosphere and released in the convergence region in the vicinity of the equator. About 900 calories are accumulated as the air flows from 20 N to the equator. If this heat is released throughout the layer from the surface to 300 mbs, the air will be

heated about 5 C. Comparison with the University of Washington water vapor fluxes showed that the aircraft turbulent flux system yielded fluxes that were about 25% too low. If a correction is made for this deficiency, then the contribution of evaporated Arabian Sea water to the heating of the equatorial air is between 6 and 7 C. Such a heating is an appreciable contribution to the energy that drives the monsoon circulation.

The turbulent exchange of energy between sea and air has two minor contributions to the weather of India and the Arabian Sea in addition to the contribution to the driving force of the monsoon circulation. The accumulation of water vapor in the lower layer of the atmosphere over the Arabian Sea eventually produces cumulus clouds. These clouds are able to form only after the air under the temperature inversion becomes saturated. Generally, a trajectory of 2 to 300 kilometers over the water is required before cumulus are formed. Clouds appear near the coast of southern India since the air frequently moves from the northwest over this part of the Arabian Sea. A complete description of these clouds is given by Bunker and Chaffee (1968).

A very strong, extensive sea- and land-breeze is set up along the west coast of India by the heating of the land by the sun. The details of the strength and extent of this system has been described by Nicholson (1965). While the sea-breeze system is an interesting phenomenon because of its great extent, it has only a minor effect upon the monsoon circulation through increasing the turbulence and modifying the gradients along the coast.

2. Relation between the Southwest Monsoon and the Turbulent Fluxes

The stress of the southwest monsoon winds produces currents in the Arabian Sea which set off a chain of events that has a great influence upon the distribution of wind strength and weather over the Arabian Sea and India. The monthly surface currents charts presented by Wooster et. al., (1967) show the rapid development of the Somali current and the circulation of water over the Arabian Sea. The off-shore component of the Somali current produces strong upwelling of cold water near the coast. Wooster's maps show the first appearance of cold water in May and minimum temperatures in August. The detailed charts presented by Warren, Stommel, and Swallow (1966) show that water with a temperature of only 14C appears off the coast near Ras Mabber (9 N).

The cold water cools the air rapidly. Estimates based on the dropsondes show that the heat exchange is about 2.5 mcal cm^{-2} sec^{-1} in a limited region over the coldest water. This value is about 10 times the average over the Arabian Sea.

About 200 kilometers offshore a band of cool air is formed which extends about 400 to 500 kilometers in the crosswind direction. See Figure 16. This band of cool air produced a thermal wind jet as shown in Figure 18. Downwind of the localized cold water, the air is reheated by both the warmer sea water and the warmer air aloft. As the air is warmed the thermal winds diminish and the jet disappears over the Eastern Arabian Sea as shown in Figure 18. The slackening of the winds contributes to the convergence of air measured over the eastern Arabian Sea by Miller and Keshavamurthy (1968). This low-level convergence in turn lifts the surface air, thereby partially releasing the latent instability of the air. Cumulus clouds and showers are produced and the water vapor of the lower air is distributed throughout a thicker layer of air. When the monsoon air finally reaches India, it is moist to 3 or 4 km. The lifting of the air by the mountains releases the instability of the air, and cumulonimbus clouds can rise to greater heights because of the pre-moistened environmental air. Thus greater cloudiness and shower activity over the eastern Arabian Sea and a greater intensity of rainfall over the mountains can be traced to the shearing stress of the air on the water.

Pisharoty (1965) has shown that the transport of water vapor across the equator into the Arabian Sea area is about one third the transport of water vapor across the west coast of India. The difference in transport is made up by evaporation from the sea. This flux divergence corresponds to roughly 0.3 gm cm^{-2} day^{-1} evaporation. This value agrees well with the fluxes computed by Suryamaryna and Sikka (1965) from ship observations and with the fluxes presented in this report for the eastern Arabian Sea. Thus it is seen that the intensity of rainfall over India is very dependent upon the evaporation over the Arabian Sea.

V Remarks on Special Phenomena Observed Over the Indian Ocean

A. Cloud Lines Off the Indian West Coast

In the course of extended observational programs, interesting phenomena are occasionally observed in certain regions which result from the combination of several independent processes. Such phenomena may have little significance from the point of view of large-scale circulations and air-sea interactions but they may be very instructive and give greater insight into many small-scale or regional processes of the atmosphere.

One example of such phenomena is the cloud lines formed downwind of the mountains of India during the northeast monsoon and described by Bunker (1967). It was shown that winds blowing from the east through the mountain valleys produced lines of cumulus clouds and greatly increased the turbulence. In the article, it was not pertinent to the argument to mention that large values of the shearing stress were observed. From Table C it is seen that on 19 February 1964 when the aircraft penetrated a cloud line perpendicular to the coast, the shearing stresses increased from a few tenths of a dyne cm^{-2} to a maximum of 13.5 dynes cm^{-2}. Such a large transfer of momentum can arise only from the rather violent uplift of high velocity air and downdrafts of low velocity air. This observation of a large, local transfer of momentum may be insignificant in terms of the momentum balance between the atmosphere and the earth, but it is of value to know that such stresses can occur between local wind systems.

It is noted also that the fluxes of sensible and latent heat attained large positive and negative values in this region of easterly winds. These values are not interpreted as true values of the turbulent flux, but rather as indications of localized overturning of the air. To explain these transports, one would have to resort to a specific vertical distribution of humidity and temperature in conjunction with a particular vertical velocity distribution. Such a description would be of little value except for explaining the present case. However, the fact that large extremes of fluxes can occur in regions of horizontal wind shears and cumulus clouds gives insight into the processes operating in atmosphere and aids in the interpretation of extremes observed elsewhere.

B. Crosswind Variations of the Southwest Monsoon Air

On 22 August 1964 a crosswind flight was made from Bombay to 5.5 N, 76.2 E about 100 km offshore. Thirty-three turbulence runs were made below 500 meters

and 11 runs were made between 2065 and 2085 meters, several of which were through cumulus clouds. The surface streamlines showed a broad steady flow of air from the southwest with a weak 20 knot maximum extending from Somalia across the Arabian Sea, India, the Bay of Bengal and into Burma. No vortices were present over the Arabian Sea or western India. Shower activity was generally confined to north of 12 N. Numerous cumulus rose to 4 km with one observed at 5 N rising to 10 km.

To show the relation of the turbulent fluctuations and latent heat fluxes to the larger scale variations of the monsoon air, plots of potential temperature and mixing ratio against latitude are presented in Figures 27 and 28. The potential temperatures and mixing ratios were computed from the output of the recording psychrometer. For the first 5 degrees of latitude of the low-level outbound leg of the flight, values were computed for each 20 seconds. The rest of the values were read and computed each 5 minutes. The numbers printed on the temperature trace of Figure 27 give the altitude of the aircraft. All other altitudes on the figure were 500 meters. Above the temperatures and humidities the values of σ_w , σ_q and $L\overline{w'q'}$ taken from Table C are plotted. The bars under these quantities indicate the distance over which the turbulence runs extended.

The most noticeable characteristic of the psychrometric traces is the wide range of values through which they fluctuate. Further, it is seen that they fluctuate with a wide range of frequencies or wavelengths. The distance between the individual 20 second points is about 1.5 kilometers. There is considerable variation between adjacent points. Larger scales of variation show much greater amplitude, such as those at 17.4 n and 14.5 N. Notes written on the psychrograph strip chart show that many of these large variations are associated with showers and cumulus activity. The cool, moist disturbance at 17.4 N preceded a shower with low scud clouds. At 16.4 N the aircraft was in a relatively clear area and approaching a wall of cumulus clouds. Here the mixing ratio shows considerable point-to-point variation and the increased value of σ_q shows that the variation extended into the higher frequency range. During the approach to the cloud wall, and during its penetration, the latent heat fluxes became strongly negative. It is believed that these negative fluxes are an indication of subsiding moist air ejected in some manner from the wall of cumulus clouds.

Figure 28 presents the psychrograph and turbulence data obtained during the return leg of the flight at 2075 meters. Temperatures and humidities were read from the trace each 5 minutes. These points show large variations with the largest variations associated with the penetration of cumulus clouds. As mentioned earlier, the largest cumulus cloud was avoided. A feature that did not appear in the low-level flight data, but which is very conspicuous in this higher level flight is the increase of mixing ratio with latitude and the decrease of potential temperature with latitude. Since showers were occurring over the northern section of the flight path, the cooling and moistening of the air were produced both by a general convergence and uplift of the air and by the action of the cumulus clouds.

The turbulence and fluctuation parameters show large variations along the flight path. The smooth runs with small variations and fluxes were in the clear regions between the cumulus clouds. The turbulent runs at 12 N were made while penetrating an active cumulonimbus cloud. The highest value of σ_w, 174 cm sec^{-1}, observed during the Indian Ocean observations, was made within

this cumulonimbus cloud. Positive latent heat fluxes of 3.6 and 2.7 mcal cm^{-2} sec^{-1} were observed in adjacent sections of this active cloud. The observations at 12.6 N were made within a wall of cumulus clouds similar to the wall observed on the outbound leg at 16.4 N. Here again, large negative values of the water vapor flux were observed, suggesting that moist parcels were subsiding out of the cumulus clouds.

C. Kinetic Energy Flux and Dissipation

At a late stage in the reduction of the turbulence data, it was decided to determine the kinetic energy budget of the monsoon wind systems. Consequently, the computer program was changed to include the transport of the turbulent kinetic energy by the turbulent gusts. This was done by forming the average value of the individual values of $\frac{1}{2}\rho(K.E.)'w'$, where $(K.E.)'$ was defined as $3/2(u'^2 + w'^2)$. The factor of 3/2 was used to account for the lateral turbulent component which was not measured. The flux of kinetic energy was computed for about half of the runs.

The dissipation of the energy, ϵ, was computed from the production and flux since the spectral range of the turbulent measurements does not extend into the inertial subrange. The equation used for the computation is:

$$\epsilon = u^{*2}\frac{\partial u}{\partial z} + \frac{gH}{c_p \rho T} - \frac{\partial \overline{e'w'}}{\partial z} \qquad (7)$$

Where u* is the friction velocity, $\partial u/\partial z$ is the vertical wind shear, H is the sensible heat flux, and $\partial \overline{e'w'}/\partial z$ is the gradient of the kinetic energy flux. The terms were evaluated from average values in different layers for the northeast and southwest monsoon systems.

Confidence in the precision of the determination of the dissipation of the energy is rather low. The equation expresses the dissipation as the sum or difference of large quantities. Two of these quantities, the friction velocity computed from the shearing stress, and the flux of kinetic energy, suffer from severe sampling variations. The flux of kinetic energy determinations, while generally forming a homogeneous group of data, occasionally displays points greater than the mean by a factor of 1000. One such point is the flux of energy measured in the shear zone off southern India on 19 February 1964. This point was not included in the averages used to determine the dissipation. Figure 29 shows the height variation of the three terms of the equation and the dissipation. It is seen that most of the turbulent kinetic energy is generated in the lowest 300 meters by the shearing stress and the wind gradient. In the lowest 25 meters the buoyancy of the air generates a small amount of kinetic energy. Above 25 meters the air is stable and kinetic energy is absorbed. The flux term shows that kinetic energy is transported upward away from the layer of generation by mechanical means. The net result of these processes is that the dissipation of energy is lower than the generation of energy by mechanical means at levels above 150m through the actions of negative buoyancy and the vertical flux of energy.

The energy budget for the southwest monsoon season is presented in Figure 30. In this case, the values are less certain because of wider variations in the measured terms both near the surface and in the cloud layer. The buoyancy term is negligible since the air is slightly stable. The flux

term is difficult to evaluate because of the wide excursions in the cloud layer. The conclusion reached from these values is that the energy is dissipated in the layer in which it is generated.

No attempt is made to evaluate the energy budget in the region of the low-level jet off Somalia because of the scanty, uncertain data. It is hoped that in the future more measurements with better equipment will be made in this interesting and important region.

References

Bunker, Andrew F., 1955: Turbulence and shearing stresses measured over the North Atlantic Ocean by an airplane-acceleration technique. J. Meteor., Vol. 12, 445-455.

--- 1960: Heat and water-vapor fluxes in air flowing southward over the western North Atlantic Ocean. J. Meteor., Vol. 17, 52-63.

--- 1962: Water-vapor distribution in the sub-cloud tradewind air. WHOI Ref. No. 62-2. Unpub. Mans. 44 pp.

--- 1963: Comments on vertical air velocity measurements. J. Atmos. Sci., Vol. 20, 242-243.

--- 1965: A low-level jet produced by air, sea, and land interactions. Proc. of Sea-Air Inter. Conf., Tech. Note 9-SAIL-1, ESSA, Weather Bureau, 225-238.

--- 1967: Cloud formations leeward of India during the Northeast Monsoon. J. Atmos. Sci., Vol. 24, 497-507.

--- and M. Chaffee, 1968: Indian Ocean clouds. Int. Ind. Ocean. Exp., Met. Mongr. 5., East-West Center Press, Honolulu. In press.

Colon, J., 1964: On interactions between the southwest monsoon current and the sea surface over the Arabian Sea. Ind. J. Met. Geophys., 15, 183-200.

Fleagle, R. G., F. I. Badgley, and Y. Hsueh, 1967: Calculations of turbulent fluxes by integral methods. J. Atmos. Sci., Vol. 24, 356-373.

Jacobs, W. C., 1942: On the energy exchange between sea and atmosphere. J. Mar. Res., 5, 37-66.

Miller, F. R., and R. N. Keshavamurthy, 1967: Structure of an Arabian Sea summer monsoon system. Int. Ind. Ocean. Exp., Met. Mongr. 1, East-West Center Press, Honolulu.

--- and C. Jefferies, 1967: Mean monthly sea-surface temperatures of the Indian Ocean during the IIOE. HIG-67-14, 6 pp., tables and charts.

Nicholson, J. R., 1965: On the character of the Bombay sea-breeze. In: P. R. Pisharoty (Ed.), Proc. Sym. Meteor. Results of IIOE. 86-96.

Pisharoty, P. R., 1965: Evaporation from the Arabian Sea and the Indian southwest monsoon. In: P. R. Pisharoty (Ed.), Proc. Sym. Meteor. Results of IIOE. 43-54.

Ramage, C. S., 1968: Problems of a Monsoon Ocean. Weather, Vol. XXIII, 28-37.

Srivastava, R. C., and C. Ronne, 1966: Salt Particles and haze in the Indian monsoon air. Ind. J. Meteor. Geophys., Vol. 17, 587-590.

Suryanarayana, R. and D. R. Sikka, 1965: Evaporation over the Indian Ocean

during 1963. In: P. R. Pisharoty (Ed.), Proc. Sym. Meteor. Results of IIOE, 68-69.

Swallow, J. C., and J. G. Bruce, 1966: Current measurements off the Somali Coast during the southwest monsoon of 1964. Deep-Sea Research, Vol. 13, 861-888.

Telford, J. W., and J. Warner, 1962: On the measurement from an aircraft of buoyancy and vertical air velocity in cloud. J. Atmos. Sci., 19, 415-423.

--- 1963: Reply, J. Atmos. Sci., Vol. 20, 244.

Warren, Bruce, Henry Stommel, and J. C. Swallow, 1966: Water masses and patterns of flow in the Somali Basin during the southwest monsoon of 1964. Deep-Sea Research, Vol. 13, 825-860.

Wooster, Warren S., Milner B. Schaefer, and Margaret K. Robinson, 1967: Atlas of the Arabian Sea for Fishery Oceanography. IMR Ref. No. 67-12, Univ. Calif., La Jolla.

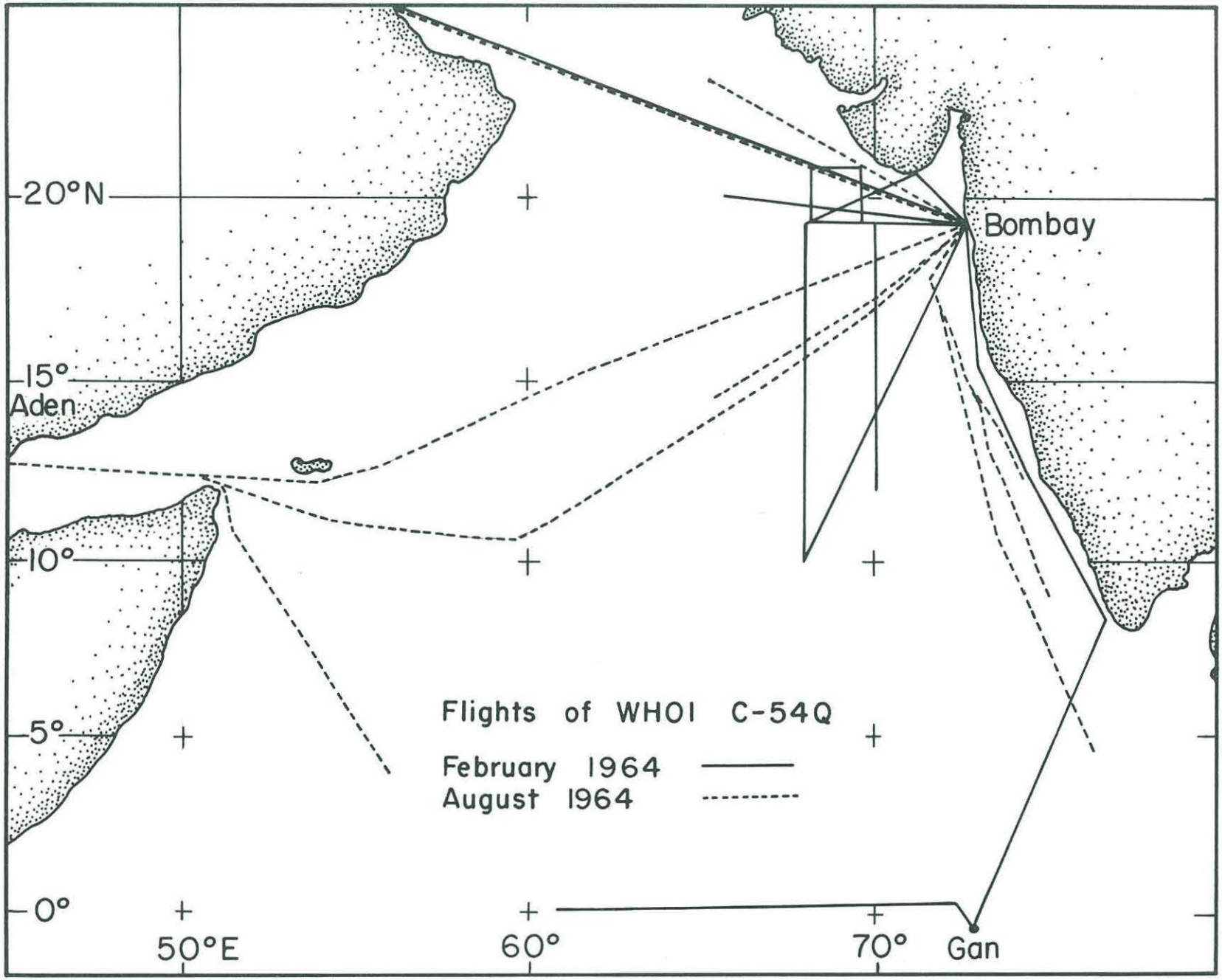

Figure 1. Flight paths flown during 1964 while making turbulence observations over the Arabian Sea.

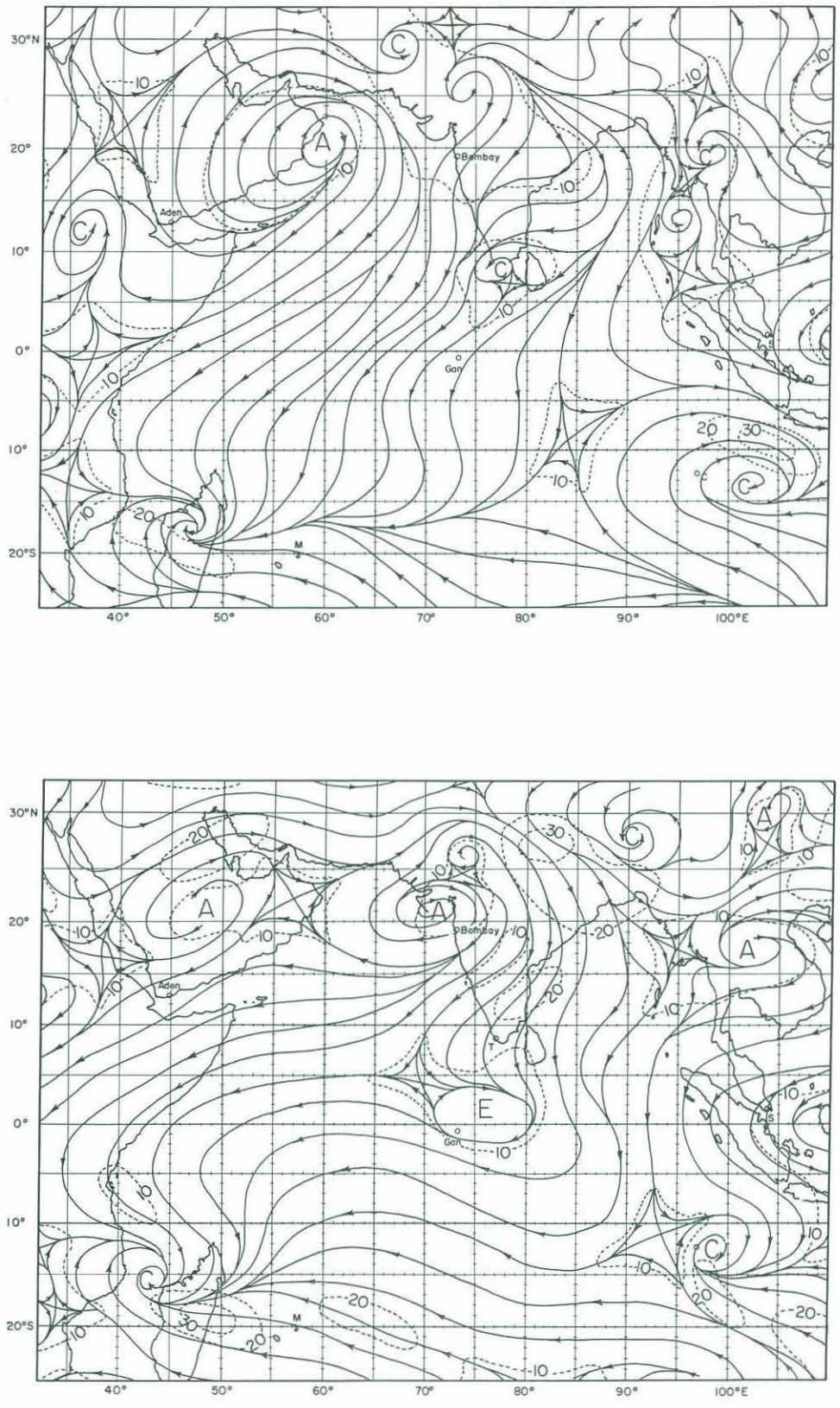

Figure 2. Streamline charts for 8 March 1964. The top chart shows the surface streamlines and isovels which are typical of the northeast monsoon. The bottom chart gives the 700 mb streamlines and isovels.

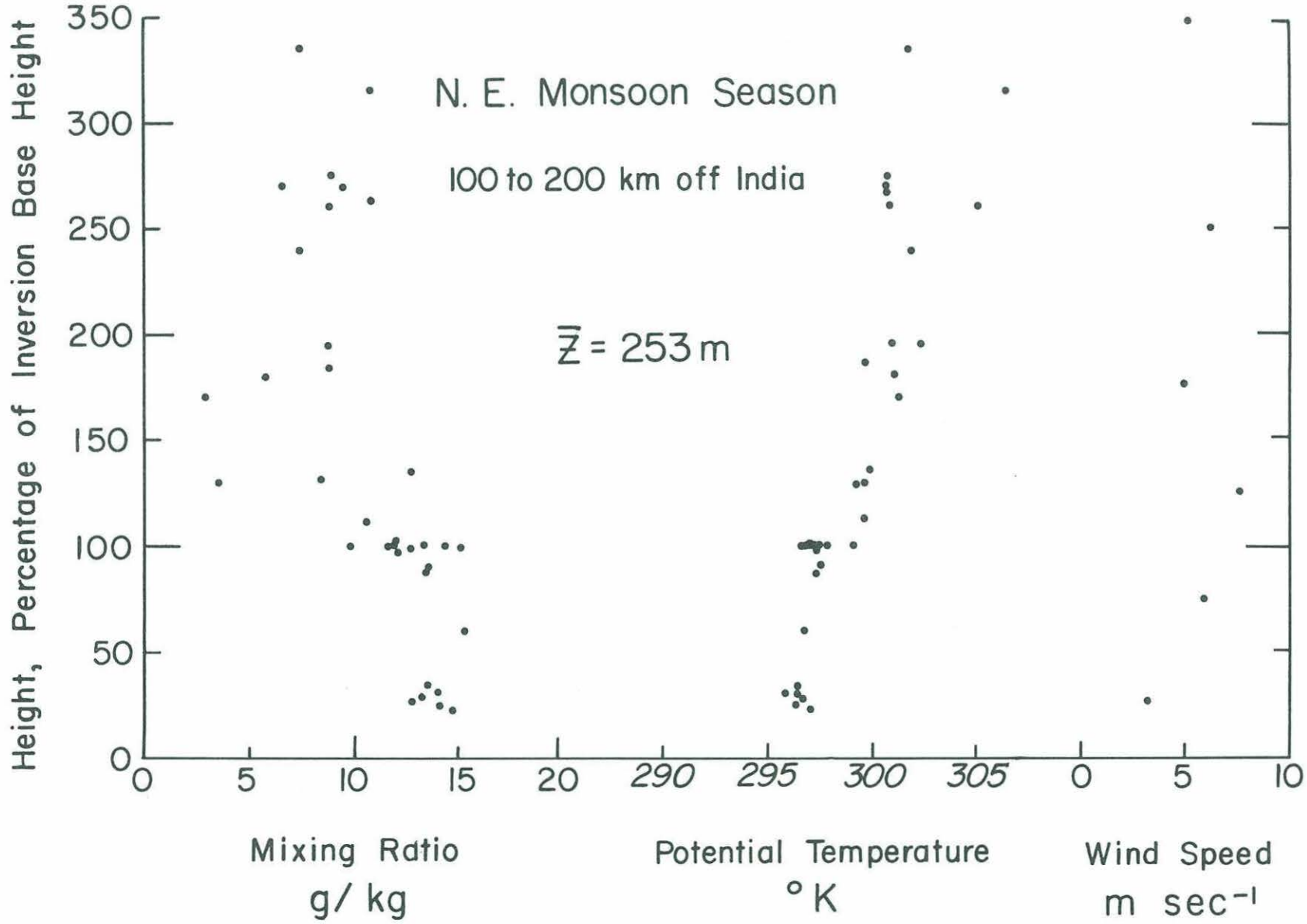

Figure 3. Height distribution of mixing ratio, potential temperature, and wind speed. Heights are expressed in terms of the height of the inversion which averaged 253 m.

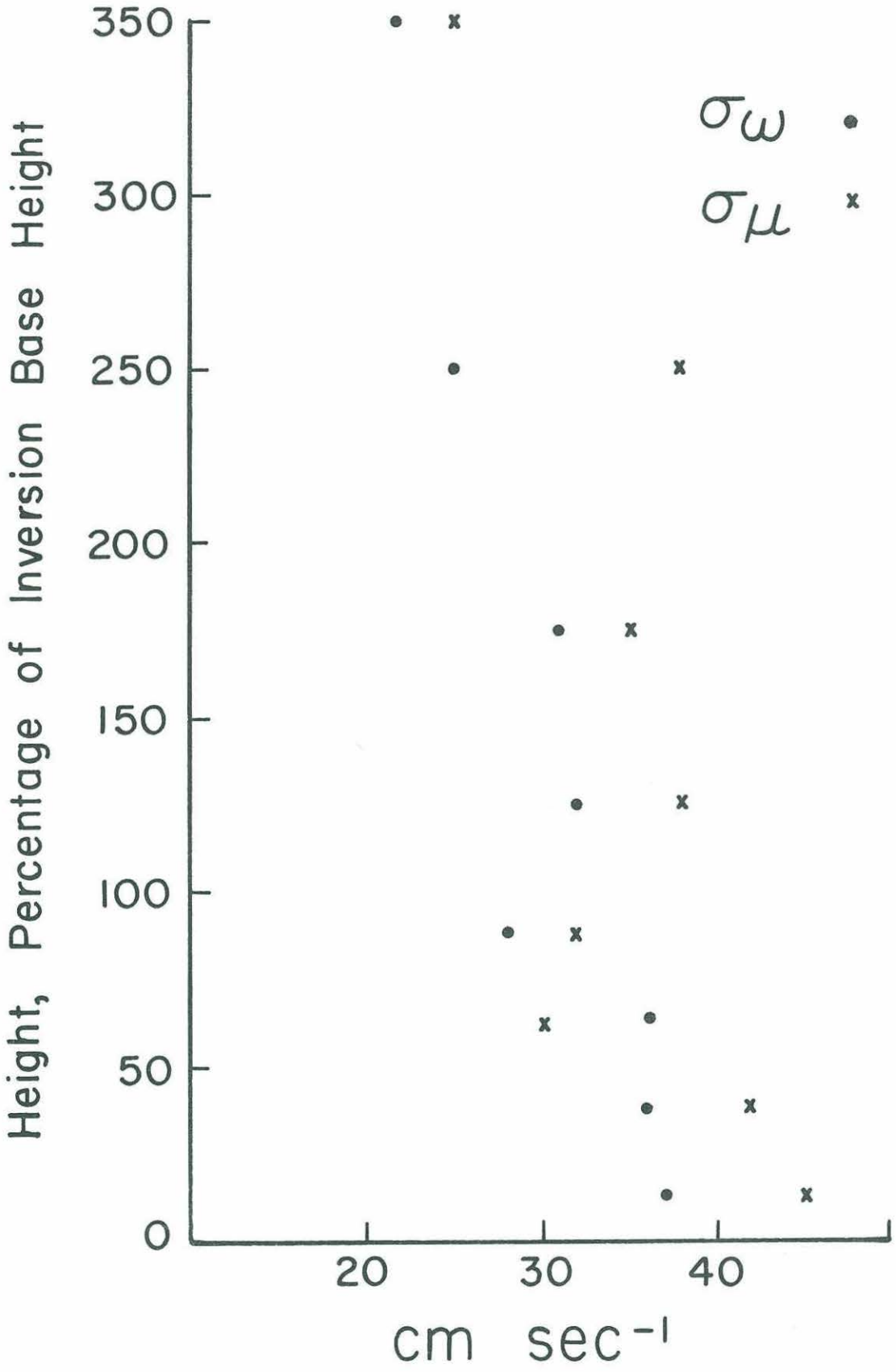

Figure 4. Height distribution of the root-mean-square values of the horizontal and vertical components of the turbulence.

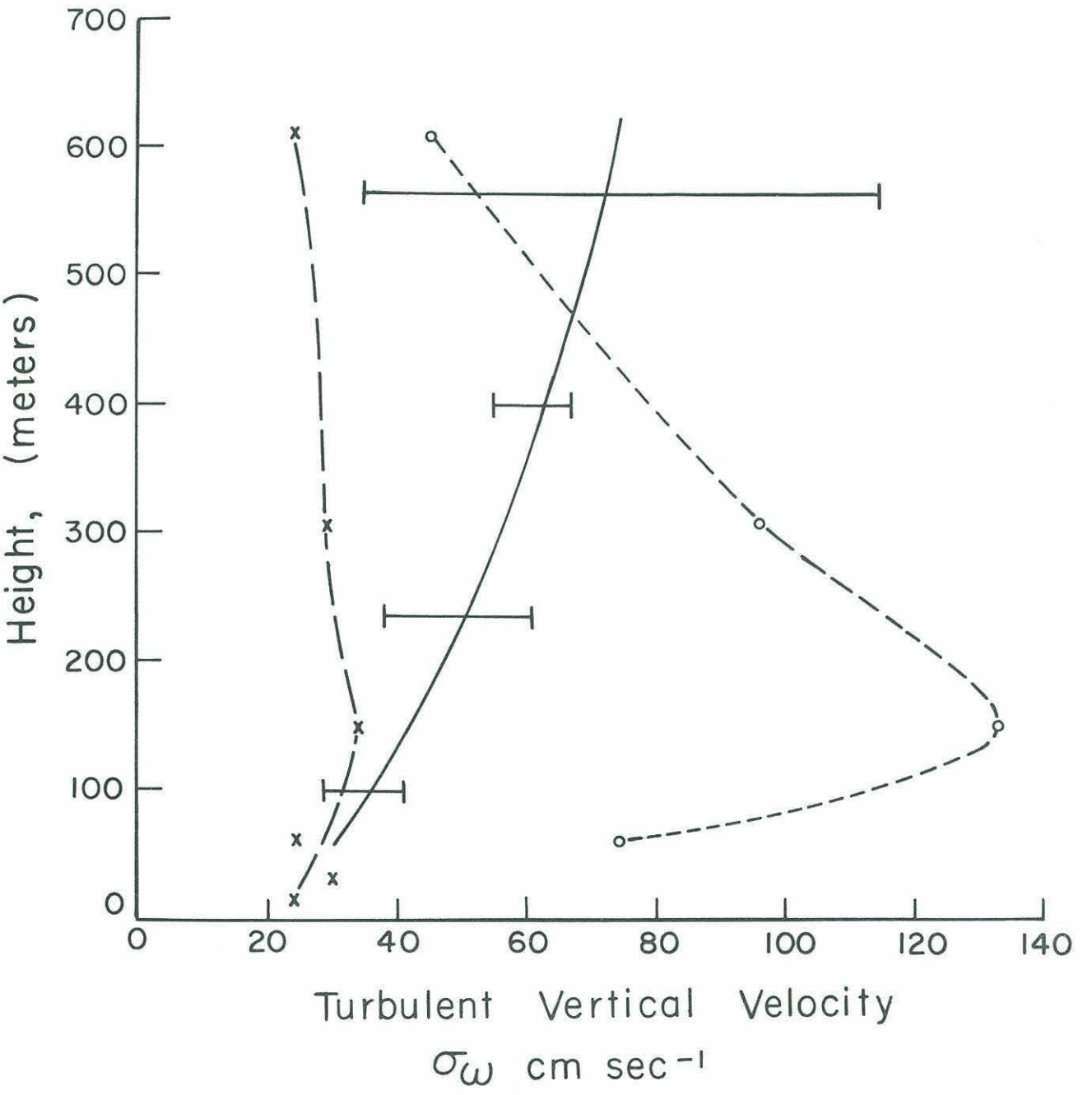

Figure 5. Height variations of the vertical turbulent velocities in three regions of the world.

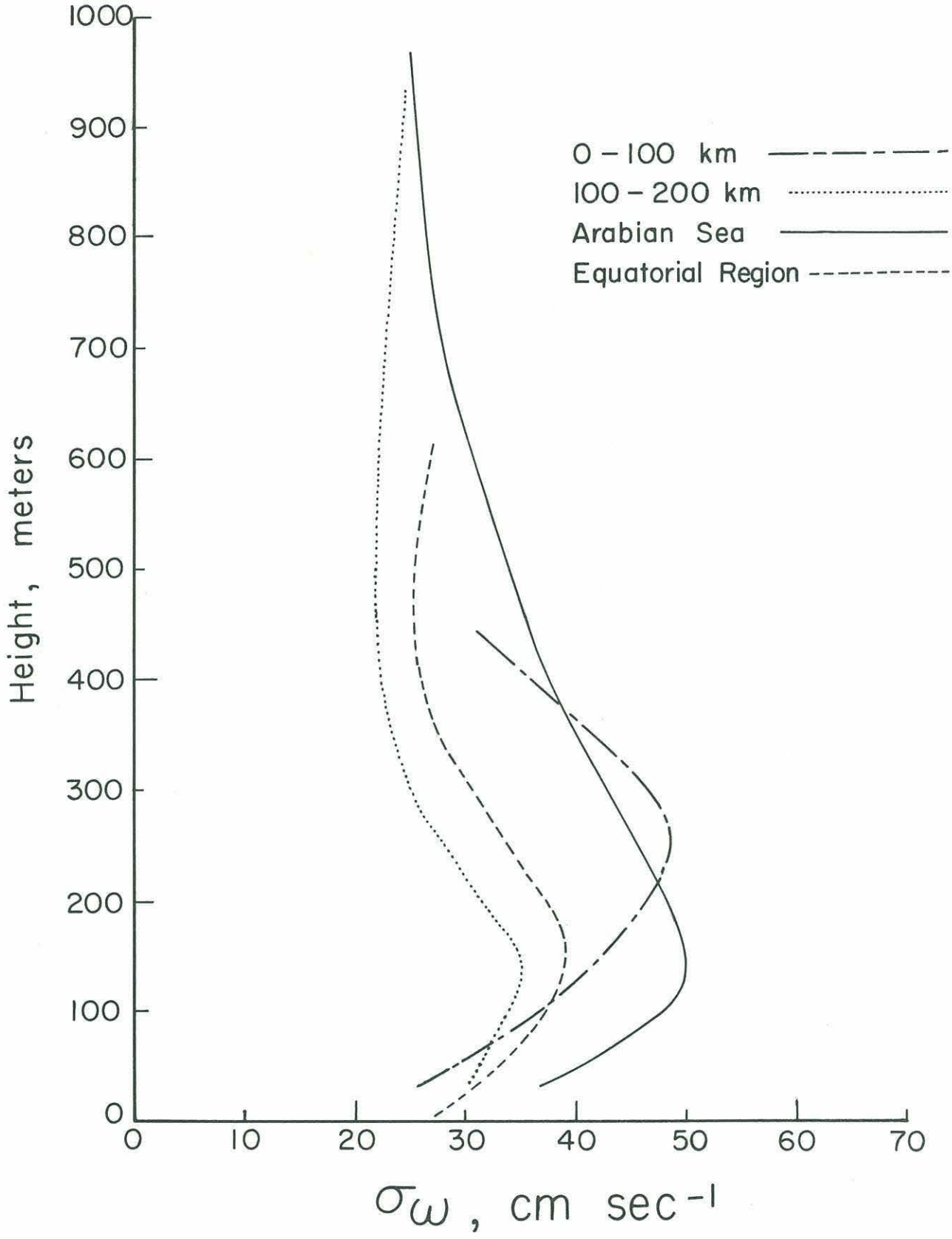

Figure 6. Height distribution of the vertical turbulent velocities in four regions of the Arabian Sea and Indian Ocean during the northeast monsoon.

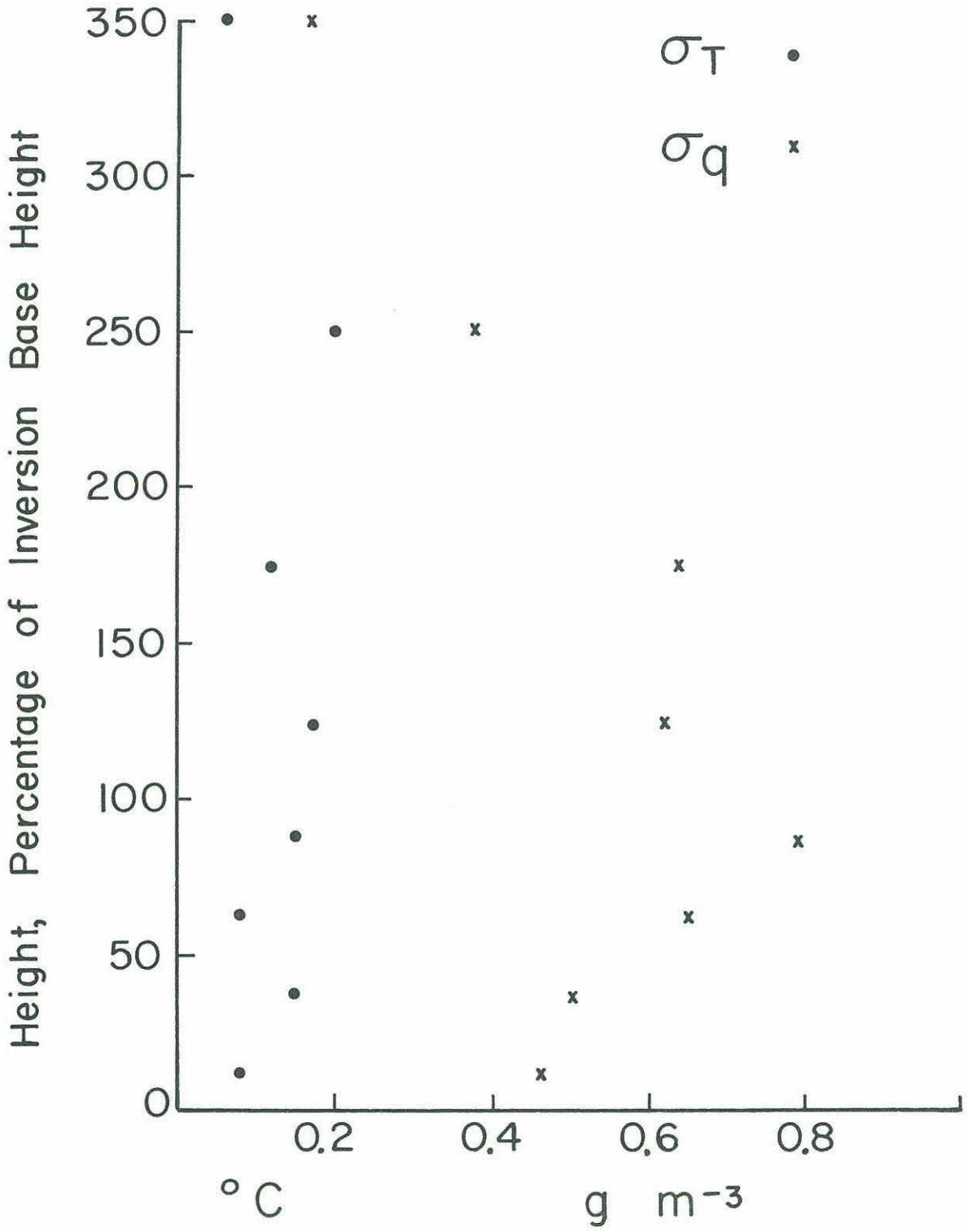

Figure 7. Height distribution of temperature and specific humidity fluctuations during the northeast monsoon over the Arabian Sea.

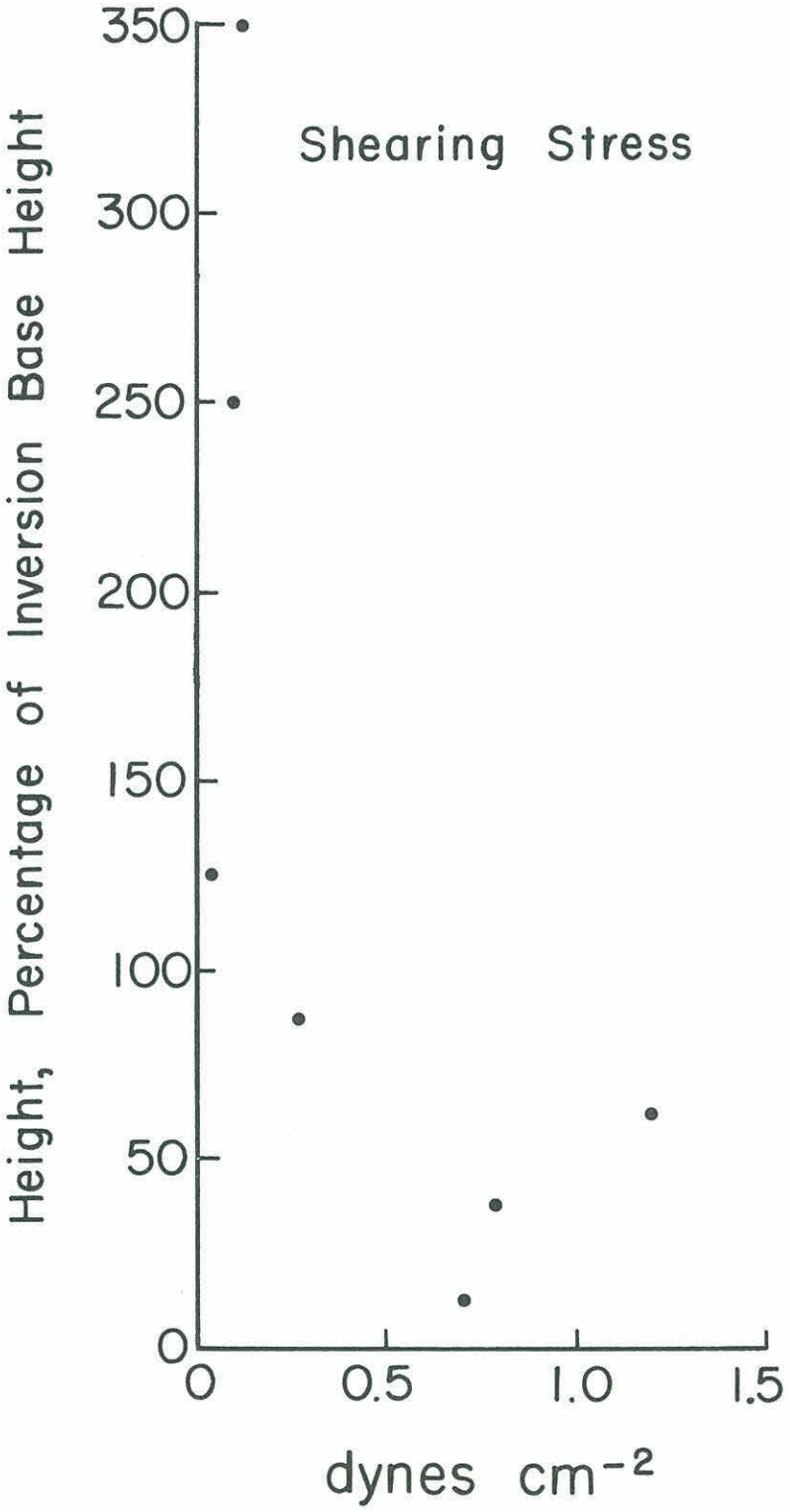

Figure 9. Height distribution of the shearing stress over the Arabian Sea during the northeast monsoon.

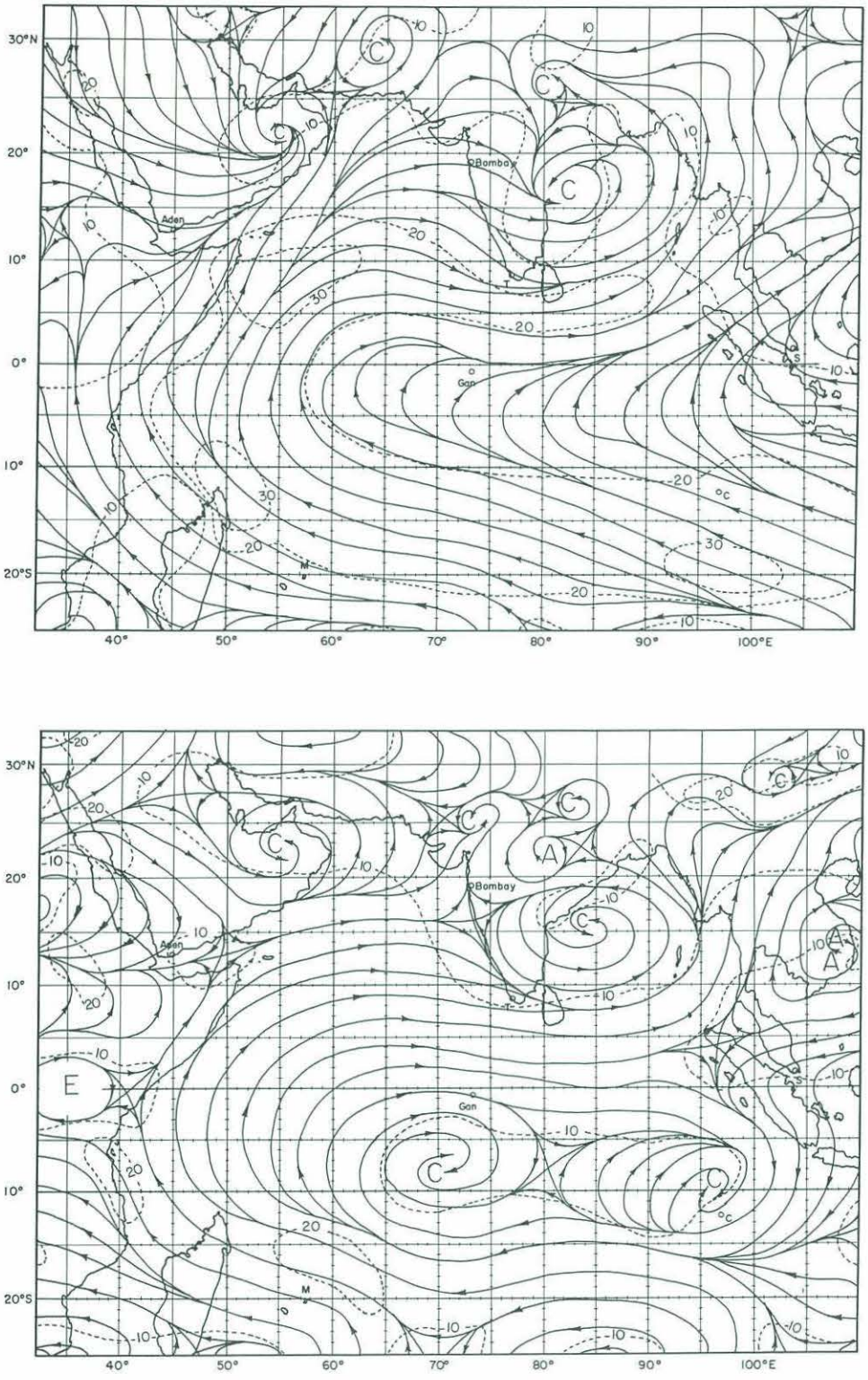

Figure 10. Streamline charts for 30 August 1964. The top chart shows the surface streamlines and isovels which are typical of the southwest monsoon. The bottom chart gives the 700 mb level streamlines and isovels.

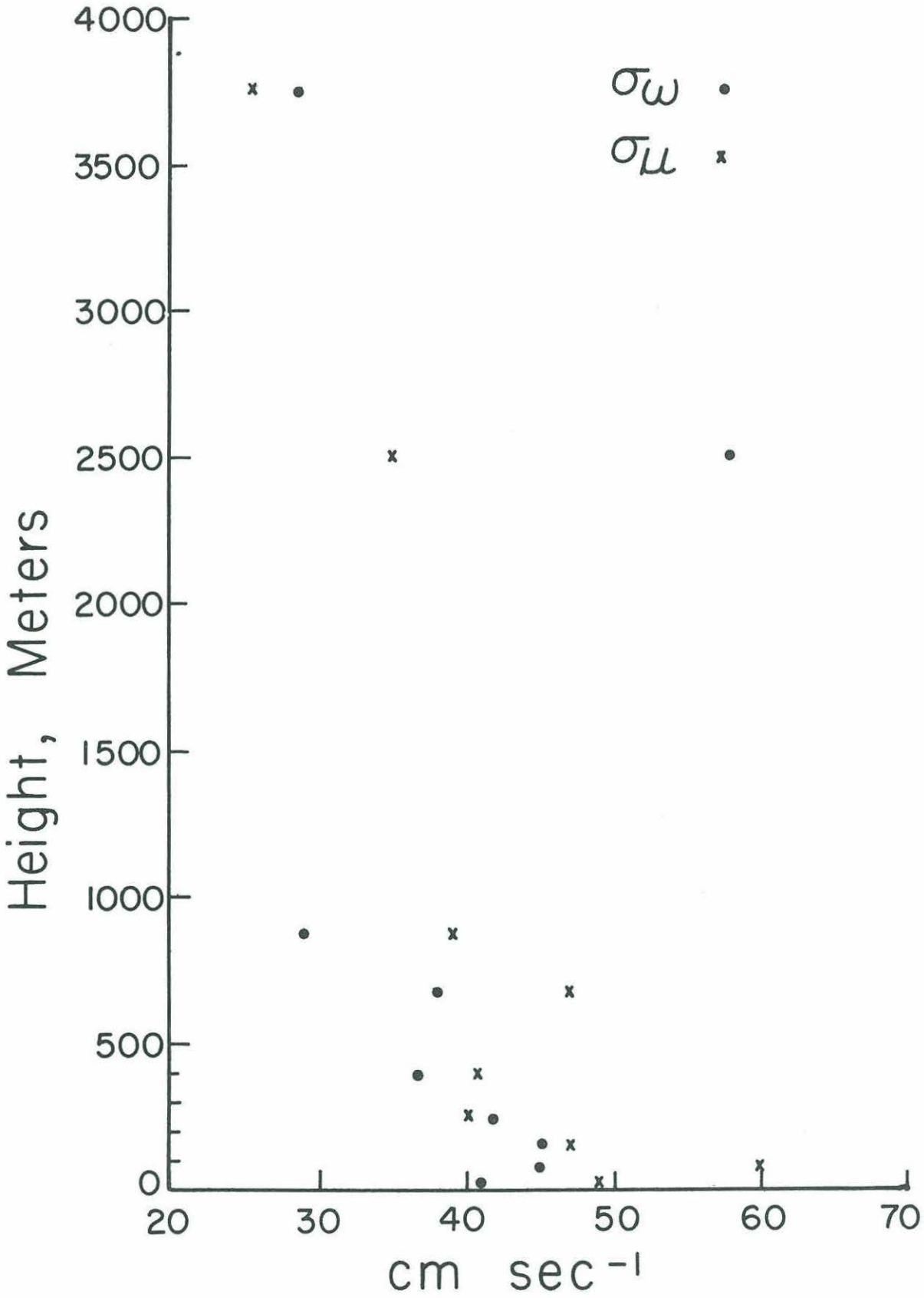

Figure 12. Height distribution of the horizontal and vertical components of turbulence over the Arabian Sea east of 65E during the south west monsoon.

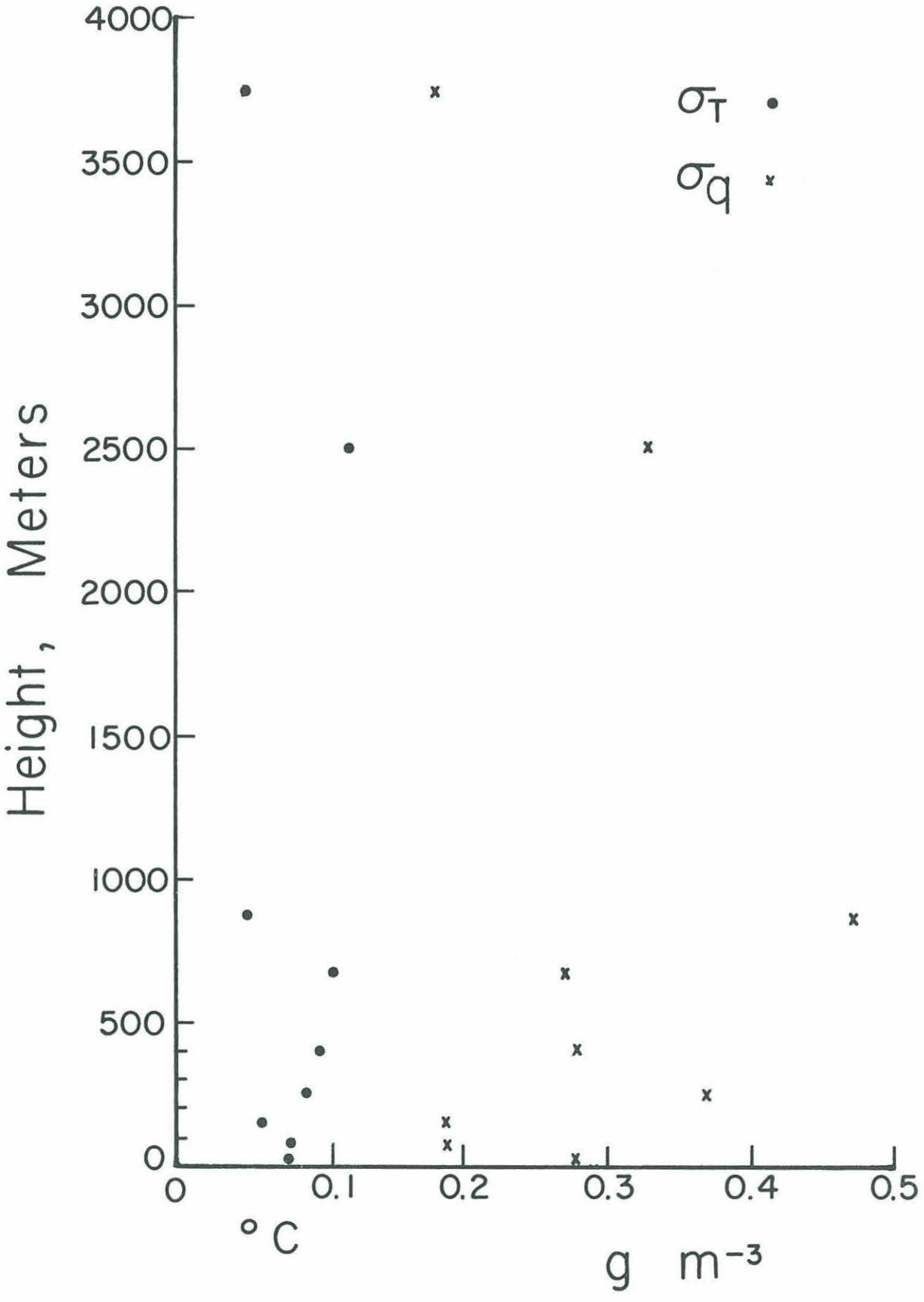

Figure 13. Height distribution of temperature and specific humidity fluctuations over the Arabian Sea east of 65E during the southwest monsoon.

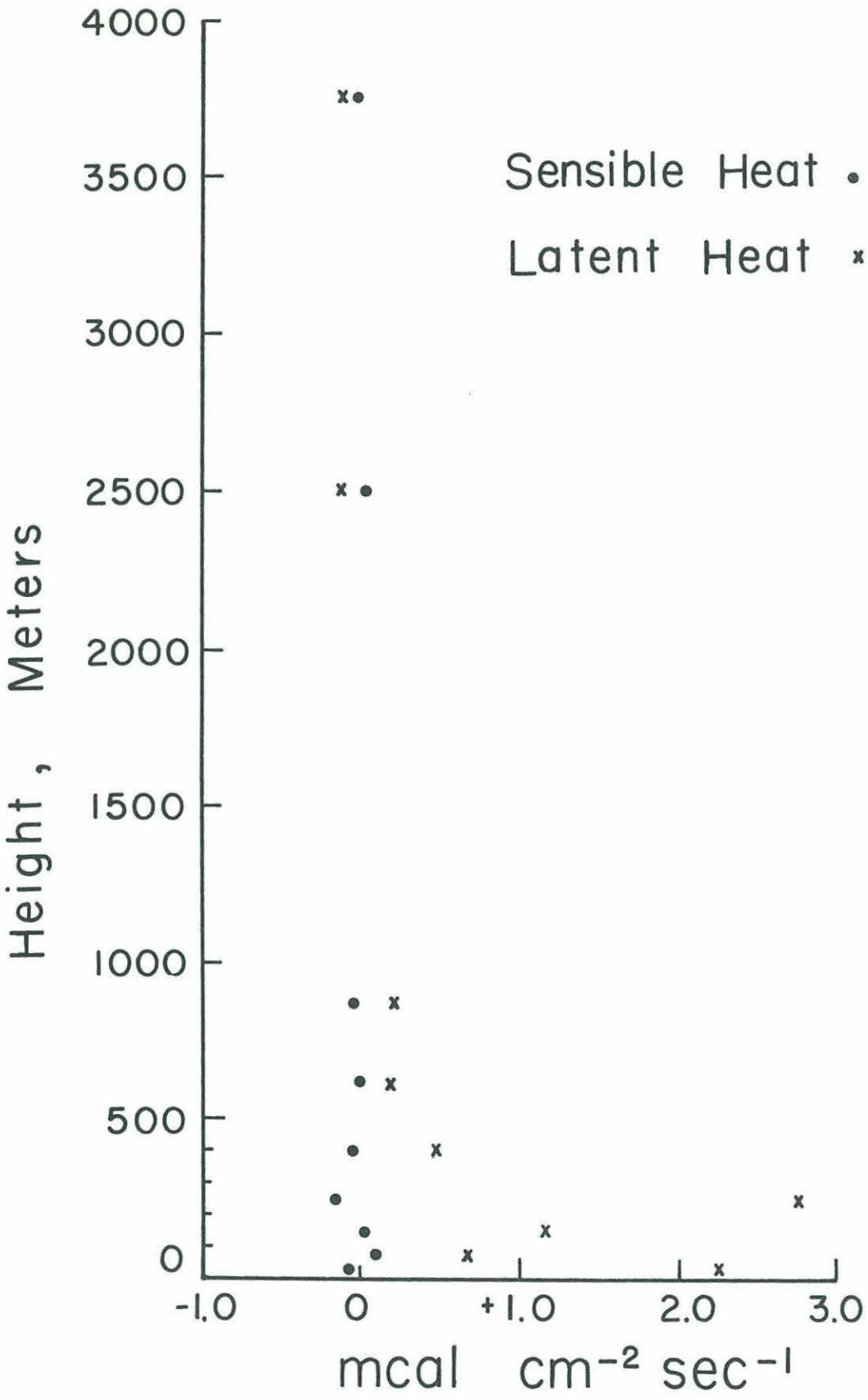

Figure 14. Height distribution of sensible and latent heat fluxes over the Arabian Sea east of 65E during the southeast monsoon.

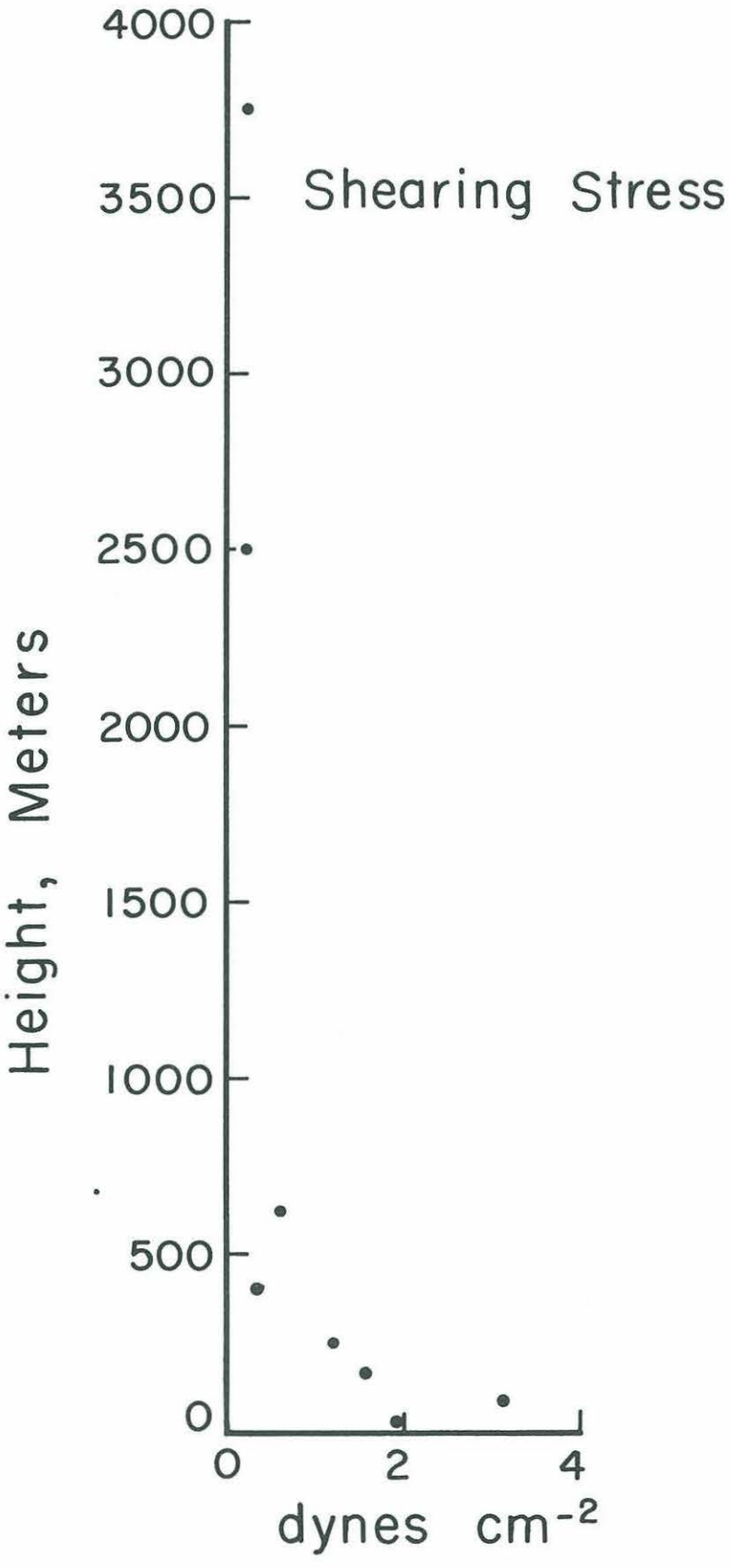

Figure 15. Height distribution of the shearing stress over the Arabian Sea east of 65E during the southwest monsoon.

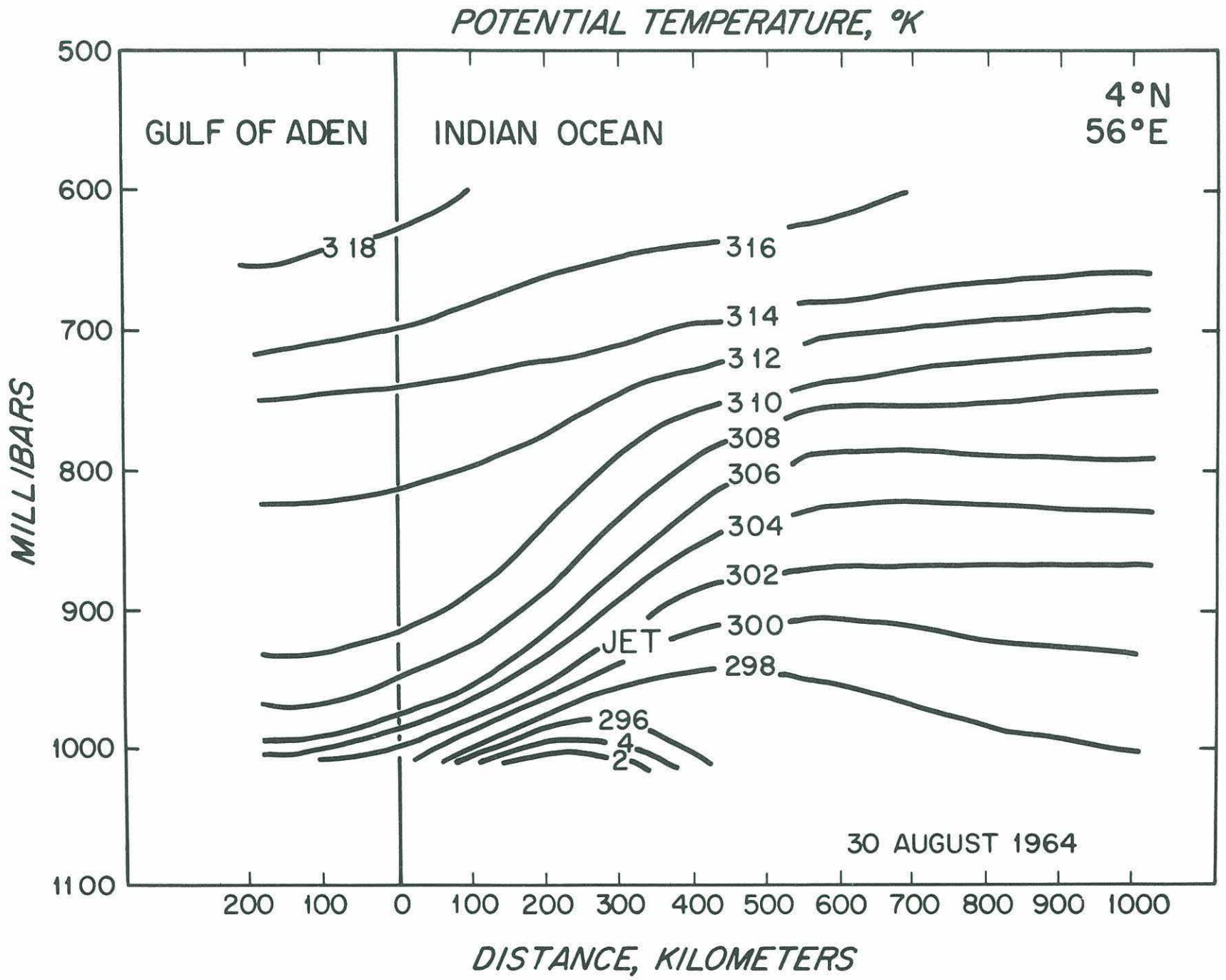

Figure 16. Potential temperature vertical cross-section from the Gulf of Aden, across cold upwelling water, to 4N, 56E during the southwest monsoon.

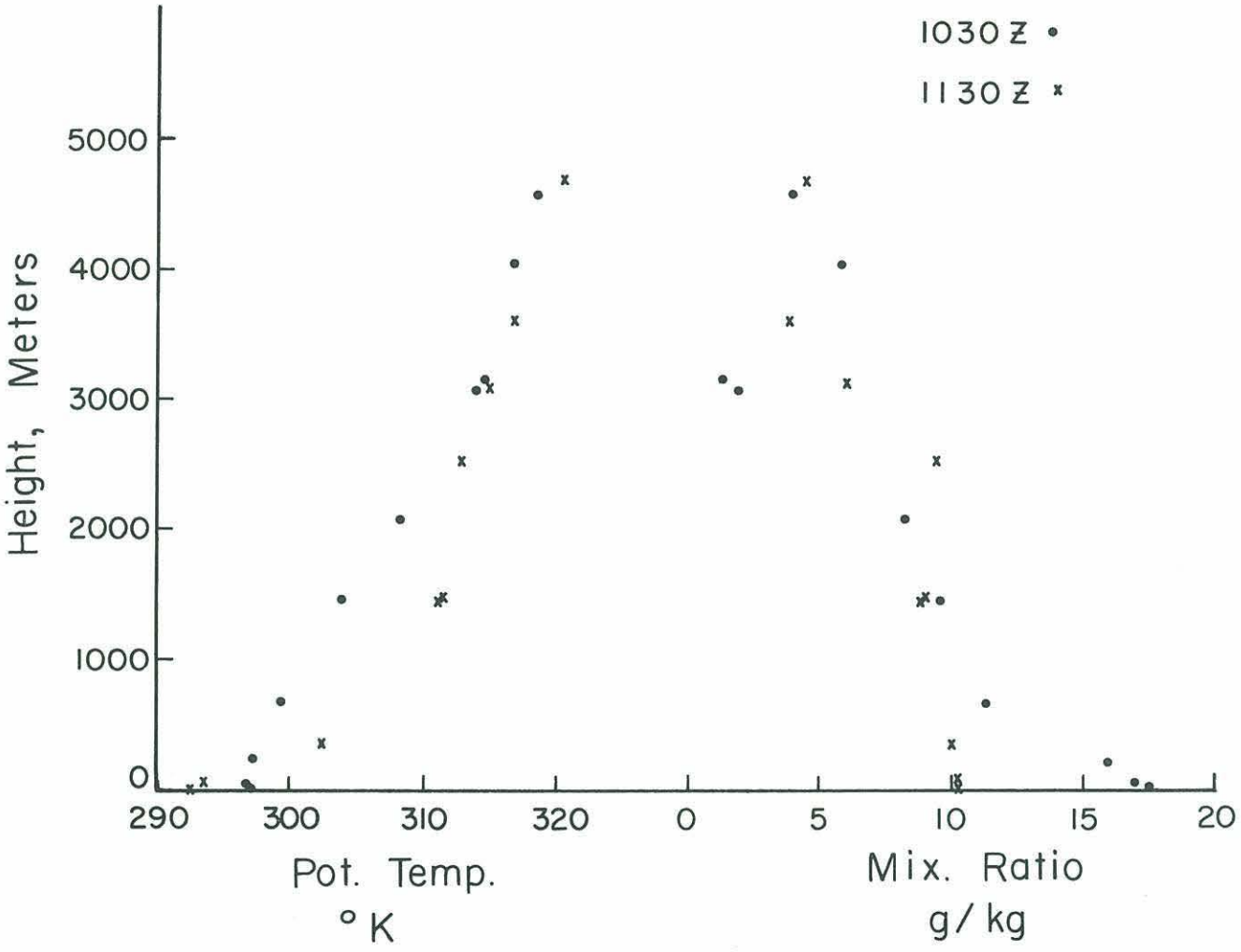

Figure 17. Height distributions of potential temperature and mixing ratio from two dropsondes released 30 August 1964 off the Somali Coast. One dropsonde fell in the region of the air cooled by upwelling water.

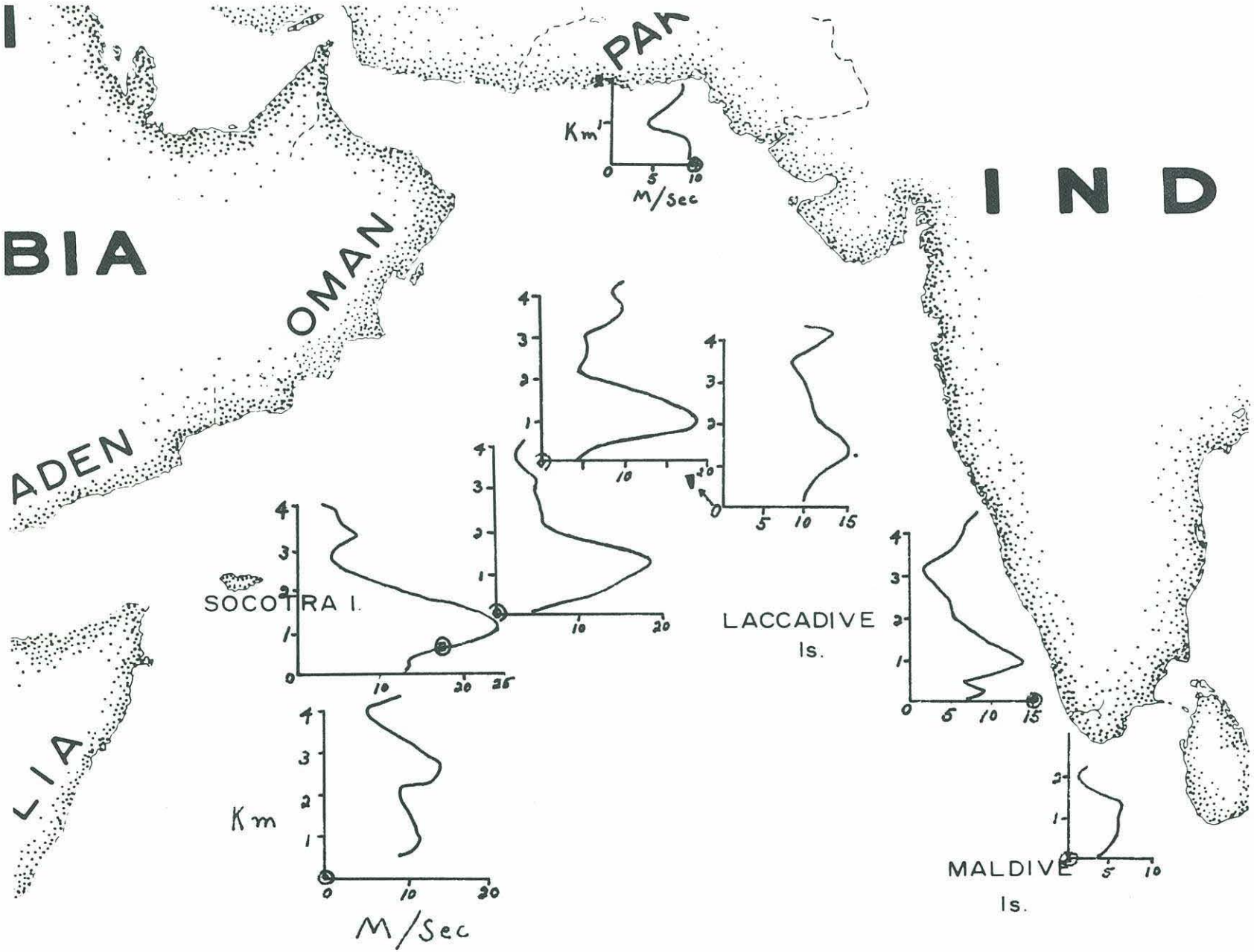

Figure 18. Vertical profiles of the wind over various regions of the Arabian Sea during the southwest monsoon season. Observations were made from the aircraft by Doppler radar.

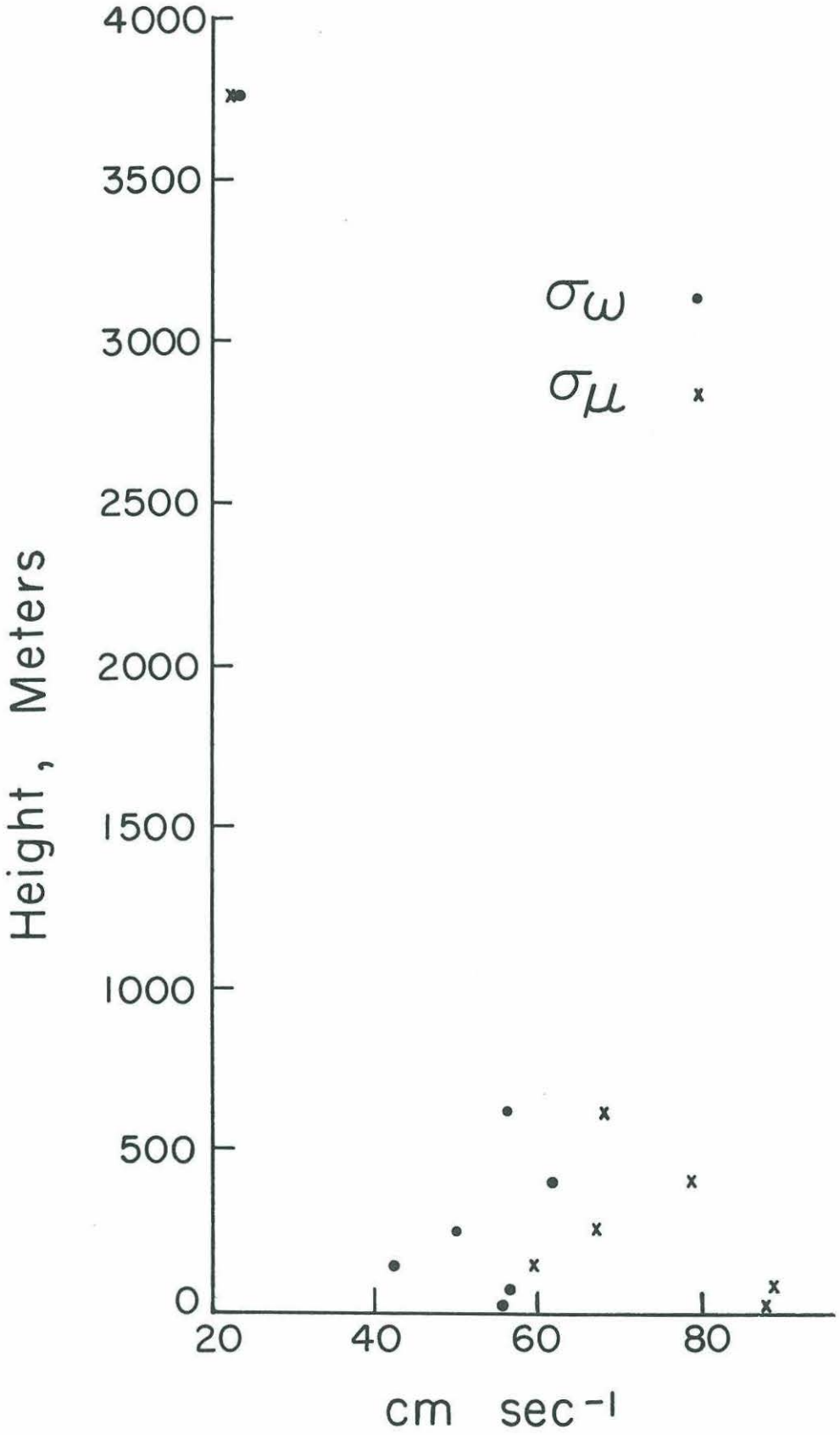

Figure 19. Height distribution of the horizontal and vertical components of the turbulence over the Arabian Sea west of 65E during the southwest monsoon.

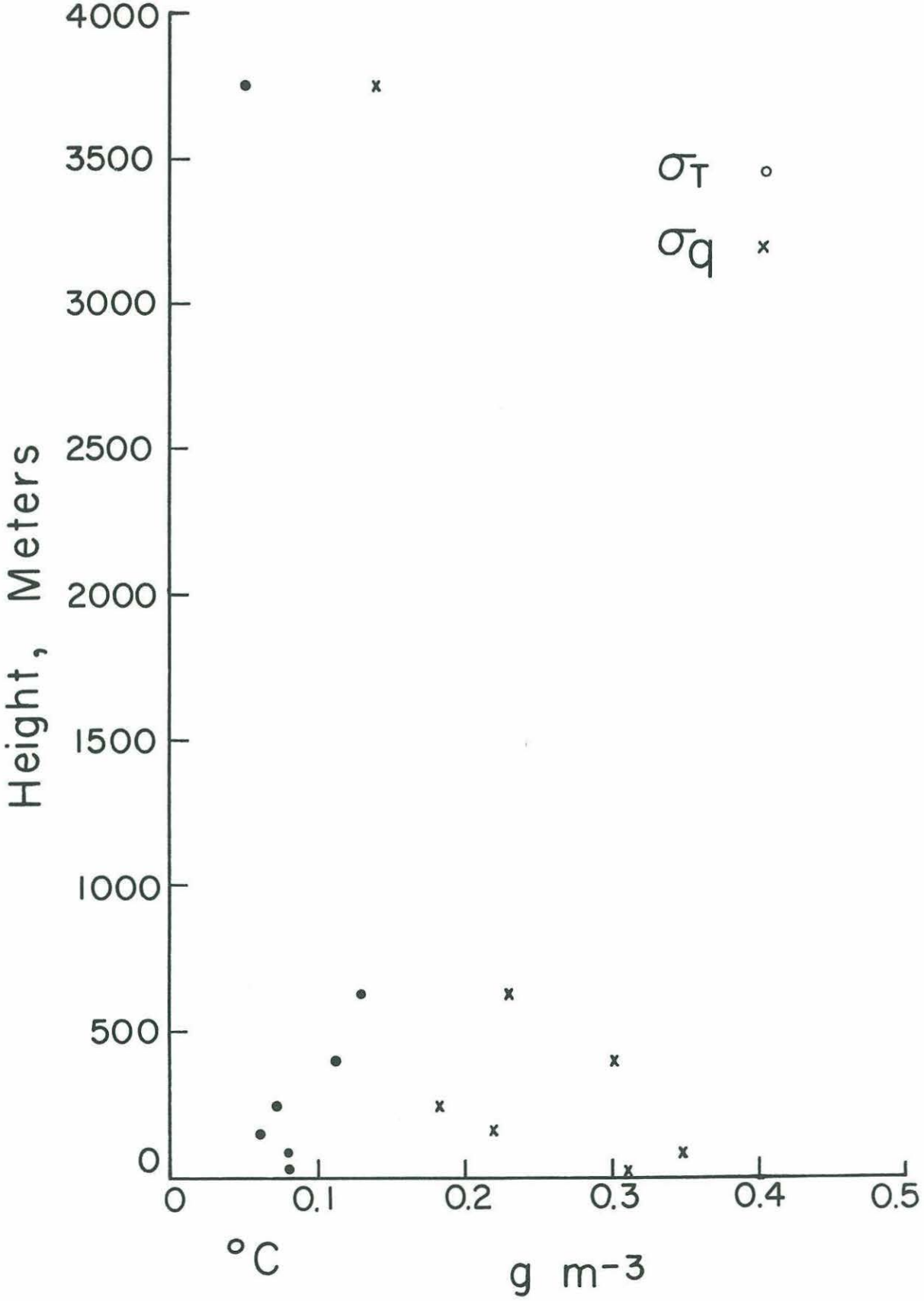

Figure 20. Height distribution of the temperature and specific humidity fluctuations over the Arabian Sea west of 65E during the southwest monsoon.

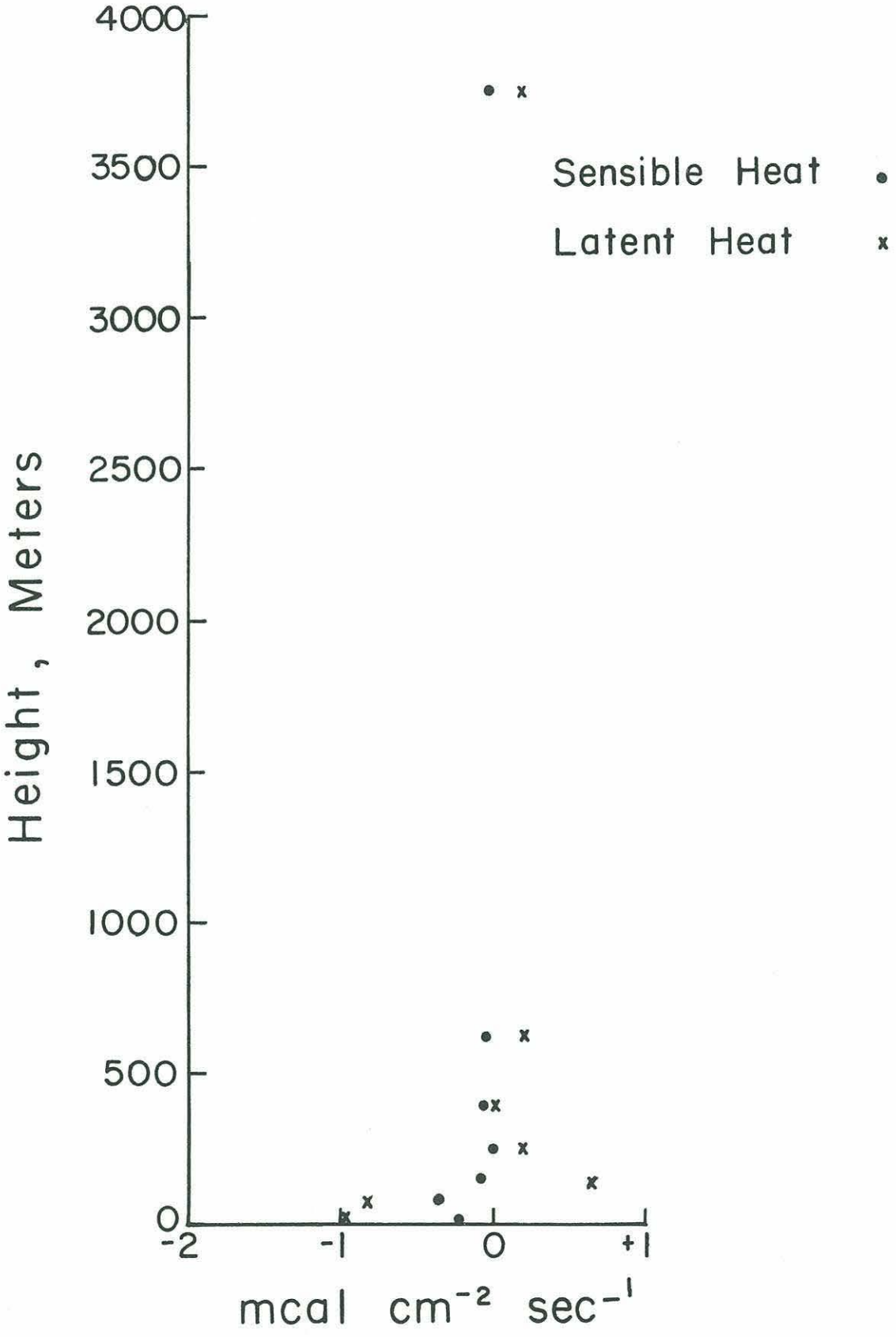

Figure 21. Height distribution of the sensible and latent heat fluxes over the Arabian Sea west of 65E during the southwest monsoon.

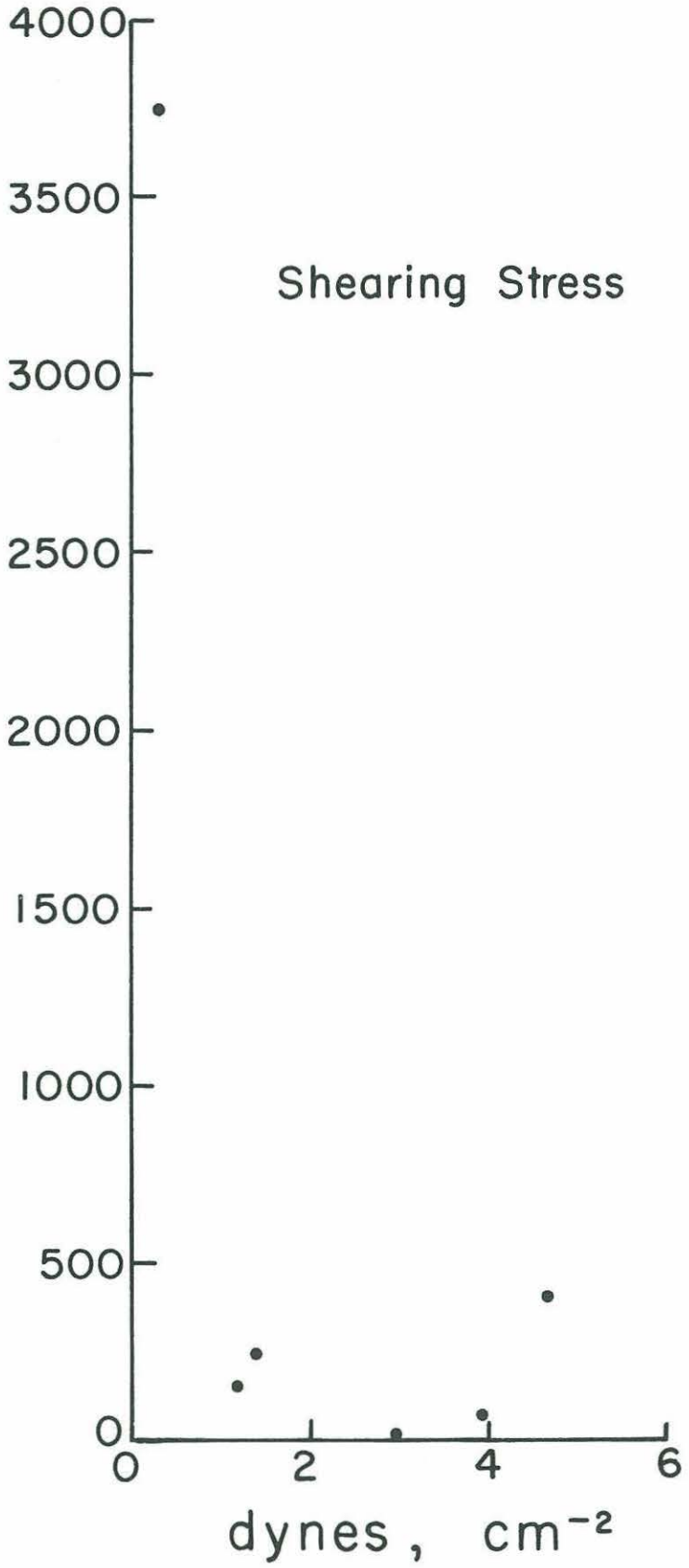

Figure 22. Height distribution of the shearing stress over the Arabian Sea west of 65E during the southwest monsoon.

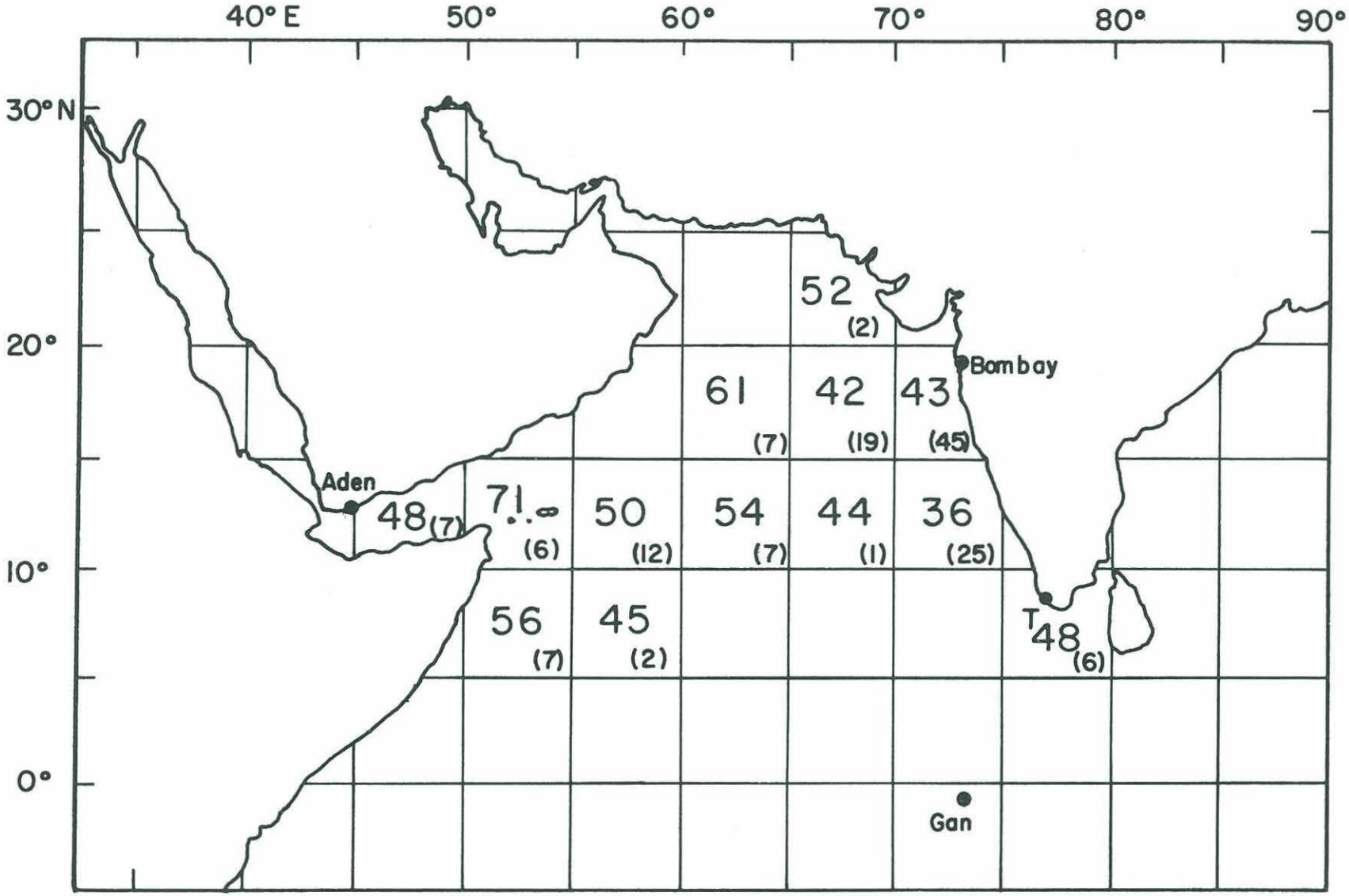

Figure 23. Chart of vertical turbulent velocities over the Arabian Sea during the southwest monsoon. Values given are averages of the root-mean-square velocities from the surface to 475 meters. Values are in cm sec^{-1}. Figures in parentheses give the number of observations.

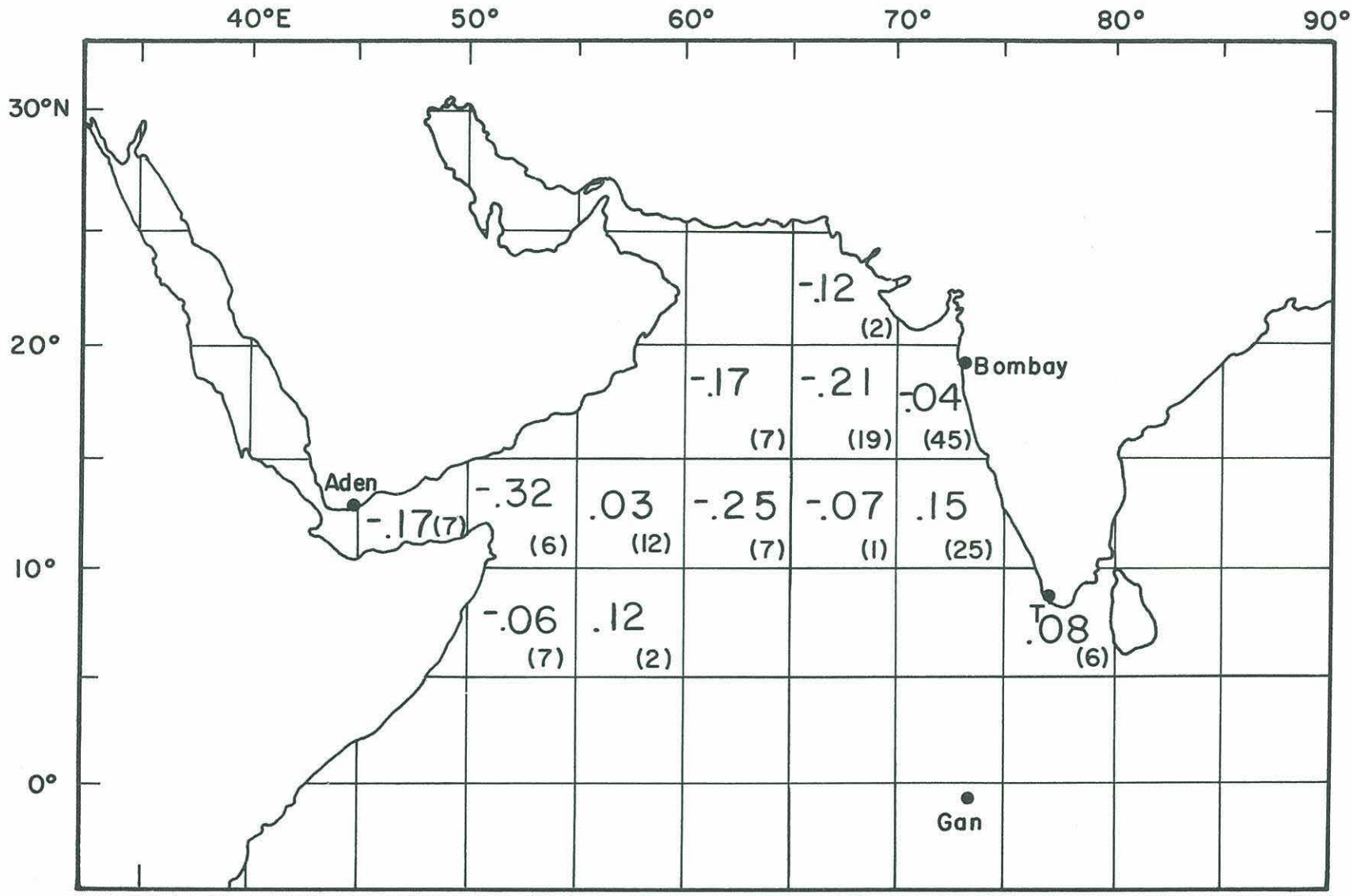

Figure 24. Chart of sensible heat flux over the Arabian Sea during the southwest monsoon. Values are averaged from the surface to 475 meters and expressed in milli-calories cm^{-2} sec^{-1}. Figures in parentheses gives the number of observations.

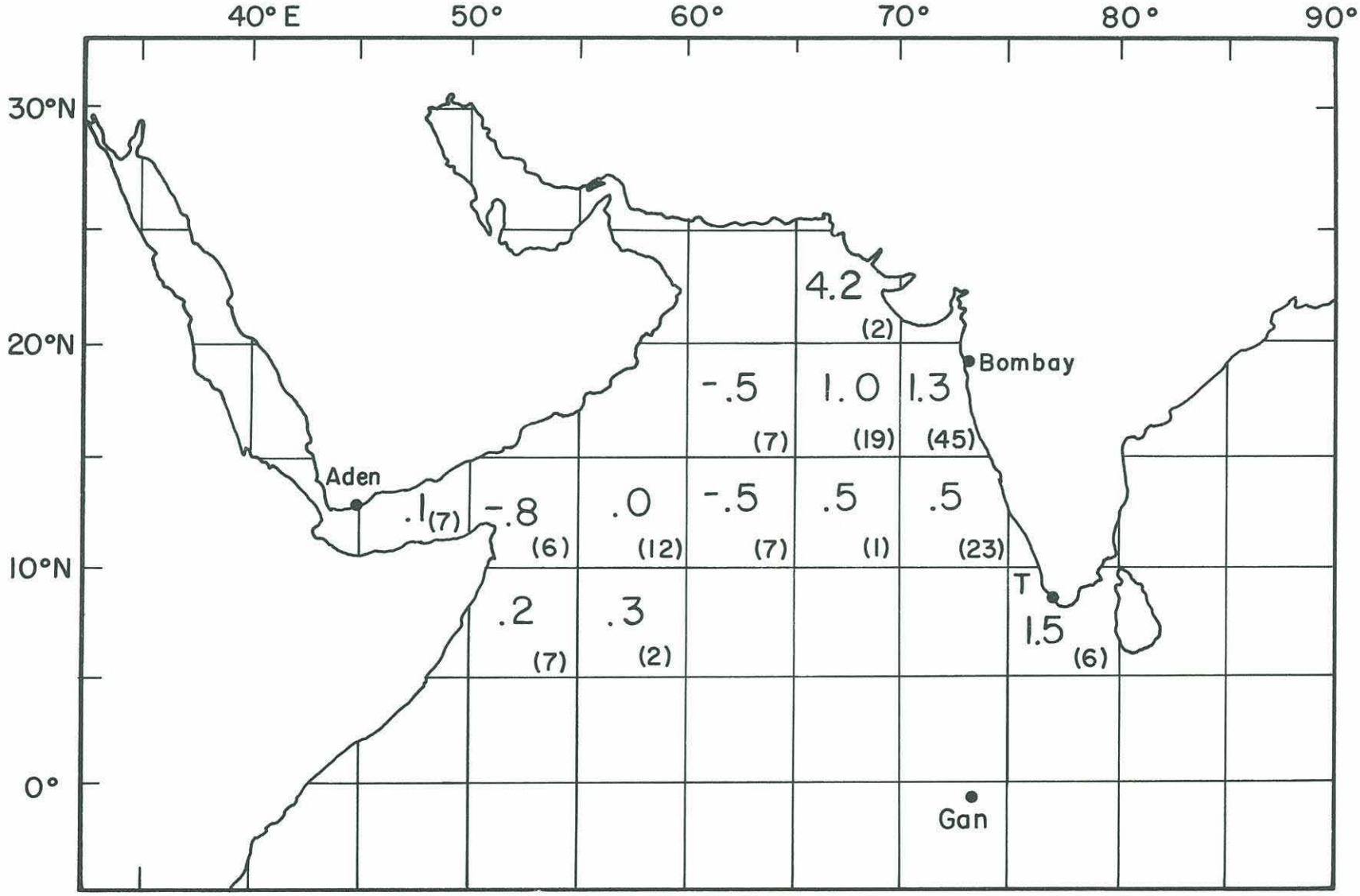

Figure 25. Chart of latent heat fluxes over the Arabian Sea during the southwest monsoon. Values are averaged from the surface to 475 meters. Values are in milli-calories cm^{-2} sec^{-1}. Figures in parentheses give the number of observations.

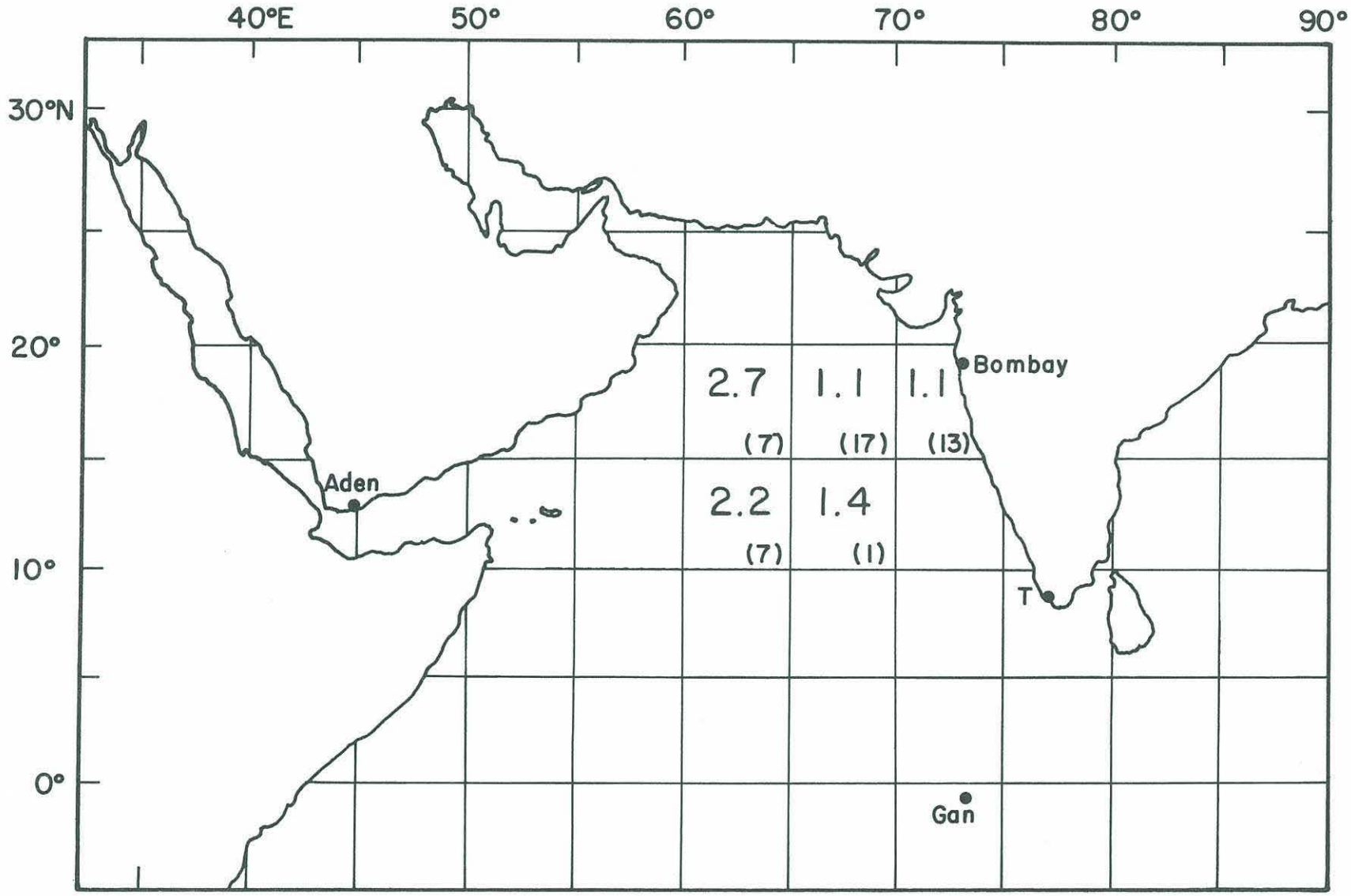

Figure 26. Chart of shearing stresses over the Arabian Sea during the southwest monsoon. Values are from upwind runs only, and averaged from the surface to 475 meters. Values are in dynes cm^{-2}. Figures in parentheses give the number of observations.

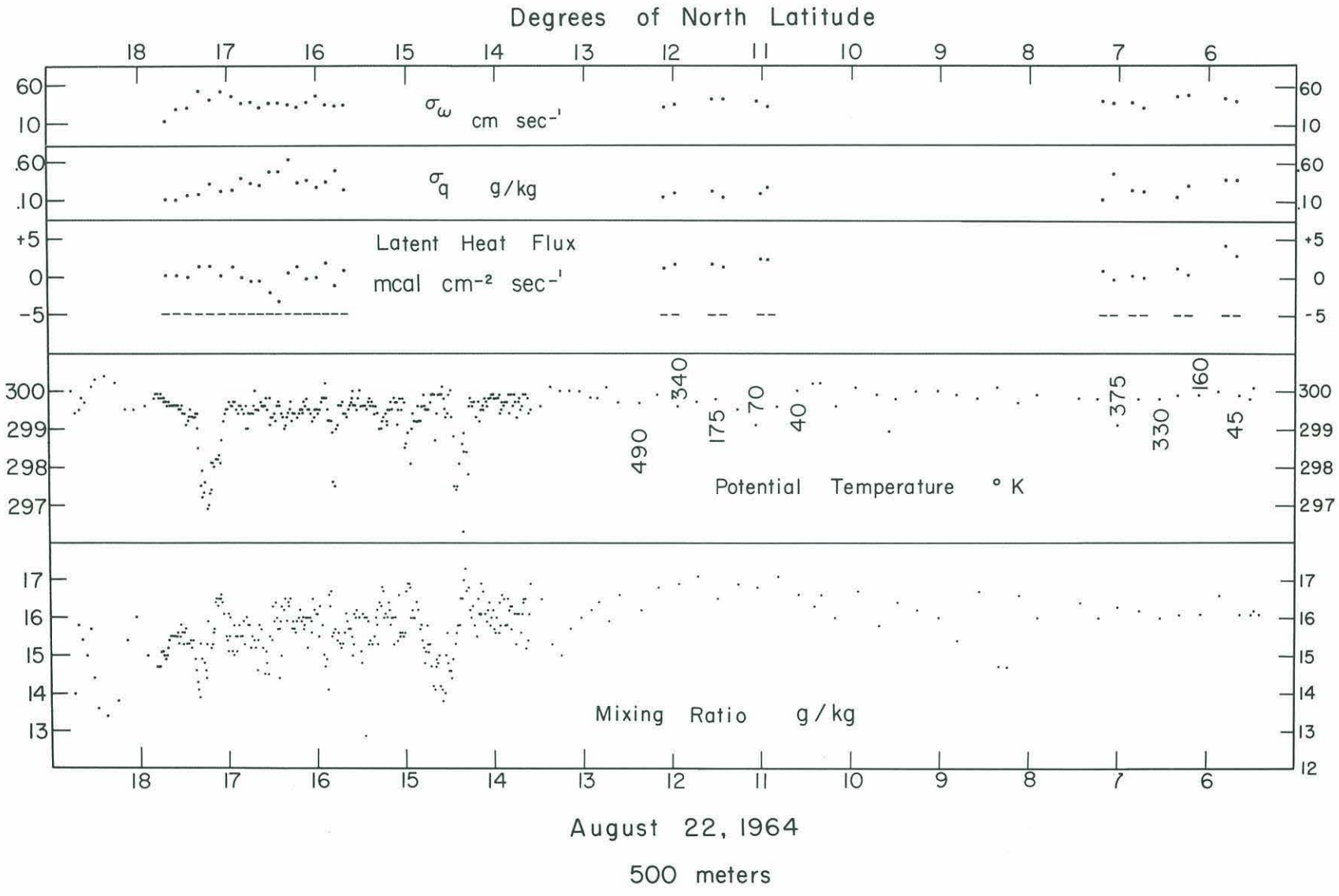

Figure 27. Cross-section of potential temperature, mixing ratio, turbulence and fluxes off the west coast of India from 19N to 6N on 22 August 1964. Drafted numbers give the aircraft height if different from 500 meters.

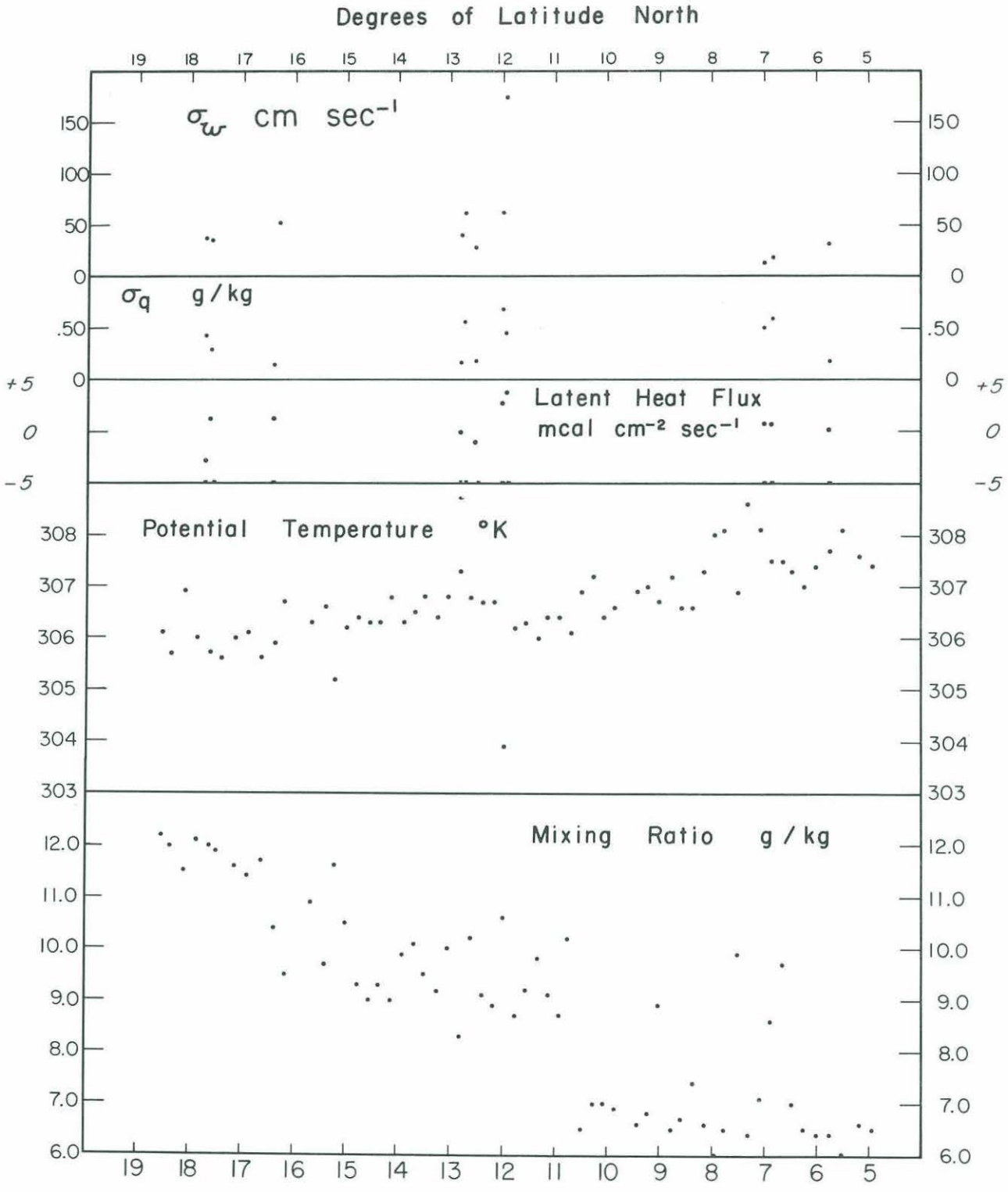

Figure 28. Cross-section of potential temperature, mixing ratio, turbulence, and fluxes off the west coast of India from 6N to 19N on 22 August 1964.

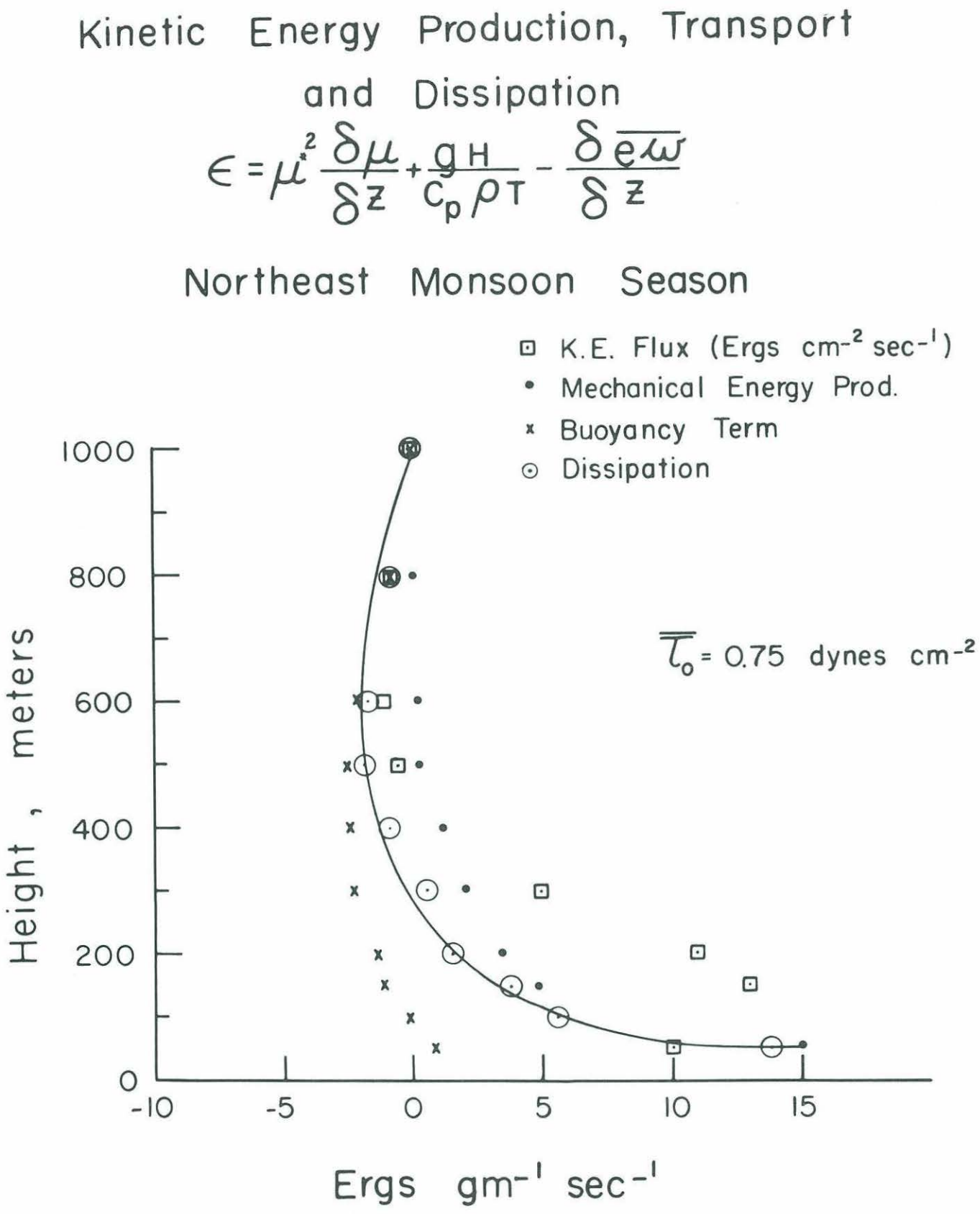

Figure 29. Height distribution of kinetic energy production, transport and dissipation during the northeast monsoon over the Arabian Sea.

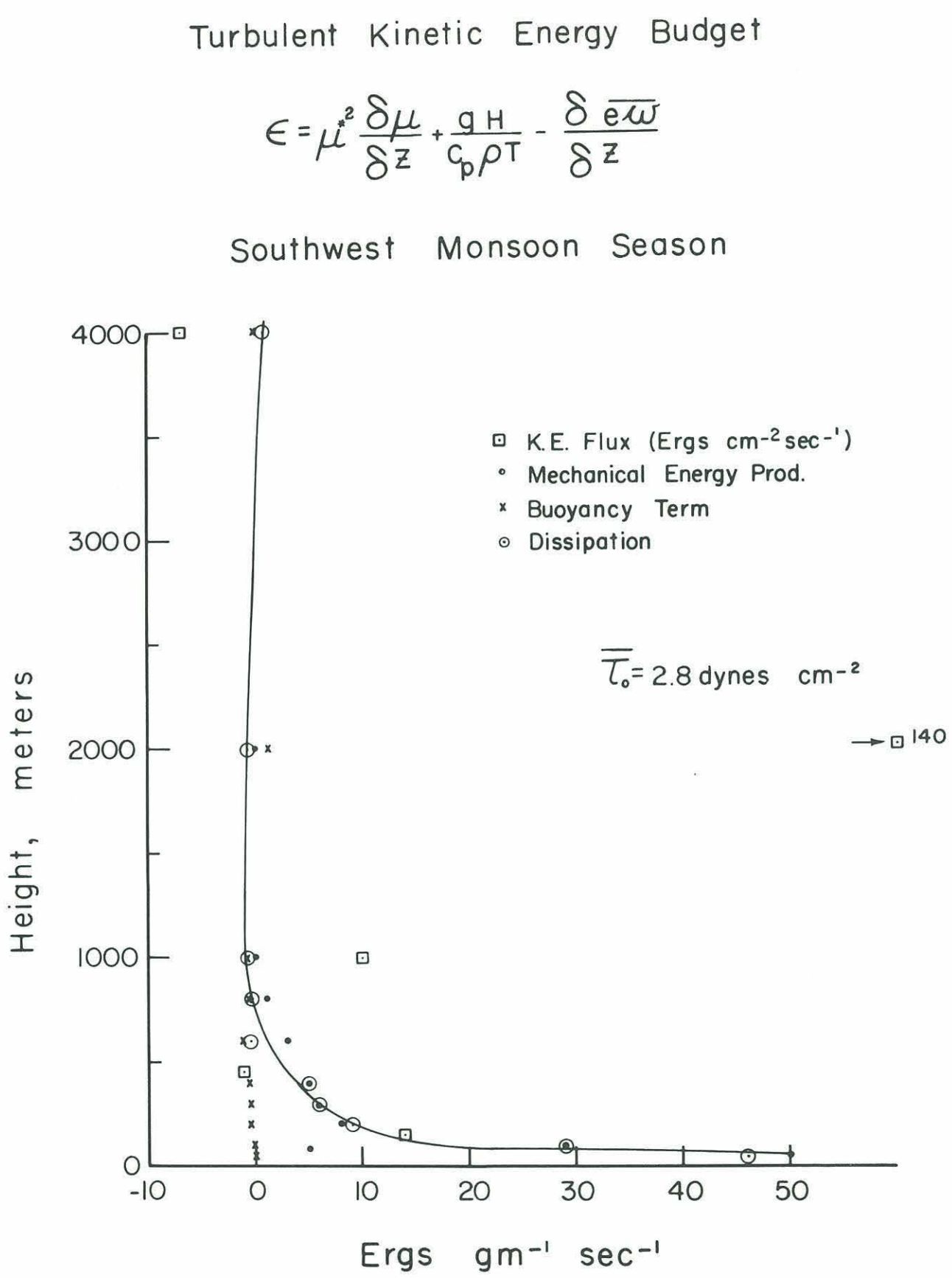

Figure 30. Height distribution of kinetic energy production, transport and dissipation during the southwest monsoon over the Arabian Sea.

Woods Hole Oceanographic Institution
Reference No. 68-62

TURBULENCE AND TURBULENT FLUXES OVER THE INDIAN OCEAN by Andrew F. Bunker. 31 pages plus figures and tables. September 1968. Grants G-22389 and GA-1490.

Observations of the turbulence and turbulent fluxes of heat, water vapor, and momentum over the Indian Ocean are presented and discussed. Data was obtained from 10 meters above the sea surface to 5000 meters in both northeast and southwest monsoon atmospheres. Height, spatial, and seasonal variations of the turbulence parameters are discussed. The flux of water vapor from the sea to the atmosphere is shown to be an important energy source for both monsoon systems.

1. Indian Ocean
2. Turbulence and turbulent fluxes
3. Monsoon systems

I. Bunker, Andrew F.
II. G-22389
III. GA-1490

This Card is UNCLASSIFIED

Woods Hole Oceanographic Institution
Reference No. 68-62

TURBULENCE AND TURBULENT FLUXES OVER THE INDIAN OCEAN by Andrew F. Bunker. 31 pages plus figures and tables. September 1968. Grants G-22389 and GA-1490.

Observations of the turbulence and turbulent fluxes of heat, water vapor, and momentum over the Indian Ocean are presented and discussed. Data was obtained from 10 meters above the sea surface to 5000 meters in both northeast and southwest monsoon atmospheres. Height, spatial, and seasonal variations of the turbulence parameters are discussed. The flux of water vapor from the sea to the atmosphere is shown to be an important energy source for both monsoon systems.

1. Indian Ocean
2. Turbulence and turbulent fluxes
3. Monsoon systems

I. Bunker, Andrew F.
II. G-22389
III. GA-1490

This Card is UNCLASSIFIED

Woods Hole Oceanographic Institution
Reference No. 68-62

TURBULENCE AND TURBULENT FLUXES OVER THE INDIAN OCEAN by Andrew F. Bunker. 31 pages plus figures and tables. September 1968. Grants G-22389 and GA-1490.

Observations of the turbulence and turbulent fluxes of heat, water vapor, and momentum over the Indian Ocean are presented and discussed. Data was obtained from 10 meters above the sea surface to 5000 meters in both northeast and southwest monsoon atmospheres. Height, spatial, and seasonal variations of the turbulence parameters are discussed. The flux of water vapor from the sea to the atmosphere is shown to be an important energy source for both monsoon systems.

1. Indian Ocean
2. Turbulence and turbulent fluxes
3. Monsoon systems

I. Bunker, Andrew F.
II. G-22389
III. GA-1490

This Card is UNCLASSIFIED

Woods Hole Oceanographic Institution
Reference No. 68-62

TURBULENCE AND TURBULENT FLUXES OVER THE INDIAN OCEAN by Andrew F. Bunker. 31 pages plus figures and tables. September 1968. Grants G-22389 and GA-1490.

Observations of the turbulence and turbulent fluxes of heat, water vapor, and momentum over the Indian Ocean are presented and discussed. Data was obtained from 10 meters above the sea surface to 5000 meters in both northeast and southwest monsoon atmospheres. Height, spatial, and seasonal variations of the turbulence parameters are discussed. The flux of water vapor from the sea to the atmosphere is shown to be an important energy source for both monsoon systems.

1. Indian Ocean
2. Turbulence and turbulent fluxes
3. Monsoon systems

I. Bunker, Andrew F.
II. G-22389
III. GA-1490

This Card is UNCLASSIFIED